Magneto-Elastic Coupling within the Stoner Model

by

Stefan Johannes Hilbert

A Master's Thesis

Submitted in partial fulfilment of the requirements

for the award of

Master of Philosophy of Loughborough University

Loughborough, August 2001

Abstract

Based on the Stoner Model for a single band in the mean field approximation (MFA), aspects of the interaction between lattice deformation and magnetisation of itinerant electron systems are studied.

The derivation of the Hartree-Fock-Stoner (HFS) Hamiltonian is reviewed for a single band starting from a general Hamiltonian describing band electrons. The finite-temperature properties of the model, including the various magnetic states and the ferromagnetic-to-paramagnetic phase transition, are briefly discussed within MFA.

The HFS Hamiltonian is applied to a single band with a rectangular density of states (DOS). The finite temperature magnetic properties of the system are studied using MFA. The model is extended to incorporate the interaction of lattice and magnetic degrees of freedom by introducing a dependence of the bandwidth on the lattice parameter. The effects of local variations of the lattice parameter are studied by introducing a local bandwidth and treating the variations as fluctuations. The results are compared to experimental magnetisation measurements of Invar alloys. Furthermore, magnetostriction and magnetic contributions to the thermal expansion are discussed within the model. Finally, effects of particle exchanges are considered within the model.

Acknowledgements

Contents

1 Introduction

The observation of magnetic phenomena goes back to ancient times (Mattis [1]). Although classical physics has had some success in describing macroscopic effects of magnetism, one could not understand the microscopic origins of magnetism until the rise of modern physics at the beginning of the twentieth century. On a microscopic scale, magnetism is a quantum mechanical phenomenon. In fact, in a purely classical model, a system can not exhibit any magnetic moment even in the presence of a magnetic field (Bohr-van Leeuwen theorem [1]).

Quantum theory of magnetism has been developed from two opposite starting points: the localised model and the band model. In the localised model, first introduced by Heisenberg in 1928 [2], each electron remains localised on an atom, where the intra-atomic electron-electron interactions are large and determine the magnetic moment of the atom. The inter-atomic forces are much smaller and compete with thermal disorder to define the magnetic order of the material.

The band model goes back to the works of Bloch [3], Mott [4], Slater [5] and Stoner [6-9] in the late 1920's and 1930's. In the band model, the magnetic carriers are itinerant and move in the average field of the other electrons and the ion cores. Weak electron-electron interactions form the ordered magnetic states characterised by different numbers of spin-up and spin-down electrons. Itinerant magnetism has been discussed, for example, by Herring [10], Blandin [11], Gautier [12] and Capellmann [13].

The model, which is among those most widely used to study itinerant magnetism, is that developed by Stoner [6-9]. Starting from the paramagnetic density of states (DOS), the electron-electron interactions are incorporated into the Stoner model by adding an exchange term quadratic in the magnetisation. In the earlier works, a parabolic form of the DOS has been used. Later, other band shapes and overlapping bands where considered, too. A rectangular shape has been discussed, for example, by Watanabe [14], Hunt [15] and Wohlfarth [16]. Using a rectangular shape has the advantage that the main formulae can be obtained in closed algebraic form. Reviews of the Stoner model have been given by Stoner [17] and by Wohlfarth [18].

Of particular interest in the field of magnetism is the interaction of magnetic and lattice degrees of freedom. The phenomena arising from this interaction range from magneto-volume instabilities in $REMn_2$ compounds [19] to the unusual properties of Invar

materials. Invar materials, first found by C. E. Guillaume in 1897 [20], are characterised by a low or even negative thermal expansion in a wide range around room temperature, which is attributed to the coupling of magnetic moment and lattice. A discussion of the Invar problem has been given by Wassermann [21].

Stoner-type models have frequently been used to discuss the effects of the interaction of magnetic and lattice degrees of freedom in itinerant electron systems. Mathon and Wohlfarth successfully explained many properties of $Fe_{65}Ni_{35}$ Invar using a Stoner model for weak itinerant ferromagnetism [22,23]. An itinerant model with distance-dependent bandwidth was suggested by Shiga and Nakamura [24]. Results for the distance-dependence of the d-bandwidth in transition metals where used by Janak and Williams [25] to describe the anomalous large volumes of the magnetic transition metals iron and nickel by giant internal magnetic pressure.

The aim of this work is to study aspects of the interaction between lattice deformation and magnetisation of itinerant electron systems based on the Stoner Model for a single band within mean field approximation (MFA). After a brief discussion of the localised model and its shortcomings following this chapter, the derivation of the Hartree-Fock-Stoner (HFS) Hamiltonian for a single band will be reviewed in chapter 3. The eigenstates of the HFS Hamiltonian will be discussed and the Stoner criterion at zero temperature will be derived. The interaction of electrons with an external magnetic field will be included into the model in chapter 4.

In chapter 5, the zero-temperature properties of the Stoner model will be investigated by applying the HFS Hamiltonian to a band with a rectangular DOS. This case will then be generalised to a non-rectangular density of states to support the findings from the study of the rectangular DOS. The finite-temperature properties of the Stoner model, including the various magnetic states and the ferromagnetic-to-paramagnetic phase transition, will be discussed within MFA in chapter 6.

In chapter 7, the MFA will be used to study the finite-temperature properties of the single band with rectangular DOS. The dependence of the magnetisation, the susceptibility and the Curie temperature on the system parameters will be analysed using analytical calculations in conjunction with numerical methods.

In chapter 8, the Stoner model for a single rectangular band will be extended to incorporate the interaction of lattice and magnetic degrees of freedom by assuming a dependence of the bandwidth on the lattice parameter. The effects of local variations of the lattice parameter will be studied by introducing a local bandwidth and treating the variations as fluctuations.

The results will be compared to experimental findings in Invar alloys. Furthermore, the magnetic contribution to the thermal expansion and magnetostriction will be discussed within this model. In chapter 9, an attempt will be made to include the effect of particle exchange between the single band and other parts of the electronic structure into the model. The work will be concluded with a summary and suggestions for future work in chapter 10.

The discussion in chapter 2, chapter 3 and chapter 6 will mainly follow the works by Blandin [11] and Gautier [12]. For experimental data of ferromagnetic materials, the books by Wohlfarth [26] and by Borzorth [27] will be used. The work of Wassermann [21] will be used as reference for Invar. For questions concerning solid state physics, the books by Kittel [28] and Ashcroft/Mermin [29] will be used as reference. The books by Nolting [30-33] will be used for theoretical questions.

2   The Localised Model and its Shortcomings

2.1   The Localised Model

Since this work is concerned with aspects of itinerant magnetism, the localised model will be discussed only briefly. Many localised models are based on the Heisenberg Hamiltonian

$$H = -\sum_{ij} J_{ij}\, \mathbf{S}_i \cdot \mathbf{S}_j \qquad (2.1)$$

with spin $\mathbf{S}_i$ localised on site i interacting with spin $\mathbf{S}_j$ localised on site j by an inter-atomic force J_{ij} which depends only on the distance between sites i and j. This Hamiltonian may be analysed within a mean field approximation. Using this approximation, the model may be solved yielding qualitatively many properties, which are found in most magnetic materials. One example is the approximation of the magnetic high-temperature susceptibility, which is obtained as

$$\chi = \frac{g^2 \mu_B^2\, S(S+1)}{3k_B(T-T_P)} \qquad (2.2)$$

with the spin quantum number S, the Bohr magneton μ_B, the Landé factor g, the Boltzmann constant k_B, the temperature T and the paramagnetic Curie temperature T_P.

In the localised model, spin waves can be introduced as elementary excitations in the magnetically ordered state at low temperatures. For a ferromagnet, the low-temperature saturation magnetisation is obtained as

$$M(T) = M(0)(1 - \alpha\, T^{3/2}) \qquad (2.3)$$

where $M(0) = g\mu_B S$ per atom.

In the Hamiltonian, J is regarded as a phenomenological parameter. In his original work, Heisenberg introduced J as the direct exchange integral between electrons of the same spin located in different orbitals. However, in ionic crystals, J is due to super-exchange and in rare earth metals, J is due to an indirect mechanism (RKKY) caused by the polarisation of the conduction electrons.

2.2 The Shortcomings of the Localised Model

However, many magnetic materials show properties, which can not be explained in a localised model such as the Heisenberg model. For example, the saturation moments should be an integral number of Bohr magnetons μ_B, but the measured saturation magnetisation of many transition metals and their alloys are fractional. For iron, cobalt and nickel, the moments are 2.22 μ_B, 1.7 μ_B and 0.6 μ_B, respectively. The measured Curie constants $C = g^2\mu_B^2 S(S+1)/(3k_B)$ of the magnetic susceptibility (2.2) do not lead to integer multiples of values of 1/2 for S. Furthermore, the spins derived from the measured Curie constant do not agree with the spins derived from the measured saturation magnetisation moments in the framework of the localised model. In some cases, the measured temperature dependence of the high temperature susceptibility follows only approximately a Curie law. Above the Curie Temperature T_C, some materials, such as chromium, do not show any spin fluctuations, as would be expected, if a Heisenberg model where applicable.

In transition metals, the partially filled d-electron states are the origin of the magnetism. De Haas-van Alphen experiments carried out on these materials clearly indicate the existence of a Fermi surface for d-electrons. Transport properties of transition metals show that d-electrons participate in the conduction process. In particular, the galvano-magnetic properties of iron, cobalt and nickel can only be explained if the magnetic electrons are assumed to be itinerant.

To understand these properties, the magnetic degrees of freedom can not be considered alone. In addition, the degrees of freedom associated with the itinerancy of the electrons have to be taken into account. The d-electrons in transition metals, showing itinerant character, have to be described within a band model, where the electron-electron interactions may stabilise various magnetic states in the metal.

3 The Derivation of the Stoner Model

3.1 The General Band Hamiltonian

In modern physics, the dynamics of a system is described with a Hamiltonian H. In quantum theory, H is an operator acting on a set of vectors $|\varphi\rangle$ of a Hilbert space, which represent the possible states of the system. The usual method for describing a quantum mechanical system comprising a large number of particles is by second quantisation.

In second quantisation, the Hamiltonian for a many-electron system, like a d-electron band in a solid, takes the form

$$H = \sum_{\alpha\beta} T_{\alpha\beta}\, a_\alpha^+ a_\beta + \tfrac{1}{2} \sum_{\alpha\beta\gamma\delta} U_{\alpha\beta\gamma\delta}\, a_\alpha^+ a_\beta^+ a_\delta a_\gamma \tag{3.1}$$

with α, β, γ and δ each characterising a one-electron state, which together form a basis in the one-electron Hilbert space. The operators a_α^+ and a_α are the creation and annihilation operators of the state α, respectively. The matrix elements of the 'kinetic energy'

$$T_{\alpha\beta} = \left\langle \alpha \left| \frac{\mathbf{p}^2}{2m} + V(\mathbf{r}) \right| \beta \right\rangle \tag{3.2}$$

comprise the one-electron kinetic energy $\mathbf{p}^2/2m$ and the one-electron potential $V(\mathbf{r})$. The Coulomb matrix elements

$$U_{\alpha\beta\gamma\delta} = \left\langle \alpha^{(1)}\beta^{(2)} \left| \frac{e^2}{|\mathbf{r}^{(1)} - \mathbf{r}^{(2)}|} \right| \gamma^{(1)}\delta^{(2)} \right\rangle \tag{3.3}$$

describe the electron-electron Coulomb interaction.

One way is to use localised atomic orbital-like states as the one-electron states for the description of the band electrons. A more common way to describe band electrons is to use the states derived by exploiting the translation symmetry of the crystal. The set of vectors representing this translation symmetry is called Bravais lattice and can be identified with the crystal lattice points by taking one of the crystal vectors as origin. The Bravais lattice $\mathcal{B}$ can be generated by three linear independent vectors $\mathbf{a}_i$ $(i \in \{1,2,3\})$:

$$\mathcal{B} = \{ n_1\,\mathbf{a}_1 + n_2\,\mathbf{a}_2 + n_3\,\mathbf{a}_3 \mid n_1, n_2, n_3 \in \mathbb{Z} \} \tag{3.4}$$

These vectors are called primitive vectors of the lattice. A volume of space is called a primitive cell if it fills all of space without either overlapping itself or leaving voids when translated through all the vectors in the Bravais lattice. A special choice of the primitive cell is the Wigner-Seitz cell, which is the region of space around a lattice point that is closer to this point than to any other lattice point.

With the choice of the Bravais lattice of a crystal, the reciprocal lattice is defined by:

$$\mathcal{K} = \{ \mathbf{k} \,|\, e^{i\mathbf{k}\cdot\mathbf{R}} = 1 \;\; \forall \mathbf{R} \in \mathcal{B} \} \tag{3.5}$$

The reciprocal lattice is itself a Bravais lattice with the original Bravais lattice as its reciprocal lattice. The Wigner-Seitz cell of the reciprocal lattice is called the first Brillouin zone.

In a crystalline solid, the one-electron potential $V(\mathbf{r})$ and with it the kinetic energy, carry as symmetry the periodicity of the crystal lattice. Following from group theory, the eigenstates of the kinetic energy then transform according to this symmetry. A way to express this relation is the celebrated Bloch Theorem: The eigenstates of the one-electron Hamiltonian

$$H = \frac{\mathbf{p}^2}{2m} + V(\mathbf{r}) \quad \text{with} \quad V(\mathbf{r}) = V(\mathbf{r} + \mathbf{R}) \;\; \forall \mathbf{R} \in \mathcal{B} \tag{3.6}$$

can be chosen to have in space the form

$$\Psi_{\mathbf{k}\,l}(\mathbf{r}) = u_{\mathbf{k}\,l}(\mathbf{r})\, e^{i\mathbf{k}\cdot\mathbf{r}} \tag{3.7}$$

with the function

$$u_{\mathbf{k}\,l}(\mathbf{r}) = u_{\mathbf{k}\,l}(\mathbf{r} + \mathbf{R}) \quad \forall \mathbf{R} \in \mathcal{B} \tag{3.8}$$

having the periodicity of a primitive cell. Here $\mathbf{k}$ is a vector in the first Brillouin zone of the reciprocal lattice and l is a set of additional quantum numbers needed to characterise the different eigenstates $\Psi_{\mathbf{k}\,l}$.

The states satisfying (3.7) are called Bloch states. As eigenstates of the kinetic energy of Hamiltonian (3.1), they diagonalise the kinetic part. However, in general, the kinetic part and the Coulomb part of the Hamiltonian can not be diagonalised simultaneously.

3.2 The Single Band Hamiltonian

For a single band in a solid formed by N atoms, the states α, β, γ and δ in the Hamiltonian (3.1) can each be characterised by their spin $\sigma \in \{\uparrow, \downarrow\}$ and indices $i, j, k, l \in \{1, ..., N\}$ representing the atom to which the orbital state belongs to:

$$H = \sum_{\substack{ij \\ \sigma\sigma'}} T_{\substack{ij \\ \sigma\sigma'}} a_{i\sigma}^+ a_{j\sigma'} + \tfrac{1}{2} \sum_{\substack{ijkl \\ \sigma\sigma'\sigma''\sigma'''}} U_{\substack{ijkl \\ \sigma\sigma'\sigma''\sigma'''}} a_{i\sigma}^+ a_{j\sigma'}^+ a_{l\sigma'''} a_{k\sigma''} \qquad (3.9)$$

Since the operators T and U of the Hamiltonian act only on the spatial part of the states

$$T_{\substack{ij \\ \sigma\sigma'}} = \langle i\sigma | T | j\sigma' \rangle = \langle i | \frac{\mathbf{p}^2}{2m_e} + V(\mathbf{r}) | j \rangle \langle \sigma | \sigma' \rangle = T_{ij} \delta_{\sigma,\sigma'} \qquad (3.10)$$

$$U_{\substack{ijkl \\ \sigma\sigma'\sigma''\sigma'''}} = \left\langle i\sigma^{(1)} j\sigma'^{(2)} \left| \frac{e^2}{|\mathbf{r}^{(1)} - \mathbf{r}^{(2)}|} \right| k\sigma''^{(1)} l\sigma'''^{(2)} \right\rangle$$

$$= \left\langle i^{(1)} j^{(2)} \left| \frac{e^2}{|\mathbf{r}^{(1)} - \mathbf{r}^{(2)}|} \right| k^{(1)} l^{(2)} \right\rangle \langle \sigma | \sigma'' \rangle \langle \sigma' | \sigma''' \rangle = U_{ijkl} \delta_{\sigma,\sigma''} \delta_{\sigma',\sigma'''} \qquad (3.11)$$

the Hamiltonian (3.9) transforms to:

$$H = \sum_{\substack{ij \\ \sigma}} T_{ij} a_{i\sigma}^+ a_{j\sigma} + \tfrac{1}{2} \sum_{\substack{ijkl \\ \sigma\sigma'}} U_{ijkl} a_{i\sigma}^+ a_{j\sigma'}^+ a_{l\sigma'} a_{k\sigma} \qquad (3.12)$$

For the tightly bound d-electrons in transition metals the orbital states are localised to the site i. Therefore, the Coulomb matrix elements involving only one site are much larger than the ones involving different sites. If all the Coulomb interactions U_{ijkl} except the ones involving only one site are neglected, i.e.

$$U_{ijkl} = U \, \delta_{i,j,k,l} \qquad (3.13)$$

with

$$\delta_{i,j,...,l} = \begin{cases} 1 & \text{if } i = j = ... = l \\ 0 & \text{otherwise} \end{cases} \qquad (3.14)$$

as a generalised Kronecker Delta function, and because the electrons, being fermions, obey the Pauli principle, the Coulomb part of (3.12) can be simplified further

$$\tfrac{1}{2} \sum_{\substack{ijkl \\ \sigma\sigma'}} U \delta_{i,j,k,l} \, a_{i\sigma}^+ a_{j\sigma'}^+ a_{l\sigma'} a_{k\sigma} = \tfrac{1}{2} U \sum_{i\sigma\sigma'} a_{i\sigma}^+ a_{i\sigma'}^+ a_{i\sigma'} a_{i\sigma}$$

$$= \tfrac{1}{2} U \sum_{i\sigma} a_{i\sigma}^+ a_{i-\sigma}^+ a_{i-\sigma} a_{i\sigma} = \tfrac{1}{2} U \sum_{i\sigma} n_{i\sigma} n_{i-\sigma} = U \sum_i n_{i\uparrow} n_{i\downarrow} \qquad (3.15)$$

leading to the Hamiltonian:

$$H = \sum_{ij\sigma} T_{ij}\, a^+_{i\sigma}\, a_{j\sigma} + U \sum_i n_{i\uparrow}\, n_{i\downarrow} \tag{3.16}$$

For a non-zero number of both spin-up and spin-down electrons on a site, the contribution from the Coulomb part of the site to the energy (3.16) is always positive. This contribution becomes zero if electrons occupying the site are only of one spin direction. In a band model, a spin polarisation causes the contribution of the kinetic part to increase, because electrons from states of one spin have to be shifted to previously unoccupied states of the other spin with higher energy. Consequently, the Coulomb part in (3.16) shows a preference for spin polarisation on each site, while the kinetic part shows a preference for an equal number of spin-up and spin-down electrons.

3.3 The Hartree-Fock-Stoner Hamiltonian

The appropriate one-particle-states to describe band electrons are the Bloch states. It follows from Bloch's theorem that the kinetic part of the Hamiltonian (3.16) can be diagonalised using the Bloch states $|k\sigma\rangle$ for electrons in a single band

$$\sum_{\substack{ij\\\sigma}} T_{ij}\, a^+_{i\sigma}\, a_{j\sigma} = \sum_{kk'\sigma} \varepsilon(k)\, \delta_{k,k'}\, a^+_{k\sigma} a_{k'\sigma} = \sum_{k\sigma} \varepsilon(k)\, n_{k\sigma} \tag{3.17}$$

with $\varepsilon(k)$ as their kinetic energy. For real materials, the $\varepsilon(k)$ are fairly complicated to estimate and the approximations needed to calculate them add another uncertainty to the calculations.

For the compact atomic d-electron orbitals in transition metals, the overlap of the electronic wavefunctions of neighbouring atoms is usually small. The bands created by the overlapping electron orbitals are quite narrow. Thus, it is a good first approximation to describe the d-band states by a linear combination of the atomic d-orbitals. More precisely, this means that the Bloch states $|k\sigma\rangle$ can be approximated by the Fourier transform of the orbital states. Conversely, the Wannier states

$$|R_i\sigma\rangle = \frac{1}{\sqrt{N}} \sum_k e^{-i\,k\cdot R_i} |k\sigma\rangle \tag{3.18}$$

as the inverse Fourier transform of the Bloch states with R_i as the lattice vector of the site i may be approximated by the atomic orbital $|i\sigma\rangle$. More generally, one may assume that the

Wannier states $|\,\mathbf{R}_i\sigma\rangle$ for a narrow band are localised to site i and show properties very close to the atomic orbitals. Under this assumption, the calculations of the previous section remain valid by taking the orbital functions as the Wannier functions.

Applying the relations

$$a_{j\sigma}^+ = \frac{1}{\sqrt{N}}\sum_{\mathbf{k}} e^{-i\mathbf{k}\cdot\mathbf{R}_j} a_{\mathbf{k}\sigma}^+ \qquad \text{and} \qquad a_{j\sigma} = \frac{1}{\sqrt{N}}\sum_{\mathbf{k}} e^{i\mathbf{k}\cdot\mathbf{R}_j} a_{\mathbf{k}\sigma} \tag{3.19}$$

between the creators and annihilators of the Bloch and Wannier states, the Coulomb part of Hamiltonian (3.16) becomes

$$\begin{aligned}
U\sum_j n_{j\uparrow} n_{j\downarrow} &= U\sum_j a_{j\uparrow}^+ a_{j\uparrow} a_{j\downarrow}^+ a_{j\downarrow} \\[2mm]
&= \frac{U}{N^2}\sum_{\mathbf{k}_1\mathbf{k}_2\mathbf{k}_3\mathbf{k}_4}\sum_j e^{i(-\mathbf{k}_1+\mathbf{k}_2-\mathbf{k}_3+\mathbf{k}_4)\mathbf{R}_j} a_{\mathbf{k}_1\uparrow}^+ a_{\mathbf{k}_2\uparrow} a_{\mathbf{k}_3\downarrow}^+ a_{\mathbf{k}_4\downarrow} \\[2mm]
&= \frac{U}{N}\sum_{\mathbf{k}_1\mathbf{k}_2\mathbf{k}_3\mathbf{k}_4}\delta_{-\mathbf{k}_1+\mathbf{k}_2-\mathbf{k}_3+\mathbf{k}_4}\, a_{\mathbf{k}_1\uparrow}^+ a_{\mathbf{k}_2\uparrow} a_{\mathbf{k}_3\downarrow}^+ a_{\mathbf{k}_4\downarrow} \\[2mm]
&= \frac{U}{N}\sum_{\mathbf{k}_2\mathbf{k}_3\mathbf{k}_4} a_{\mathbf{k}_2-\mathbf{k}_3+\mathbf{k}_4\uparrow}^+ a_{\mathbf{k}_2\uparrow} a_{\mathbf{k}_3\downarrow}^+ a_{\mathbf{k}_4\downarrow} \\[2mm]
&= \frac{U}{N}\sum_{\mathbf{k}\mathbf{k}'\mathbf{q}} a_{\mathbf{k}-\mathbf{q},\uparrow}^+ a_{\mathbf{k}\uparrow} a_{\mathbf{k}'+\mathbf{q},\downarrow}^+ a_{\mathbf{k}'\downarrow}
\end{aligned} \tag{3.20}$$

by observing the sum form of the discrete delta function:

$$\delta_{\mathbf{k}} = \frac{1}{N}\sum_{\mathbf{R}} e^{i\,\mathbf{k}\cdot\mathbf{R}} = \begin{cases} 1 & \mathbf{k}=0 \\ 0 & \mathbf{k}\neq 0 \end{cases} \tag{3.21}$$

The Hamiltonian (3.16) then takes the form:

$$H = \sum_{\mathbf{k}\sigma}\varepsilon(\mathbf{k})\, n_{\mathbf{k}\sigma} + \frac{U}{N}\sum_{\mathbf{k}\mathbf{k}'\mathbf{q}} a_{\mathbf{k}-\mathbf{q},\uparrow}^+ a_{\mathbf{k}\uparrow} a_{\mathbf{k}'+\mathbf{q},\downarrow}^+ a_{\mathbf{k}'\downarrow} \tag{3.22}$$

In a Hartree-Fock approximation (HFA) one takes only those parts of the Hamiltonian, which lead to number operators, which are build only of occupation number operators $n_{anystate}$. This originates from taking Slater determinants

$$|HF\rangle = \sqrt{N!}\,|k_1\sigma_1,\ldots,k_n\sigma_n\rangle^{(-)} = \frac{1}{\sqrt{N!}}\begin{vmatrix} \left|k_1\sigma_1^{(1)}\right\rangle & \left|k_1\sigma_1^{(2)}\right\rangle & \cdots & \left|k_1\sigma_1^{(n)}\right\rangle \\[2mm] \left|k_2\sigma_2^{(1)}\right\rangle & \left|k_2\sigma_2^{(2)}\right\rangle & \cdots & \left|k_2\sigma_2^{(n)}\right\rangle \\[2mm] \vdots & \vdots & \ddots & \vdots \\[2mm] \left|k_n\sigma_n^{(1)}\right\rangle & \left|k_n\sigma_n^{(2)}\right\rangle & \cdots & \left|k_n\sigma_n^{(n)}\right\rangle \end{vmatrix} \tag{3.23}$$

as antisymmetric test functions in the variation method

$$\langle H \rangle_\varphi = \frac{\langle \varphi | H | \varphi \rangle}{\langle \varphi | \varphi \rangle} \tag{3.24}$$

where all non-number parts of H do not contribute. The Slater determinants (3.23) are identical - apart from a normalisation constant - with the Fock states $\left| n_{k_1\sigma_1}, ..., n_{k_n\sigma_n} \right\rangle^{(-)}$. Fock states $\left| n_{\alpha_1}, n_{\alpha_2}, ... \right\rangle^{(\pm)}$ are the usual way to describe states in the second quantisation formalism.

Making the Hartree-Fock approximation for the Coulomb part of Hamiltonian (3.22) and neglecting all contributions with $q \neq 0$

$$\begin{aligned}
H &= \sum_{k\,\sigma} \varepsilon(k)\, n_{k\sigma} + \frac{U}{N} \sum_{kk'q} a^+_{k-q,\uparrow} a_{k\uparrow} a^+_{k'+q,\downarrow} a_{k'\downarrow} \\
&\stackrel{HF}{=} \sum_{k\,\sigma} \varepsilon(k)\, n_{k\sigma} + \frac{U}{N} \sum_{kk'} a^+_{k\uparrow} a_{k\uparrow} a^+_{k'\downarrow} a_{k'\downarrow} = \sum_{k\,\sigma} \varepsilon(k)\, n_{k\sigma} + \frac{U}{N} \sum_{k} n_{k\uparrow} \sum_{k'} n_{k'\downarrow}
\end{aligned} \tag{3.25}$$

one obtains the Hartree-Fock Hamiltonian:

$$H = \sum_{k\,\sigma} \varepsilon(k)\, n_{k\sigma} + \frac{U}{N} n_\uparrow n_\downarrow \qquad \text{with} \qquad n_\sigma = \sum_{k} n_{k\,\sigma} \tag{3.26}$$

For the description of band magnetism, this Hamiltonian was first introduced by Stoner. Therefore, Hamiltonian (3.26) is also referred to as Hartree-Fock-Stoner Hamiltonian. The Hamiltonian (3.26) can be written in the form

$$H = \sum_{k\sigma} \varepsilon(k)\, n_{k\sigma} + \tfrac{1}{2} \sum_{\substack{kk' \\ \sigma\sigma'}} \left(\frac{U}{N} - \frac{U}{N} \delta_{\sigma,\sigma'} \right) n_{k\sigma}\, n_{k'\sigma'} \tag{3.27}$$

where it is apparent that in this approximation the direct and the exchange term of the two states $|k\sigma\rangle$ and $|k'\sigma'\rangle$ are both determined by the intra-atomic Coulomb repulsion.

3.4 The Density-of-States Approximation

In a solid, the number of atoms N is usually very large. In the limit of a large crystal, the allowed values for k in a sum of the form $\sum_{k\,\sigma} Q(k,\sigma)$ are quasi-continuous and the sum can be approximated by an integral

$$\sum_{k\sigma} Q(k,\sigma) = \sum_{\sigma} \int Q(k,\sigma)\, \tilde{D}_\sigma(k)\, dk \tag{3.28}$$

by using the density of states $\tilde{D}_\sigma(k)$ as a continuum approximation of the distribution of the one-electron states $|k\sigma\rangle$ in k-space. If, as is often the case, the quantities $Q(k,\sigma)$ depend on k only through the one-electron energies $\varepsilon(k)$, the sum can be expressed as:

$$\sum_{k\sigma} Q(k,\sigma) = \sum_{\sigma} \int Q(\varepsilon(k),\sigma)\, \tilde{D}_\sigma(k)\, dk = \sum_{\sigma} \int_{-\infty}^{\infty} Q(\varepsilon,\sigma)\, D_\sigma(\varepsilon)\, d\varepsilon \tag{3.29}$$

The integral over the k-space with the weight $\tilde{D}_\sigma(k)$ is replaced by an integral over the one-electron energies ε with the weight $D_\sigma(\varepsilon)$. The density of states $D_\sigma(\varepsilon)$ is the continuum approximation for the distribution of the states over the one-electron energies ε. In the models used here, the density of states $D_\sigma(\varepsilon)$ does not depend on the occupation of the states and the spin-up and spin-down densities are identical:

$$D_\uparrow(\varepsilon) \equiv D_\downarrow(\varepsilon) =: D(\varepsilon) \tag{3.30}$$

Therefore, the spin indices for $D_\uparrow(\varepsilon)$ and $D_\downarrow(\varepsilon)$ can be dropped and the density of states for both spins may be denoted as $D(\varepsilon)$. In this approximation, the HFS Hamiltonian (3.26) can then be written as

$$H = \sum_{\sigma} \int_{-\infty}^{\infty} \varepsilon\, n_\sigma(\varepsilon)\, D(\varepsilon)\, d\varepsilon + U\, n_\uparrow n_\downarrow \tag{3.31}$$

with $n_\sigma(\varepsilon)$ as the continuum approximation of the occupation numbers of the states with spin σ and one-electron energies ε,

$$n_\sigma = \sum_{k} n_{k\sigma} = \int_{-\infty}^{\infty} n_\sigma(\varepsilon)\, D(\varepsilon)\, d\varepsilon \tag{3.32}$$

as the number of spin-up and spin-down electrons and

$$n = n_\uparrow + n_\downarrow \tag{3.33}$$

as the total number of electrons. $D(\varepsilon)$, and consequently H, n, $n_\uparrow$ and $n_\downarrow$ are normalised such as to be measured per atom in order to exclude a dependence on sample size.

3.5 The Eigenstates of the Hartree-Fock-Stoner Hamiltonian

The eigenstates of the Hartree-Fock Hamiltonian (3.26) are the Slater determinants (3.23), the eigenstates for the system without electron-electron interactions:

$$H = \sum_{k\,\sigma} \varepsilon(k)\, n_{k\sigma} \tag{3.34}$$

This is evident from the way the Hamiltonian has been derived. The Slater determinants (3.23) are eigenstates of the occupation number operator $n_{k\sigma}$. In the Hartree-Fock approximation, those parts of the Hamiltonian are neglected, which can not be represented as a function of $n_{k\sigma}$, which would cause the Slater determinant (3.23) not to be an eigenstate of the Hamiltonian.

After having been derived using a variation method, Hamiltonian (3.26) has to be used to find the states that minimise the total energy. The minimal value of the total energy and the corresponding state may then be used as an approximation for the ground state and the ground state energy. The deviations of this state and energy from the real ground state of the full many-body Hamiltonian (3.9) are due to correlations, the effect of which may be difficult to quantify.

The eigenstates of Hamiltonian (3.26) representing a completely ferromagnetic state are the Slater determinants with either all or none of the states of one spin direction occupied, i.e. $\exists \sigma \in \{\uparrow, \downarrow\}$ such that $\left(\left(n_{k\sigma} = 0\ \forall k\right) \vee \left(n_{k\sigma} = 1\ \forall k\right)\right)$. These states are also eigenstates of the Hamiltonian (3.22). The Slater determinant for the fully ferromagnetic state with

$$n_{k\sigma} = \begin{cases} 1 & \text{if } \varepsilon(k) \le \varepsilon_{F\sigma} \\ 0 & \text{if } \varepsilon(k) > \varepsilon_{F\sigma} \end{cases} \tag{3.35}$$

where $\varepsilon_{F\sigma}$ is a spin-dependent Fermi energy, is the state of lowest energy for maximum spin polarisation and given total number of electrons. A Slater determinant representing a partial ferromagnetic state, where $\left(\left(\exists k : n_{k\sigma} = 0\right) \wedge \left(\exists k : n_{k\sigma} = 1\right)\right) \forall \sigma \in \{\uparrow, \downarrow\}$, is not an eigenstate of Hamiltonian (3.22).

The Hamiltonian (3.26) is invariant under rotation. For an eigenstate of the Hamiltonian with finite magnetisation, the rotational symmetry of the system is broken. Nevertheless, these eigenstates are degenerate with respect to the polarisation direction due to the rotational symmetry of the Hamiltonian. The degeneracy is lifted by application of an external magnetic field. This will be discussed in more detail in chapter 4.

3.6 The Stoner Criterion

As the main feature of the Hartree-Fock-Stoner Hamiltonian (3.26), the magnetic properties of the system in this approximation are governed by its band structure and its band filling. Several studies of the criteria for the onset and stability of different ferromagnetic states have been carried out for the Stoner model [34] and other, more general models [35,36,37].

To study the stability of the paramagnetic state at low temperature within the Stoner model, an electron band containing n electrons with density of states $D(\varepsilon)$ for both spin-up and spin-down electrons and a Fermi energy ε_F located inside the band is considered. For the paramagnetic state, the occupation numbers at zero temperature are:

$$n_{k\sigma} = \begin{cases} 1 & if \ \varepsilon(\mathbf{k}) \le \varepsilon_F \\ 0 & if \ \varepsilon(\mathbf{k}) > \varepsilon_F \end{cases} \quad and \quad n_\sigma = \sum_{\mathbf{k}} n_{k\sigma} = \frac{n}{2} \tag{3.36}$$
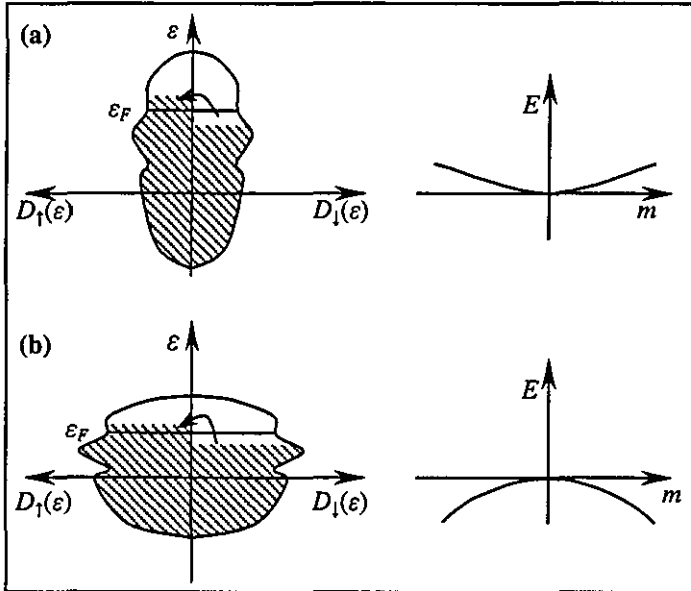
Fig. 3.1: The Stoner Criterion. For wide bands (a), the shift of electrons from the spin-down to the spin-up states raises the energy, whereas for narrow bands (b) the energy of the system is lowed by this process.

If all the spin-down electrons in a shell of infinitesimal thickness δE located directly below the Fermi surface are shifted to the free spin-up states located directly above the Fermi level, the change in the kinetic energy

$$\Delta T = \int_{\varepsilon_F}^{\varepsilon_F + \delta E} \varepsilon \ D(\varepsilon) \ d\varepsilon + \int_{\varepsilon_F}^{\varepsilon_F - \delta E} \varepsilon \ D(\varepsilon) \ d\varepsilon = D(\varepsilon_F) \delta E^2 \tag{3.37}$$

and the change in the Coulomb energy

$$\Delta U = U\left(\frac{n}{2} + D(\varepsilon_F)\delta E\right)\left(\frac{n}{2} - D(\varepsilon_F)\delta E\right) - U\frac{n^2}{4} = -U D(\varepsilon_F)^2 \delta E^2 \tag{3.38}$$

yield a total change in the electronic energy:

$$\Delta E = \Delta T + \Delta U = (1 - U D(\varepsilon_F))D(\varepsilon_F)\delta E^2 \tag{3.39}$$

For $U D(\varepsilon_F) < 1$ the total change in energy ΔE by a small spin polarisation is positive, whereas for $U D(\varepsilon_F) > 1$, the change in energy ΔE is negative. From this consideration, the Stoner criterion follows: For $U D(\varepsilon_F) < 1$ the paramagnetic state is energetically locally stable, while for $U D(\varepsilon_F) > 1$ the paramagnetic state is unstable.

More generally, this means that for a wide band, where the DOS at the Fermi level $D(\varepsilon_F)$ is small, the paramagnetic state is stable, whereas for bands, which are sufficiently narrow and therefore exhibit a large $D(\varepsilon_F)$, the ferromagnetic state is favoured. With a similar stability analysis based on the density of states and its derivatives, one can derive approximate criteria for the stability of magnetisation values [34].

4   The Inclusion of an External Magnetic Field

Until now, the model has been treated without consideration of an external magnetic field. In this work, only Pauli spin paramagnetism is considered. Diamagnetic and higher order interaction of electrons with a magnetic field are usually very small and are thus neglected here. However, it can be shown [33] that the diamagnetic or Landau susceptibility χ_L for free electrons is negative and one third in magnitude of the paramagnetic or Pauli susceptibility χ_P. In some metals, the deviation of the effective electron mass from the free electron mass even causes the Landau susceptibility to dominate the Pauli susceptibility [33]. Furthermore, all interactions of the orbital angular momentum with the magnetic field are neglected. In crystals, permanent moments arising from orbital angular momentum usually vanish, which is known as the quenching of orbital angular momentum [29].

4.1   The Hamiltonian

In a magnetic field, the degeneracy of the one-electron energies ε_k with respect to their magnetic quantum number along the field direction is lifted [32]. Therefore, it is convenient to choose the spin quantisation axis in direction of the applied field. This preserves the states (3.23) as eigenstates of the Hamiltonian including interactions with an external magnetic field. Since the z-component of the spin **S** in a Cartesian coordinate system is chosen for characterisation of the states (3.23), the direction of the external magnetic field has to be chosen as the z-axis. With the approximations used here, the additional part in the Hamiltonian for the interaction of an electron in a state $|k\ \sigma\rangle$ with an external magnetic field $\mathbf{B}_0 = (0,0,-B_0)$ is then

$$-2\frac{\mu_B}{\hbar}\mathbf{S}\cdot\mathbf{B}_0 = -\mu_B\, B_0\,\overline{\sigma} \tag{4.1}$$

with **S** as the spin of the electron and μ_B as the Bohr magneton [32]. Here the notation

$$\overline{\sigma} = \begin{cases} +1 & for \quad \sigma = \uparrow \\ -1 & for \quad \sigma = \downarrow \end{cases} \tag{4.2}$$

has been used for brevity.

This yields the spin-dependent one-electron energies

$$\varepsilon_{\mathbf{k}\,\sigma} = \varepsilon(\mathbf{k}) - \mu_B \, B_0 \, \overline{\sigma} \tag{4.3}$$

which replace the $\varepsilon(\mathbf{k})$ in (3.26) [33]. The Hartree-Fock-Stoner Hamiltonian (3.26) then becomes

$$\begin{aligned}
H &= \sum_{\mathbf{k}\,\sigma} \left(\varepsilon(\mathbf{k}) - \mu_B B_0 \overline{\sigma} \right) n_{\mathbf{k}\sigma} + \frac{U}{N} n_\uparrow \, n_\downarrow \\
&= \sum_{\mathbf{k}\,\sigma} \varepsilon(\mathbf{k}) \, n_{\mathbf{k}\sigma} + \frac{U}{N} n_\uparrow \, n_\downarrow - \mu_B B_0 (n_\uparrow - n_\downarrow)
\end{aligned} \tag{4.4}$$

with $n_\sigma = \sum_{\mathbf{k}} n_{\mathbf{k}\,\sigma}$. The difference $n_\uparrow - n_\downarrow$ is the spin polarisation:

$$m = \sum_{\mathbf{k}\,\sigma} \overline{\sigma} \, n_{\mathbf{k}\,\sigma} = n_\uparrow - n_\downarrow \tag{4.5}$$

In the next chapter, it will be shown that m or its expectation value is the magnetisation of the system measured in Bohr magnetons $\mu_B = \dfrac{e\hbar}{2m_e c} = 9.2732 \times 10^{-24} \, \text{J T}^{-1}$.

The Hamiltonian (4.4) can be written in compact form as

$$H = \sum_{\mathbf{k}\,\sigma} \overline{\varepsilon}_{\mathbf{k}\,\sigma} \, n_{\mathbf{k}\,\sigma} \tag{4.6}$$

with

$$\overline{\varepsilon}_{\mathbf{k}\,\sigma} = \varepsilon(\mathbf{k}) + \frac{U}{2N} \sum_{\mathbf{k}} n_{\mathbf{k}\,-\sigma} - \mu_B \, B_0 \, \overline{\sigma} \tag{4.7}$$

as an effective one-electron energy. In the density-of-states approximation (see 3.4), the Hamiltonian takes the form:

$$H = \sum_{\sigma} \int_{-\infty}^{\infty} \varepsilon \, n_\sigma(\varepsilon) \, D(\varepsilon) \, d\varepsilon + U \, n_\uparrow \, n_\downarrow \tag{4.8}$$

with

$$n_\sigma = \sum_{\mathbf{k}} n_{\mathbf{k}\sigma} = \int_{-\infty}^{\infty} n_\sigma(\varepsilon) \, D(\varepsilon) \, d\varepsilon \tag{4.9}$$

as the number of spin-up and spin-down electrons and

$$n = \sum_{\mathbf{k}\,\sigma} n_{\mathbf{k}\sigma} = \sum_{\sigma} n_{\sigma} = \sum_{\sigma} \int_{-\infty}^{\infty} n_{\sigma}(\varepsilon)\, D(\varepsilon)\, d\varepsilon \qquad (4.10)$$

as the total number of electrons. $D(\varepsilon)$, H, n, $n_{\uparrow}$ and $n_{\downarrow}$ are normalised.

In the absence of an external magnetic field, the possible directions of the magnetisation are degenerate due to spherical symmetry of the Hamiltonian. A non-zero external field breaks this symmetry. If only fields are considered, which point in a fixed direction, one can choose the spin quantisation axis along the field direction and the spin-up electrons to have lower energy than the spin-down electrons, which amounts to assuming $B_0 \geq 0$ for $\mathbf{B_0} = (0,0,-B_0)$. For an external magnetic field with changing direction, this can not be achieved. However, any change of the direction of the magnetic field without a change in its strength just rotates the magnetisation in the field direction, but does not change the energy. In this model, there is no energy needed to change the direction of the magnetisation.

4.2 The Magnetisation

The magnetisation **M** is defined as the derivative of the system's free energy F with respect to the external magnetic field $\mathbf{B_0}$. The magnetisation is usually normalised by the volume or the number of atoms to eliminate the dependence on sample size. This is not done here explicitly, since the free energy is already taken per atom in the density-of-states approximation. In general, the magnetisation is a vector quantity as well as the magnetic field. However, the system studied here can be seen as one-dimensional with an external field $\mathbf{B_0} = (0,0,-B_0)$ and a magnetisation $\mathbf{M} = (0,0,M)$.

Now it will be shown that the spin polarisation defined by (4.5) is the magnetisation of the system measured in Bohr magnetons. With (4.5), the Hamiltonian can be written as:

$$H = \sum_{\mathbf{k}\,\sigma} \varepsilon(\mathbf{k})\, n_{\mathbf{k}\sigma} + \frac{U}{N} n_{\uparrow}\, n_{\downarrow} - \mu_B B_0 m \qquad (4.11)$$

By means of the internal energy $\langle H \rangle$ as the expectation value of the Hamiltonian, the entropy S and the temperature T, the system's free energy can be written as: $F = \langle H \rangle - T\,S$.

The magnetisation is then calculated as:

$$M = -\left(\frac{\partial F}{\partial B_0}\right)_{T,V,n} = -\left(\frac{\partial F}{\partial B_0}\right)_{T,V,n,m} - \left(\frac{\partial F}{\partial\langle m\rangle}\right)_{T,V,n,B}\left(\frac{\partial\langle m\rangle}{\partial B_0}\right)_{T,V,n} \tag{4.12}$$

The spin polarisation $\langle m\rangle$ is considered as an internal degree of freedom and it therefore minimises the free energy of the system. This implies that the term $\left(\partial F/\partial\langle m\rangle\right)_{T,V,n,B}$ vanishes for a proper minimum, i.e. a minimum lying inside the region of possible magnetisation values. For a minimum at the boundary, infinitesimal changes of B do not change m, and therefore, the term $\left(\partial\langle m\rangle/\partial B_0\right)_{T,V,n}$ vanishes.

Therefore:

$$M = -\left(\frac{\partial F}{\partial B_0}\right)_{T,V,n,m} = -\left(\frac{\partial\langle H\rangle}{\partial B_0}\right)_{T,V,n,m} + T\left(\frac{\partial S}{\partial B_0}\right)_{T,V,n,m} \tag{4.13}$$

Furthermore, the entropy is not explicitly dependent on the magnetic field. Hence:

$$M = -\left(\frac{\partial\langle H\rangle}{\partial B_0}\right)_{T,V,n,m} = \mu_B\langle m\rangle \tag{4.14}$$

The spin polarisation m is indeed the magnetisation measured in Bohr magnetons.

4.3 The Susceptibility

The susceptibility χ is defined as the second derivative of the free energy F with respect to the external magnetic field B_0. In general, it is a tensor of rank two, but in the isotropic case studied here, it is considered simply a number. With (4.12) it can be calculated as:

$$\chi(B_0,T) = -\left(\frac{\partial^2 F}{\partial B_0^2}\right)_{T,V,n} = \mu_B\left(\frac{\partial\langle m\rangle}{\partial B_0}\right)_{T,V,n} \tag{4.15}$$

For proper minima of the free energy with respect to m, where $0 = \left(\partial F/\partial\langle m\rangle\right)_{T,V,n,B_0}$, a useful relation between the susceptibility χ and the stability requirement $0 < \left(\partial^2 F/\partial\langle m\rangle^2\right)_{T,V,n,B_0}$ can be obtained by (indices T, V, n at the derivatives omitted):

$$0 = \left(\frac{\partial}{\partial B_0} \left(\frac{\partial F}{\partial \langle m \rangle} \right)_{B_0} \right) = \left(\frac{\partial}{\partial B_0} \left(\frac{\partial F}{\partial \langle m \rangle} \right)_{B_0} \right)_{\langle m \rangle} + \left(\frac{\partial^2 F}{\partial \langle m \rangle^2} \right)_{B_0} \left(\frac{\partial \langle m \rangle}{\partial B_0} \right)$$

$$= -\mu_B + \left(\frac{\partial^2 F}{\partial \langle m \rangle^2} \right)_{B_0} \frac{\chi}{\mu_B} \tag{4.16}$$

For a non-zero value of the susceptibility, this yields:

$$\left(\frac{\partial^2 F}{\partial \langle m \rangle^2} \right)_{B_0} = \mu_B^2 \, \chi^{-1} \tag{4.17}$$

Therefore, the stability of a stationary value of $\langle m \rangle$ is equivalent to a positive susceptibility.

5 The Stoner Model at Zero Temperature

5.1 The Rectangular Band at Zero Temperature

Distinguished by its simplicity, the case of a single, independent rectangular band is studied here to establish some fundamental properties of the Stoner theory. In a first step, an external magnetic field is not included into the consideration. Starting from the Hartree-Fock-Stoner Hamiltonian for a single band (3.26), the density of states approximation (3.31), (3.32) and (3.33) for a rectangular density of states

$$D(\varepsilon) = \begin{cases} 1/W & for \quad -W/2 \le \varepsilon \le W/2 \\ 0 & otherwise \end{cases} \tag{5.1}$$

with the bandwith W is applied. In the Hamiltonian, the operators are then substituted by their eigenvalues, which characterise their eigenstates, namely the Slater determinants (3.23). The resulting Hamiltonian is then used to find the ground state and its magnetic properties for different system parameters. In the model, adjustable system parameters are the total number of electrons in the band n, the strength of the on-site Coulomb repulsion U and the bandwidth W.
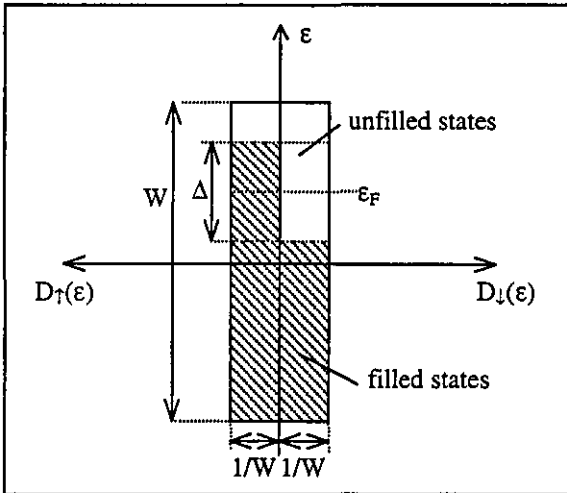
Fig. 5.1: The density of states $D_\uparrow(\varepsilon)$ for spin-up and $D_\downarrow(\varepsilon)$ for spin-down electrons and the filling of the states.
The unequal filling of the spin-up and the spin-down states gives rise to a band splitting Δ as the difference in energies of the highest filled spin-up and the spin-down band states.

The density of states (5.1) satisfies the normalisation as proposed in section 3.3, since for a single band, there are exactly one spin-up and one spin-down one-electron state per atom. Furthermore, the total number of electrons n in the band is fixed to a value between zero and two. The number of spin-up electrons $n_\uparrow$ and the number of spin-down electrons $n_\downarrow$ are then related by equation (3.33).

For zero temperature, the occupation numbers $n_\sigma(\varepsilon)$ are approximated by a step function

$$n_\sigma(\varepsilon) = \begin{cases} 1 & for \quad \varepsilon \le \varepsilon_{F\sigma} \\ 0 & for \quad \varepsilon > \varepsilon_{F\sigma} \end{cases} \tag{5.2}$$

with $\varepsilon_{F\sigma}$ being the Fermi energy for spin σ as derived from the total number of electrons with spin σ:

$$n_\sigma = \int_{-\infty}^{\varepsilon_{F\sigma}} D(\varepsilon)\, d\varepsilon = \int_{-W/2}^{\varepsilon_{F\sigma}} \frac{1}{W}\, d\varepsilon = \frac{1}{2} + \frac{\varepsilon_{F\sigma}}{W} \tag{5.3}$$

The occupation numbers (5.2) are the occupation numbers of the Slater determinant with lowest energy for a fixed number of up- and down-spin electrons.

The paramagnetic Fermi energy ε_F defined by

$$n = \sum_\sigma \int_{-\infty}^{\varepsilon_F} D(\varepsilon)\, d\varepsilon = 2 \int_{-W/2}^{\varepsilon_F} \frac{1}{W}\, d\varepsilon = 1 + \frac{2\varepsilon_F}{W} \tag{5.4}$$

is determined by the total number of electrons n and the bandwidth W:

$$\varepsilon_F = (n-1)\frac{W}{2} \tag{5.5}$$

The spin polarisation or magnetisation (per atom, measured in μ_B) is defined by

$$m = n_\uparrow - n_\downarrow \tag{5.6}$$

and can take values in the interval $[-m_{max}, m_{max}]$ with

$$m_{max} = \min\{n, 2-n\} \tag{5.7}$$

as the saturation magnetisation.

The magnetisation m is assumed to be an internal degree of freedom of the system. Hence, its actual value minimises the system's free energy F, which for zero temperature is identical to the internal energy H

$$F = H = \sum_\sigma \int_{-\infty}^{\infty} \varepsilon\, n_\sigma(\varepsilon)\, D(\varepsilon)\, d\varepsilon + U\, n_\uparrow n_\downarrow \tag{5.8}$$

with the kinetic energy as the first term and the Coulomb repulsion as the second term. It is now the aim to express all the quantities in (5.8) in terms of the external system parameters W, U, n and B_0 and the internal degree of freedom m and then to minimise (5.8) with respect to m.

Using (3.33) and (5.6), the number of spin-up and spin-down electrons can be expressed by:

$$n_\uparrow = \frac{n}{2} + \frac{m}{2} \quad \text{and} \quad n_\downarrow = \frac{n}{2} - \frac{m}{2} \tag{5.9}$$

By introducing the band splitting energy

$$\Delta = mW \tag{5.10}$$

and using (5.3), (5.4), (5.5) and (5.9), one finds for the Fermi energies the relations:

$$\varepsilon_{F\uparrow} = \varepsilon_F + \frac{\Delta}{2} = (n - 1 + m)\frac{W}{2} \quad \text{and}$$

$$\tag{5.11}$$

$$\varepsilon_{F\downarrow} = \varepsilon_F + \frac{\Delta}{2} = (n - 1 - m)\frac{W}{2}$$

With these relations, the magnetisation dependence of the free energy is calculated as:

$$F = \sum_\sigma \int_{-\infty}^{\infty} \varepsilon \, n_\sigma(\varepsilon) \, D(\varepsilon) \, d\varepsilon + U \, n_\uparrow n_\downarrow$$

$$= \int_{-W/2}^{\varepsilon_{F\uparrow}} \varepsilon \, D(\varepsilon) \, d\varepsilon + \int_{-W/2}^{\varepsilon_{F\downarrow}} \varepsilon \, D(\varepsilon) \, d\varepsilon + \frac{U}{4} n_\uparrow n_\downarrow$$

$$\tag{5.12}$$

$$= \int_{-W/2}^{(n-1+m)W/2} \frac{\varepsilon}{W} \, d\varepsilon + \int_{-W/2}^{(n-1-m)W/2} \frac{\varepsilon}{W} \, d\varepsilon + \frac{U}{4}(n + m)(n - m)$$

$$= \frac{W}{4}(n^2 - 2n + m^2) + \frac{U}{4}(n^2 - m^2)$$

Minimising the magnetisation-dependent part of the free energy

$$\Delta F(m) = (W - U)\frac{m^2}{4} \tag{5.13}$$

with respect to the magnetisation leads to:

$$m = \begin{cases} \pm m_{max} & \text{for} \quad W < U \\ 0 & \text{for} \quad W > U \end{cases} \tag{5.14}$$

This dependence of the magnetisation on the bandwidth W reflects the Stoner criterion discussed in section 3.6. For a DOS at the Fermi level $D(\varepsilon_F) = 1/W$, the paramagnetic state becomes unstable for $W < U$. For a rectangular band shape in the Stoner model, all magnetisation values between zero and maximum magnetisation are generally not stable.

Therefore, for the rectangular band and within the framework of Stoner theory, the magnetisation shows a first order phase transition from zero to maximum as a function of the bandwidth at $W = U$. To observe a continuous transition, a different band shape is needed in Stoner theory.

5.2 The Rectangular DOS and a Finite External Field

To include the interaction with an external magnetic field $\mathbf{B}_0 = (0,0,-B_0)$, the Hamiltonian (3.31) is modified by use of (4.3) yielding Hamiltonian (4.8). For a rectangular DOS (5.1) at $T = 0$, the calculations of section 5.1 can be straightforwardly adapted. The result for the magnetisation-dependent part of the free energy in an external magnetic field is then

$$\Delta F(m, B_0) = (W - U)\frac{m^2}{4} - \mu_B B_0\, m \tag{5.15}$$

In the paramagnetic case with $W > U$, the field dependence of the magnetisation is

$$m(B_0) = \frac{2\mu_B B_0}{W - U} \tag{5.16}$$

for field strengths $|B_0|$ lower than the saturation field strength

$$B_{0\,\text{max}} = \frac{W - U}{2\mu_B} m_{\text{max}} \tag{5.17}$$

with $m_{\text{max}} = \min\{n, 2 - n\}$ as the saturation magnetisation. For higher field strengths, the magnetisation is simply the saturation magnetisation. Therefore, the susceptibility in the paramagnetic case is zero for $|B_0| > B_{0\,\text{max}}$ and constant for field strengths $|B_0| < B_{0\,\text{max}}$:

$$\chi = \frac{2\mu_B^2}{W - U} = \frac{\chi_P}{1 - U/W} \tag{5.18}$$

The Coulomb interaction enhances the small field susceptibility by a factor $(1 - U/W)^{-1}$ compared to the Pauli susceptibility $\chi_P = 2\mu_B^2/W$ derived in the Pauli theory of spin paramagnetism, where electron-electron interactions are neglected [33].

In the ferromagnetic state for $W < U$, the magnetisation is maximal, i.e. $m = \pm m_{\text{max}} = \pm\min\{n, 2 - n\}$, and its absolute value does not depend on the external

magnetic field. Hence, the susceptibility vanishes for finite fields, as expected for a saturated magnet. The susceptibility is not definable for $B_0 = 0$.

5.3 Beyond a Rectangular DOS

For a density of states $D(\varepsilon)$ deviating from the coarse approximation of a rectangular shape, one has to start the calculation of the magnetisation dependence of the free energy F from Hamiltonian (3.31) again. Firstly, an external magnetic field is not considered. This will be included in the next section.

Of interest is only the change of the free energy ΔF caused by a non-zero magnetisation compared to the case of a zero magnetisation. Most definitions and calculations, for which the particular band shape is not important, can be taken over from the previous section, where they have been derived for a rectangular density of states. Using (3.33) and (5.6), the Coulomb part of Hamiltonian (3.31) can be expressed in a form, which is independent of the band shape:

$$U \, n_\uparrow \, n_\downarrow = \frac{U}{4} \left(n^2 - m^2 \right) \tag{5.19}$$

The Coulomb part is a function of the magnetisation m and the number of electrons n. Therefore, the change in the Coulomb part ΔU is simply:

$$\Delta U = -\frac{U}{4} \, m^2 \tag{5.20}$$

Now the change in the kinetic part ΔT has to be calculated for an arbitrary DOS. For zero temperature, the occupation numbers $n_\sigma(\varepsilon)$ are assumed to be

$$n_\sigma(\varepsilon) = \begin{cases} 1 & for \quad \varepsilon \leq \varepsilon_{F\sigma} \\ 0 & for \quad \varepsilon > \varepsilon_{F\sigma} \end{cases} \tag{5.21}$$

with $\varepsilon_{F\sigma}$ as the Fermi energy for spin σ derived from

$$n_\sigma = \int_{-\infty}^{\varepsilon_{F\sigma}} D(\varepsilon) \, d\varepsilon \tag{5.22}$$

similarly to the previous section. For convenience, the zero-point of the energy is chosen to coincide with the paramagnetic Fermi energy ε_F defined by:

$$n = \sum_{\sigma} \int_{-\infty}^{\varepsilon_F} D(\varepsilon)\, d\varepsilon \tag{5.23}$$

For the paramagnetic state, the Fermi energies $\varepsilon_{F\sigma}$ for both spin directions coincide with the paramagnetic Fermi energy $\varepsilon_F = 0$. A non-zero magnetisation causes the Fermi energy for the spin-up electrons $\varepsilon_{F\uparrow}$ to be raised from zero by $\Delta\uparrow$ and for the spin-down electrons $\varepsilon_{F\downarrow}$ to be lowered by $\Delta\downarrow$.
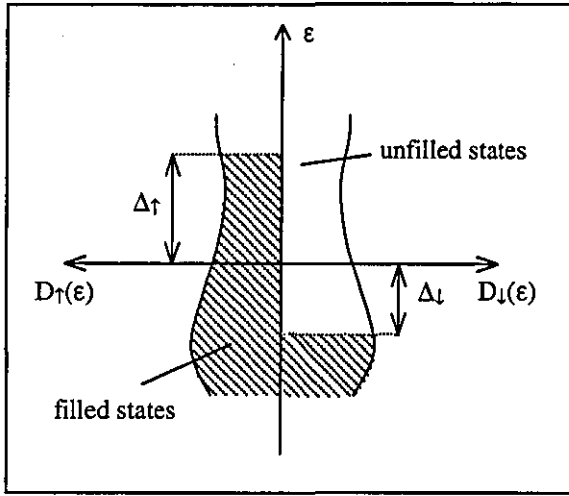

Fig. 5.2: The density of states $D_\uparrow(\varepsilon)$ for spin-up and $D_\downarrow(\varepsilon)$ for spin-down electrons and the filling of the states.

The unequal filling of the spin-up and the spin-down states band yields a shifting $\Delta\uparrow$ and $\Delta\downarrow$ of the energies of the highest filled up- and down-band states.

For an explicitly known band shape, one can perform the analysis by carrying out all the integrals involving the DOS. The conservation of the number of electrons, the magnetisation m and the change in the kinetic energy ΔT are then expressed by the integrals:

$$0 = \Delta n = \int_0^{\Delta\uparrow} D(\varepsilon)\, d\varepsilon + \int_0^{-\Delta\downarrow} D(\varepsilon)\, d\varepsilon \;\; = \int_0^{\Delta\uparrow} D(\varepsilon)\, d\varepsilon - \int_{-\Delta\downarrow}^{0} D(\varepsilon)\, d\varepsilon \tag{5.24}$$

$$m = \int_0^{\Delta\uparrow} D(\varepsilon)\, d\varepsilon - \int_0^{-\Delta\downarrow} D(\varepsilon)\, d\varepsilon = \int_{-\Delta\downarrow}^{\Delta\uparrow} D(\varepsilon)\, d\varepsilon = 2\int_0^{\Delta\uparrow} D(\varepsilon)\, d\varepsilon = 2\int_{-\Delta\downarrow}^{0} D(\varepsilon)\, d\varepsilon \tag{5.25}$$

$$\Delta T = \int_0^{\Delta\uparrow} \varepsilon\, D(\varepsilon)\, d\varepsilon + \int_0^{-\Delta\downarrow} \varepsilon\, D(\varepsilon)\, d\varepsilon = \int_0^{\Delta\uparrow} \varepsilon\, D(\varepsilon)\, d\varepsilon - \int_{-\Delta\downarrow}^{0} \varepsilon\, D(\varepsilon)\, d\varepsilon \tag{5.26}$$

Then a stability analysis of the free energy $F(m) = F(0) + \Delta T(m) + \Delta U(m)$ can be carried out by calculating the minima with respect to m. This yields the ground state value for m and possibly other metastable values for the magnetisation.

To get an expression for the stable values of m using the properties of the DOS at the Fermi level ε_F, a Taylor expansion of the DOS

$$D(\varepsilon) = \sum_{i=0}^{\infty} \frac{D_i}{i!} \varepsilon^i \qquad \text{with} \qquad D_i = \frac{\partial^i D(\varepsilon)}{\partial \varepsilon^i}\bigg|_{\varepsilon=0} \tag{5.27}$$

around $\varepsilon_F = 0$ can be applied to the integrals (5.24) to (5.26). For its validity, a smooth DOS $D(\varepsilon)$ is required in the range $-\Delta_\downarrow \leq \varepsilon \leq \Delta_\uparrow$. In practice, this is fulfilled by a regular DOS around the Fermi energy and a small magnetisation m. Application to the integral (5.26) yields a change in kinetic energy:

$$\Delta T = \int_0^{\Delta_\uparrow} \varepsilon\, D(\varepsilon)\, d\varepsilon + \int_0^{-\Delta_\downarrow} \varepsilon\, D(\varepsilon)\, d\varepsilon = \int_0^{\Delta_\uparrow} \sum_{i=0}^{\infty} \frac{D_i}{i!} \varepsilon^{i+1}\, d\varepsilon + \int_0^{-\Delta_\downarrow} \sum_{i=0}^{\infty} \frac{D_i}{i!} \varepsilon^{i+1}\, d\varepsilon$$

$$= \sum_{i=2}^{\infty} \frac{i-1}{i!} D_{i-2}\left((\Delta_\uparrow)^i + (-\Delta_\downarrow)^i \right) \tag{5.28}$$

In this formula, ΔT depends on the two energy shifts $\Delta_\uparrow$ and $\Delta_\downarrow$. These quantities are connected by the conservation law (5.24) and therefore can not be varied independently. Furthermore, the change in Coulomb energy has a simple form in terms of the magnetisation. Therefore, it seems appropriate to express $\Delta_\uparrow$ and $\Delta_\downarrow$ in terms of the magnetisation as well. Applying the Taylor expansion of the DOS to the integrals (5.25), one obtains

$$m = 2\int_0^{\Delta_\uparrow} D(\varepsilon)\, d\varepsilon = 2\int_0^{\Delta_\uparrow} \sum_{i=0}^{\infty} \frac{D_i}{i!} \varepsilon^i\, d\varepsilon = \sum_{i=1}^{\infty} 2 D_{i-1} \frac{\Delta_\uparrow^{\,i}}{i!} \tag{5.29}$$

by using the expression including only $\Delta_\uparrow$, and similarly

$$m = -2\int_{-\Delta_\downarrow}^0 D(\varepsilon)\, d\varepsilon = \sum_{i=1}^{\infty} (-1)^{i-1} 2 D_{i-1} \frac{\Delta_\downarrow^{\,i}}{i!} \tag{5.30}$$

for $\Delta_\downarrow$. These series can be inverted by application of the reversion of a power series [38]

$$y(x) = \sum_{i=0}^{\infty} a_i (x - x_0)^i \quad \Rightarrow$$

$$x(y) = x_0 + \frac{y - a_0}{a_1} - \frac{a_2(y - a_0)^2}{a_1^3} + \frac{(2a_2^2 - a_1 a_3)(y - a_0)^3}{a_1^5} + \dots \tag{5.31}$$

giving the expansion of $\Delta_\uparrow$ and $\Delta_\downarrow$ in terms of m:

$$\Delta_\uparrow = \frac{m}{2D_0} - \frac{D_1 m^2}{8D_0^3} + \frac{3D_1^2 - D_0 D_2}{48D_0^5} m^3 - \frac{15D_1^3 - 10D_0 D_1 D_2 + D_0^2 D_3}{384 D_0^7} m^4 + \dots$$

$$\Delta_\downarrow = \frac{m}{2D_0} + \frac{D_1 m^2}{8D_0^3} + \frac{3D_1^2 - D_0 D_2}{48D_0^5} m^3 + \frac{15D_1^3 - 10D_0 D_1 D_2 + D_0^2 D_3}{384 D_0^7} m^4 + \dots \tag{5.32}$$

Substituting these into expansion (5.28) of the change in the kinetic energy in terms of $\Delta_\uparrow$ and $\Delta_\downarrow$ yields the expansion

$$\Delta T(m) = \frac{1}{4D_0} m^2 + \frac{3D_1^2 - D_0 D_2}{192 D_0^5} m^4$$

$$+ \frac{105 D_0^4 - 105 D_0 D_1^2 D_2 + 10 D_0^2 D_2^2 + 15 D_0^2 D_1 D_3 - D_0^3 D_4}{23040 D_0^9} m^6 + o(m^8) \tag{5.33}$$

up to 6th order in m. It should be clear that, due to the symmetry between spin-up and spin-down, only even powers in m appear in the expansion. This procedure can be performed up to any order in m. Of course the effort in obtaining higher order coefficients in the expansion increases enormously with the order of the expansion.

The resulting Landau-type free energy with the magnetisation m as the order parameter is:

$$F(m) = F(0) + \Delta T + \Delta U - \mu_B B_0 m$$

$$= F(0) - \mu_B B_0 m + \frac{\alpha_2}{2} m^2 + \frac{\alpha_4}{4} m^4 + \frac{\alpha_6}{6} m^6 + o(m^8) \tag{5.34}$$

with:

$$\alpha_2 = \frac{1 - UD_0}{2D_0}$$

$$\alpha_4 = \frac{3D_1^2 - D_0 D_2}{48 D_0^5} \tag{5.35}$$

$$\alpha_6 = \frac{105 D_0^4 - 105 D_0 D_1^2 D_2 + 10 D_0^2 D_2^2 + 15 D_0^2 D_1 D_3 - D_0^3 D_4}{3840 D_0^9}$$

Keeping in mind that $D_0 = D(\varepsilon_F)$, this again reflects the Stoner criterion. For $D_0 U < 1$, the free energy F has a local minimum for $m = 0$ and hence, the paramagnetic state is locally stable. For $D_0 U > 1$, the point $m = 0$ becomes a maximum of F, so the paramagnetic state is unstable and the free energy has its minimal value at a finite magnetisation. For a rectangular band, all derivatives of the DOS $D(\varepsilon)$ and thus all D_i for $i \geq 1$ vanish and equation (5.34) simplifies to equation (5.13) with $1/D(\varepsilon_F) = W$.

5.4 Beyond a Rectangular DOS: A Finite External Field

For deviations from a rectangular DOS, the Hamiltonian (3.31) is modified to (4.8) by use of (4.3) to include the interaction with an external magnetic field $\mathbf{B}_0 = (0,0,-B_0)$. Calculations similar to section 5.3 yield the magnetisation dependent part of the free energy

$$F(m, B_0) = F(0,0) - \mu_B B_0 m + \sum_{i=1}^{\infty} \frac{\alpha_{2i}}{2i} m^{2i} \tag{5.36}$$

with coefficients α_2, α_4 and α_6 defined by (5.35). The formula (5.36) is valid for a smooth DOS around the Fermi level and a small magnetisation. The magnetisation m is defined by:

$$0 = \left(\frac{\partial F}{\partial m}\right)_{B_0} = \sum_{i=1}^{\infty} \alpha_{2i} \, m^{2i-1} - \mu_B B_0 \qquad \text{and} \qquad \left(\frac{\partial^2 F}{\partial m^2}\right)_{B_0} < 0 \tag{5.37}$$

For the paramagnetic state, this yields a field dependence of the magnetisation for small fields:

$$m(B_0) = \sum_{i=0}^{\infty} \beta_{2i+1} \left(\mu_B B_0\right)^{2i+1} \tag{5.38}$$

The first coefficients of (5.38) are:

$$\beta_1 = \frac{1}{\alpha_2} = \frac{2D_0}{1-UD_0}$$

$$\beta_3 = -\frac{\alpha_4}{\alpha_2^4} = \frac{-3D_1^2 + D_0 D_2}{3D_0(1-UD_0)^4}$$

$$\beta_5 = \frac{3\alpha_4^2 - \alpha_2\alpha_6}{\alpha_2^7}$$

$$= \frac{\left(3D_1^2 - D_0 D_2\right)^2}{6D_0^3(1-UD_0)^7} + \frac{-105D_1^4 + 105D_0 D_1^2 D_2 - 10D_0^2 D_2^2 - 15D_0^2 D_1 D_3 + D_0^3 D_4}{60D_0^3(1-UD_0)^6}$$

(5.39)

The paramagnetic susceptibility $\chi(B_0)$ can be obtained for $B_0 = 0$ by differentiation of (5.38) or from (5.37) by means of the Implicit Function Theorem:

$$\chi(B_0 = 0) = \frac{2\mu_B^2 D_0}{1-UD_0} = \frac{\chi_P}{1-UD_0}$$

(5.40)

The paramagnetic susceptibility is again enhanced by a factor $\left(1 - UD(\varepsilon_F)\right)^{-1}$ compared to the Pauli susceptibility $\chi_P = 2\mu_B^2 D(\varepsilon_F)$. As $UD(\varepsilon_F)$ approaches unity, the susceptibility goes to infinity, indicating an instability of the paramagnetic state for $UD(\varepsilon_F) > 1$. The result (5.40) agrees with (5.18) for a rectangular band shape. In this model, the zero-field paramagnetic susceptibility depends only on the on-site repulsion U and the density of states at the Fermi level $D(\varepsilon_F)$. Contrary to the case of a rectangular DOS, the susceptibility $\chi(B_0)$ may vary with the external field and even show singularities at points of field-induced discontinuous changes of magnetisation.

For the ferromagnetic case, the situation is more complicated. For the fully ferromagnetic state, where the magnetisation is maximal and field independent, the susceptibility vanishes. In the case of weak ferromagnetism, where the zero-field magnetisation is small, one can neglect higher order coefficients in (5.38) and use a Landau free energy description to derive the magnetisation and susceptibility. However, in the case of strong ferromagnetism, where the magnetisation may be large, the equations derived here by using a power expansion are not applicable in general. Too many coefficients in the power expansions may be needed to obtain reliable results from the calculations. Moreover, the equations derived here by using a power expansion may suffer from any problems associated with power expansions in general. They might not converge outside a certain region of parameters or if, then not to the same value as the function.

6 The Stoner Model at Finite Temperatures

6.1 The Mean Field Approximation

To study the properties of a system characterised by the Hartree-Fock Hamiltonian (3.26) at finite temperatures T, one has to use the methods of statistical physics. The interaction terms $n_{\mathbf{k}\sigma} n_{\mathbf{k'}-\sigma}$ in the Hamiltonian (3.26) make the statistical treatment difficult, since they cause the one-particle energies to depend on the occupation numbers. Here a mean field approach is used. In the mean field approximation (MFA), the product of two operators A and B is approximated by

$$
\begin{aligned}
AB &= \left(A - \langle A\rangle\right)\left(B - \langle B\rangle\right) + A\langle B\rangle + \langle A\rangle B - \langle A\rangle\langle B\rangle \\
&\overset{MFA}{\Rightarrow} A\langle B\rangle + \langle A\rangle B - \langle A\rangle\langle B\rangle
\end{aligned}
\tag{6.1}
$$

by neglecting the product of the fluctuations $\left(A - \langle A\rangle\right)\left(B - \langle B\rangle\right)$ [33].

Here, the form (4.6) with the effective one-particle energies (4.7) including the interaction with an external magnetic field $\mathbf{B}_0 = (0,0,-B_0)$ is used as a starting point for the MFA. The electron-electron interaction term $n_\uparrow n_\downarrow$ is approximated by $n_\uparrow\langle n_\downarrow\rangle + \langle n_\uparrow\rangle n_\downarrow - \langle n_\uparrow\rangle\langle n_\downarrow\rangle$. This yields the mean field Hamiltonian

$$
H = \sum_{\mathbf{k}} H_\sigma - \frac{U}{N}\langle n_\uparrow\rangle\langle n_\downarrow\rangle
\tag{6.2}
$$

with

$$
H_\sigma = \sum_{\mathbf{k}} \bar{\varepsilon}_{\mathbf{k}\sigma}\, n_{\mathbf{k}\sigma}
\tag{6.3}
$$

and the effective one-electron energies

$$
\bar{\varepsilon}_{\mathbf{k}\sigma} = \varepsilon(\mathbf{k}) + \frac{U}{N}\langle n_{-\sigma}\rangle - \mu_B B_0\bar{\sigma}
\tag{6.4}
$$

with $\bar{\sigma}$ defined in (4.2) in section 4. Next, each Hamiltonian H_σ is considered separately. This is done by regarding $\langle n_{-\sigma}\rangle$ in H_σ as an external parameter, which has to be calculated in a self-consistent manner. The resulting Hamiltonian (6.3) represents a

Hamiltonian for non-interacting electrons with one-electron energies (6.4). Hence, the expectation values of the occupation numbers $n_{\mathbf{k}\,\sigma}$

$$\left\langle n_{\mathbf{k}\,\sigma}\right\rangle = f(\bar{\varepsilon}_{\mathbf{k}\,\sigma},\mu_\sigma,\beta) \tag{6.5}$$

are given by the Fermi distribution

$$f(\varepsilon,\mu,\beta) = \frac{1}{e^{\beta(\varepsilon-\mu)}+1} \tag{6.6}$$

where $\beta = 1/k_B T$ with the Boltzmann constant k_B and the temperature T. The chemical potential μ_σ is determined by the expectation value of the spin-σ electron number:

$$\left\langle n_\sigma\right\rangle = \sum_{\mathbf{k}}\left\langle n_{\mathbf{k}\,\sigma}\right\rangle = \sum_{\mathbf{k}} f(\bar{\varepsilon}_{\mathbf{k}\,\sigma},\mu_\sigma,\beta) \tag{6.7}$$

With the internal energy

$$\left\langle H_\sigma\right\rangle = \sum_{\mathbf{k}} \bar{\varepsilon}_{\mathbf{k}\,\sigma} f(\bar{\varepsilon}_{\mathbf{k}\,\sigma},\mu_\sigma,\beta) \tag{6.8}$$

as the expectation value of the Hamiltonian H_σ and the entropy

$$\begin{aligned}
S_\sigma &= -k_B \sum_{\mathbf{k}}\left(\left\langle n_{\mathbf{k}\,\sigma}\right\rangle \ln\left\langle n_{\mathbf{k}\,\sigma}\right\rangle + (1-\left\langle n_{\mathbf{k}\,\sigma}\right\rangle)\ln(1-\left\langle n_{\mathbf{k}\,\sigma}\right\rangle)\right) \\
&= -k_B \sum_{\mathbf{k}}\left(f(\bar{\varepsilon}_{\mathbf{k}\,\sigma},\mu_\sigma,\beta)\ln f(\bar{\varepsilon}_{\mathbf{k}\,\sigma},\mu_\sigma,\beta)\right. \\
&\qquad \left. + (1-f(\bar{\varepsilon}_{\mathbf{k}\,\sigma},\mu_\sigma,\beta))\ln(1-f(\bar{\varepsilon}_{\mathbf{k}\,\sigma},\mu_\sigma,\beta))\right)
\end{aligned} \tag{6.9}$$

one can calculate the free energy of the spin-σ electrons

$$F_\sigma = F_\sigma(T,B_0,\left\langle n_\sigma\right\rangle,\left\langle n_{-\sigma}\right\rangle) = \left\langle H_\sigma\right\rangle - T\,S_\sigma \tag{6.10}$$

with the temperature, the magnetic field and the number of electrons for each spin as parameters. The whole free energy of the system is then:

$$\begin{aligned}
F &= \sum_\sigma F_\sigma(T,B_0,\left\langle n_\sigma\right\rangle,\left\langle n_{-\sigma}\right\rangle) - \frac{U}{N}\left\langle n_\uparrow\right\rangle\left\langle n_\downarrow\right\rangle \\
&= \sum_{\mathbf{k}\,\sigma}\left(\bar{\varepsilon}_{\mathbf{k}\,\sigma} f(\bar{\varepsilon}_{\mathbf{k}\,\sigma},\mu_\sigma,\beta) + k_B T\,f(\bar{\varepsilon}_{\mathbf{k}\,\sigma},\mu_\sigma,\beta)\ln f(\bar{\varepsilon}_{\mathbf{k}\,\sigma},\mu_\sigma,\beta)\right. \\
&\qquad \left. + k_B T\,(1-f(\bar{\varepsilon}_{\mathbf{k}\,\sigma},\mu_\sigma,\beta))\ln(1-f(\bar{\varepsilon}_{\mathbf{k}\,\sigma},\mu_\sigma,\beta))\right) - \frac{U}{N}\left\langle n_\uparrow\right\rangle\left\langle n_\downarrow\right\rangle
\end{aligned} \tag{6.11}$$

With the expectation value of the magnetisation

$$\langle m \rangle = \langle n_\uparrow \rangle - \langle n_\downarrow \rangle \tag{6.12}$$

and the total number of electrons

$$\langle n \rangle = \langle n_\uparrow \rangle + \langle n_\downarrow \rangle \tag{6.13}$$

one obtains:

$$\langle n_\sigma \rangle = \frac{1}{2}\left(\langle n \rangle + \overline{\sigma}\langle m \rangle \right) \tag{6.14}$$

Using the special properties of the Fermi function, the expectation values for the $n_{\mathbf{k}\,\sigma}$ can be expressed as

$$\langle n_{\mathbf{k}\,\sigma} \rangle = f(\overline{\varepsilon}_{\mathbf{k}\,\sigma}, \mu_\sigma, \beta) = f(\varepsilon_{\mathbf{k}}, \overline{\mu}_\sigma, \beta) \tag{6.15}$$

with a new chemical potential $\overline{\mu}_\sigma$ determined by:

$$\frac{1}{2}\left(\langle n \rangle + \sigma\langle m \rangle \right) = \langle n_\sigma \rangle = \sum_{\mathbf{k}} \langle n_{\mathbf{k}\,\sigma} \rangle = \sum_{\mathbf{k}} f(\varepsilon_{\mathbf{k}}, \overline{\mu}_\sigma, \beta) \tag{6.16}$$

This can be solved, at least in principle, for $\overline{\mu}_\sigma = \overline{\mu}_\sigma(T, \langle n \rangle, \langle m \rangle)$. Using (6.14) and (6.15), the free energy can then be written as:

$$\begin{aligned}
F = {} & \frac{U}{4N}\left(\langle n \rangle^2 - \langle m \rangle^2 \right) - \mu_B\, B_0 \langle m \rangle \\
& + \sum_{\mathbf{k}\,\sigma} \Big[\, \varepsilon_{\mathbf{k}}\, f(\varepsilon_{\mathbf{k}}, \overline{\mu}_\sigma, \beta) + k_B T\, f(\varepsilon_{\mathbf{k}}, \overline{\mu}_\sigma, \beta)\, \ln f(\varepsilon_{\mathbf{k}}, \overline{\mu}_\sigma, \beta) \\
& \qquad\quad + k_B T \left(1 - f(\varepsilon_{\mathbf{k}}, \overline{\mu}_\sigma, \beta) \right) \ln\left(1 - f(\varepsilon_{\mathbf{k}}, \overline{\mu}_\sigma, \beta) \right) \Big]
\end{aligned} \tag{6.17}$$

This form allows a clear physical interpretation. The first term contains the electron-electron interaction and the second term the interaction with the external field. The remaining sum is the sum of the two free energies

$$\begin{aligned}
\overline{F}_\sigma = {} & \sum_{\mathbf{k}} \Big[\, \varepsilon_{\mathbf{k}}\, f(\varepsilon_{\mathbf{k}}, \overline{\mu}_\sigma, \beta) + k_B T\, f(\varepsilon_{\mathbf{k}}, \overline{\mu}_\sigma, \beta)\, \ln f(\varepsilon_{\mathbf{k}}, \overline{\mu}_\sigma, \beta) \\
& \qquad + k_B T \left(1 - f(\varepsilon_{\mathbf{k}}, \overline{\mu}_\sigma, \beta) \right) \ln\left(1 - f(\varepsilon_{\mathbf{k}}, \overline{\mu}_\sigma, \beta) \right) \Big]
\end{aligned} \tag{6.18}$$

of non-interacting spin-σ electrons with chemical potential $\overline{\mu}_\sigma$. In these reduced free energies $\overline{F}_\sigma$, the first part of the sum represents the internal energy of non-interacting spin-σ electrons $\langle \overline{H}_\sigma \rangle$ and the last two terms contain their entropy $\overline{S}_\sigma$ and the temperature.

Within the continuum approximation with the density of states $D_\sigma(\varepsilon) = D(\varepsilon)$ of the distribution of the states $|\mathbf{k}\,\sigma\rangle$ over the energy ε, the free energy takes the form:

$$F = \frac{U}{4}\left(\langle n\rangle^2 - \langle m\rangle^2\right) - \mu_B\, B_0\langle m\rangle + \sum_\sigma \overline{F}_\sigma \tag{6.19}$$

with

$$\overline{F}_\sigma = \int\limits_{-\infty}^{\infty} D(\varepsilon)\Big[\, \varepsilon\, f(\varepsilon,\overline{\mu}_\sigma,\beta) + k_B T\, f(\varepsilon,\overline{\mu}_\sigma,\beta)\ln f(\varepsilon,\overline{\mu}_\sigma,\beta)$$
$$+ k_B T\left(1 - f(\varepsilon,\overline{\mu}_\sigma,\beta)\right)\ln\left(1 - f(\varepsilon,\overline{\mu}_\sigma,\beta)\right)\Big]\,d\varepsilon \tag{6.20}$$

Furthermore, the expectation of the number of spin-σ electrons takes the form:

$$\langle n_\sigma\rangle = \frac{1}{2}\left(\langle n\rangle + \overline{\sigma}\langle m\rangle\right) = \int\limits_{-\infty}^{\infty} D(\varepsilon)\, f(\varepsilon,\overline{\mu}_\sigma,\beta)\,d\varepsilon \tag{6.21}$$

The expectation value of the total number of electrons and the magnetisation are then:

$$\langle n\rangle = \sum_\sigma \langle n_\sigma\rangle = \sum_\sigma \int\limits_{-\infty}^{\infty} D(\varepsilon)\, f(\varepsilon,\overline{\mu}_\sigma,\beta)\,d\varepsilon \tag{6.22}$$

$$\langle m\rangle = \sum_\sigma \overline{\sigma}\langle n_\sigma\rangle = \sum_\sigma \overline{\sigma}\int\limits_{-\infty}^{\infty} D(\varepsilon)\, f(\varepsilon,\overline{\mu}_\sigma,\beta)\,d\varepsilon \tag{6.23}$$

Here, the DOS $D(\varepsilon)$, the expectation values $\langle n_\sigma\rangle$, $\langle n\rangle$ and $\langle m\rangle$ and the free energy F are normalised to be quantities per atom. The chemical potentials $\overline{\mu}_\sigma$ as a function of $\langle n\rangle$ and $\langle m\rangle$ is determined by (6.21).

After the mean field approximation is applied, operators, such as the total number of electrons, enter the equations of the model only as their expectation values. For brevity, the brackets $\langle\ \rangle$ around the symbols indicating averaging will be dropped from now on. The addition 'expectation value' will also be omitted for these quantities in the following treatment.

6.2 The Magnetisation and the Susceptibility

The magnetisation m is considered an internal degree of freedom of the system. Therefore, its actual value, which is adopted by the system in thermal equilibrium, minimises the

system free energy (6.17). At finite temperatures, the maximal possible magnetisation m_{max}, for which either $n_{k\uparrow} = 1$ or $n_{k\downarrow} = 0$ for all $\mathbf{k}$, does not minimise the free energy. A physical reason for this is the fact that thermal excitations always lead to an actual magnetisation lower than m_{max}. From the mathematical point of view, the derivative of the entropy part $- k_B T \sum_{\sigma} \bar{S}_{\sigma}$ of the free energy with respect to m goes to positive infinity as m approaches m_{max}. The same is true for a magnetisation $m = -m_{max}$. Since it can be assumed, that the free energy as a function of m is regular in the range $-m_{max} < m < m_{max}$, it follows that the free energy is minimal for a value of m within this range. Therefore, the actual value of the magnetisation m is determined by $(\partial F / \partial m)_{T,n,B} = 0$ and $(\partial^2 F / \partial m^2)_{T,n,B} > 0$. With (6.14), (6.18) and the thermodynamic relation between free energy, particle number and chemical potential, one obtains:

$$\left(\frac{\partial \bar{F}_{\sigma}}{\partial m} \right)_{T,B_0,n} = \left(\frac{\partial \bar{F}_{\sigma}}{\partial n_{\sigma}} \right)_{T,B_0,n} \left(\frac{\partial n_{\sigma}}{\partial m} \right)_{T,B_0,n} = \bar{\mu}_{\sigma} \frac{\sigma}{2} \tag{6.24}$$

as first condition for the magnetisation in the DOS approximation, this yields:

$$\begin{aligned} 0 = \left(\frac{\partial F}{\partial m} \right)_{T,B_0,n} &= \left(\frac{\partial}{\partial m} \left[\frac{U}{N} \left(n^2 - m^2 \right) - \mu_B B_0 m + \sum_{\sigma} \bar{F}_{\sigma} \right] \right)_{T,B_0,n} \\ &= -\frac{U}{2} m - \mu_B B_0 + \frac{\bar{\mu}_{\uparrow} - \bar{\mu}_{\downarrow}}{2} \end{aligned} \tag{6.25}$$

The second condition is:

$$\begin{aligned} 0 < \left(\frac{\partial^2 F}{\partial m^2} \right)_{T,B_0,n} &= -\frac{U}{2} + \frac{1}{2} \left(\frac{\partial \bar{\mu}_{\uparrow}}{\partial m} \right)_{T,B_0,n} - \frac{1}{2} \left(\frac{\partial \bar{\mu}_{\downarrow}}{\partial m} \right)_{T,B_0,n} \\ &= -\frac{U}{2} + \frac{1}{4} \left(\frac{\partial n_{\uparrow}}{\partial \bar{\mu}_{\uparrow}} \right)_{T,B_0,n}^{-1} + \frac{1}{4} \left(\frac{\partial n_{\downarrow}}{\partial \bar{\mu}_{\downarrow}} \right)_{T,B_0,n}^{-1} \end{aligned} \tag{6.26}$$

Using (4.17), one can calculate the susceptibility per atom:

$$\chi = \mu_B^2 \left(\frac{\partial^2 F}{\partial m^2} \right)_{T,B_0,n}^{-1} = \mu_B^2 \left(-\frac{U}{2} + \frac{1}{4} \left(\frac{\partial n_{\uparrow}}{\partial \bar{\mu}_{\uparrow}} \right)_{T,B_0,n}^{-1} + \frac{1}{4} \left(\frac{\partial n_{\downarrow}}{\partial \bar{\mu}_{\downarrow}} \right)_{T,B_0,n}^{-1} \right)^{-1} \tag{6.27}$$

Sometimes the band splitting Δ is used to characterise the magnetic state. It represents the shift of the reduced chemical potential of the spin-up electrons against the spin-down electrons due to an external magnetic field and the electron-electron interaction:

$$\Delta = \bar{\mu}_\uparrow - \bar{\mu}_\downarrow \tag{6.28}$$

In absence of an external field, $m = 0$ always satisfies the first condition due to symmetry between the spin-up and spin-down electrons. If the second condition is satisfied too, the paramagnetic state is stable. If for $m = 0$, the second condition is not satisfied, the stable state is ferromagnetic.

6.3 The Paramagnetic State

With setting $U = 0$, the Pauli theory of spin paramagnetism for non-interacting electrons is recovered [12,33] and therefore the Pauli susceptibility is:

$$\chi_P = \mu_B^2 \left(\frac{1}{4} \left(\frac{\partial n_\uparrow}{\partial \bar{\mu}_\uparrow} \right)^{-1}_{T,B_0,n} + \frac{1}{4} \left(\frac{\partial n_\downarrow}{\partial \bar{\mu}_\downarrow} \right)^{-1}_{T,B_0,n} \right)^{-1} \tag{6.29}$$

In the density-of-states approximation with a normalised DOS $D(\varepsilon)$, the Pauli susceptibility $\chi_P(B_0,T)$ for zero field can be calculated as [12]:

$$\chi_P(0,T) = -2\mu_B^2 \int_{-\infty}^{\infty} D(\varepsilon) \frac{\partial f(\varepsilon,\mu,T)}{\partial \varepsilon} d\varepsilon \tag{6.30}$$

with the DOS $D_\uparrow(\varepsilon) = D_\downarrow(\varepsilon) = D(\varepsilon)$ and the paramagnetic chemical potential μ determined by the electron number. For a smooth and slowly varying DOS in the range much larger than $k_B T$ around the Fermi energy ε_F, the Pauli susceptibility can be calculated by the usual expansion formula [12]

$$\chi_P(0,T) = \chi_P(0,0) \left[1 + \frac{\pi^2}{6} (k_B T)^2 \frac{D_1^2 - D_0 D_2}{D_0^2} + ... \right] \tag{6.31}$$

with the zero-temperature zero-field Pauli susceptibility

$$\chi_P(0,0) = 2\mu_B^2 D(\varepsilon_F) \tag{6.32}$$

and the D_i as the coefficients of a power expansion of $D(\varepsilon)$ around ε_F:

$$D_i = \left.\frac{\partial^i D(\varepsilon)}{\partial \varepsilon^i}\right|_{\varepsilon = \varepsilon_F} \tag{6.33}$$

The Pauli susceptibility can be used to express the susceptibility (6.27) as a function of the magnetisation as:

$$\chi(m,T) = \frac{\chi_P(m,T)}{1 - \frac{U}{2\mu_B^2}\chi_P(m,T)} \tag{6.34}$$

In the paramagnetic case, $B_0 = 0 \iff m = 0$ and therefore, the susceptibility $\chi(B_0,T)$ as a function of the external field can be written as:

$$\chi(0,T) = \frac{\chi_P(0,T)}{1 - \frac{U}{2\mu_B^2}\chi_P(0,T)} \tag{6.35}$$

According to (4.17), the susceptibility (6.35) has to be finite and positive for the paramagnetic state to be stable. Therefore:

$$1 > \frac{U}{2\mu_B^2}\chi_P(0,T) \tag{6.36}$$

This represents the Stoner criterion for finite temperatures. For $T = 0$, it reduces to the Stoner criterion discussed in section 3.6.

6.4 The Curie Temperature

If the temperature dependence of the Pauli susceptibility is known, this can be used to calculate the Curie temperature. Suppose, there is a temperature T_C, below which the paramagnetic state becomes unstable. Then above T_C, the susceptibility of the paramagnetic state (6.35) is positive, whereas below T_C, it becomes negative. With $\chi_P(0,T) > 0$ for all T, this implies a sign change of (6.35) at T_C in the denominator and therefore:

$$1 = \frac{U}{2\mu_B^2}\chi_P(0,T_C) = -U \int_{-\infty}^{\infty} D(\varepsilon)\frac{\partial f(\varepsilon,\mu,T_C)}{\partial \varepsilon} d\varepsilon \tag{6.37}$$

The paramagnetic susceptibility (6.35) is singular at $T = T_C$.

37

For a continuous transition from the paramagnetic to the ferromagnetic state, the temperature T_C can be straightforwardly identified with the Curie temperature. However, there may be a temperature range above T_C, where a ferromagnetic state is still stable. Then either the paramagnetic or the ferromagnetic state is metastable and the transition may be discontinuous and exhibit hysteresis.

6.5 Ferromagnetic States

If the paramagnetic state is unstable, then a state with finite magnetisation must be the ground state. In order to find the actual magnetisation, one has to solve the relations (6.25) and (6.26). If for $T = 0$, no magnetisation value m other than the maximum magnetisation m_{max} is stable, the equilibrium state for all magnetisation values is the saturated magnet [12]. Either the spin-up band is completely filled or the down band is empty. The density of states is zero for one of the $\overline{\mu}_\sigma$. The susceptibility vanishes, since the magnetisation does not depend on the external field. For $T \neq 0$, the magnetisation $m(T)$ for $B_0 = 0$ decreases slowly by spin reversals. There is an energy gap δ between the upper edge of the spin-up band and the unoccupied states of the spin-down band. Therefore, the decrease

of the magnetisation $\Delta m(T) := m(0) - m(T) \propto T^{3/2} \exp\left(-\dfrac{\delta}{k_B T}\right)$ for low temperatures [12].

If for $T = 0$, the stable value of the magnetisation is non-zero and smaller than the maximum magnetisation m_{max}, the equilibrium state for $B_0 = 0$ is an unsaturated magnet. The density of states $D(\overline{\mu}_\sigma) \neq 0$ for both $\overline{\mu}_\sigma$. The susceptibility is non-zero for field strengths B_0 smaller than the saturation field strength. If the magnetisation is very small, the state is called a weak ferromagnet. For $T \neq 0$, the magnetisation $m(T)$ decreases by the reversal of spins, but there is no gap for such excitations and therefore, $\Delta m(T) \propto T^2$ for low temperatures.

In both cases, the theory does not yield the Bloch law (2.3) for the low temperature magnetisation. This is clear, since in the Hartree-Fock approximation, only individual excitations are considered. Both cases show a phase transition to the paramagnetic state at a certain temperature T_C, since for very high temperatures, the entropy part of the free energy, which is minimised by $m = 0$, dominates the free energy. Above the Curie temperature T_C, the susceptibility is given by (6.35).

6.6 Other Magnetic States

In the framework of Stoner theory, further magnetic states can be explained. If, for example, the paramagnetic state is stable, but $\chi(m) < 0$ in a region $m_1 < m < m_2$ ($0 < m_1$), there is a discontinuous change of the magnetisation from a low-moment to a high-moment state driven by the external field [12]. This behaviour is called metamagnetism. One can use Maxwell's theorem (for the van der Waals theory of liquid-gas transition) to obtain the stable magnetic state.

If the system is paramagnetic at low temperatures and the zero-field susceptibility $\chi(T)$ shows a maximum when the temperature is increased, the paramagnetic state can become unstable for a temperature T with $T_S < T < T_C$, and a spontaneous magnetisation occurs in this temperature range.

The Stoner model can be extended to explain band antiferromagnetism. In the simplest case, this is done by introducing two identical sublattices. One sublattice is obtained from the other by translation and inversion of the spins. The magnetic moments of all sites of the first sublattice are equal and opposite to those of the second sublattice. This model can be further extended to more complicated commensurate and incommensurate magnetic structures [10,39].

All these behaviours have been observed for transition metals, their alloys and compounds. For example, Ni, Co, Ni_3Fe and CoFe are strong ferromagnets, Fe is an unsaturated ferromagnets, $ZrZn_2$, Sc_3In and YNi_3 are weak ferromagnets, $ThCo_5$ and $Co_{2-x}Se_x$ are metamagnets. Spontaneous thermal magnetisation can be observed for Y_2Ni_7 [12].

6.7 Spin Waves

For the low-temperature magnetisation in the ferromagnetic state, only individual excitations were considered, which have finite excitation energy [11]. An individual excitation

$$\left| \Psi_{\mathbf{k}\,\mathbf{q}} \right\rangle = a^{+}_{\mathbf{k}+\mathbf{q}\downarrow} a_{\mathbf{k}\uparrow} \left| \Psi_{fund} \right\rangle \tag{6.38}$$

out of the ground state $\left| \Psi_{fund} \right\rangle$, which lowers the magnetisation by one unit, has an excitation energy of approximately $U\!\left(n_\uparrow - n_\downarrow\right)$ for small q. These excitations are called Stoner excitations. Collective excitations, such as spin waves, should have an excitation energy proportional to $\mathbf{q}^2$, but these can not be described within this framework. The

simplest way to model collective excitations is to build up 'spin waves' by linear combinations of individual excitations. These are no true spin waves, because electron-hole excitations of the same spin are missing. Within a random phase approximation, one finds in addition to a pseudo-continuum of individual excitations, a collective excitation with energies proportional to $\mathbf{q}^2$ for small $\mathbf{q}$. Using Bose-Einstein statistics for these excitations, one finds again the Bloch law (2.3) for the low temperature magnetisation of a ferromagnetic system. In the same manner, one can introduce spin-wave excitations for a non-magnetic state in a finite external field.

6.8   The Discussion of the Stoner Model

The Hartree-Fock-Stoner theory has been widely used for explaining the properties of ferromagnetic metals and alloys. With the intra-atomic interactions, the magnetic properties depend only on the shape of the density of states.

The theory provides an explanation of the non-integral values of the saturation magnetisation in Bohr magnetons. In particular, experimental findings of magnetic properties at zero temperatures, such as the Slater-Pauling curve, are well explained by this model [11]. The saturation magnetisation m_{sat} of strongly ferromagnetic metals and alloys for zero-temperatures is explained by the dependence of $m_{\max}$ on the band filling n.

The model also explains why the susceptibility may be different from the Curie-Weiss susceptibility (2.2). There is no a priori reason for the susceptibility given by (6.35) should be proportional to $(T - T_C)^{-1}$ for high temperatures. If this is the case, then it is not surprising that the Curie constant does not lead to half-integer values of the magnetisation in Bohr magnetons. Furthermore, the Stoner model may explain why the magnetic entropy is different from what is expected by a Heisenberg model. Finally, the Stoner model is in accordance with all the experiments, which show the existence of d-bands.

The details of the finite temperature magnetic properties of real materials are not well explained by the Stoner model. Especially, the Curie temperatures for ferromagnetic materials calculated with the Stoner model are too high by a factor five to ten compared to the experimental values [13]. The Stoner model can not explain the quite good agreement of the susceptibilities of most transition metals and alloys with the Curie-Weiss law. In addition, the Stoner model has difficulties to explain weak ferromagnetism [37].

The breakdown of the Stoner theory is believed due to the neglect of electron-electron correlations in the Hartree-Fock and the mean field approximation [13]. Furthermore, no collective excitations, which have energies much smaller than individual excitations, are considered in the model. Therefore, the calculated low-temperature magnetisation does not lead to the observed Bloch law (2.3), and the calculated Curie temperature for ferromagnetic materials is much too high [13].

In conclusion, the Stoner model gives a qualitatively satisfactory explanation of many properties of transition metals and alloys. For a deeper understanding of their properties, the electron-electron interactions have to be treated in a more sophisticated manner.

7 The Rectangular Band at Finite Temperatures

In this chapter, the mean field approximation will be used to study the finite temperature properties of the Stoner model for a rectangular density of states. A rectangular DOS has the advantage that a large part of the calculations can be carried out analytically. However, in the further studies, it will not be possible to refrain completely from numerical methods.

7.1 The Free Energy of the Rectangular Band

As mentioned above, many expressions for the case of a rectangular density of states can be derived analytically. However, these expressions are rather complicated and therefore, the assistance of mathematical software [38] has been enlisted for the calculations. With the rectangular DOS

$$
D(\varepsilon) = \begin{cases} 1/W & for \quad -W/2 \le \varepsilon \le W/2 \\ 0 & otherwise \end{cases}
\tag{7.1}
$$

and equations (6.19) to (6.23) of the mean field approximation, one obtains the following expressions for the free energy, the electron numbers and the magnetisation:

$$
F = \frac{U}{4}\left(n^2 - m^2\right) - \mu_B B_0 m + \sum_\sigma \overline{F}_\sigma
\tag{7.2}
$$

$$
\overline{F}_\sigma = \int_{-W/2}^{W/2} \frac{1}{W}\Big[\, \varepsilon \, f(\varepsilon,\overline{\mu}_\sigma,\beta) + k_B T \, f(\varepsilon,\overline{\mu}_\sigma,\beta) \ln f(\varepsilon,\overline{\mu}_\sigma,\beta) \\ + k_B T \left(1 - f(\varepsilon,\overline{\mu}_\sigma,\beta)\right)\ln\left(1 - f(\varepsilon,\overline{\mu}_\sigma,\beta)\right) \Big]\, d\varepsilon
\tag{7.3}
$$

$$
n_\sigma = \frac{1}{2}\left(n + \overline{\sigma}\, m\right) = \int_{-W/2}^{W} \frac{1}{W} f(\varepsilon,\overline{\mu}_\sigma,\beta)\, d\varepsilon
\tag{7.4}
$$

$$
n = \sum_\sigma n_\sigma = \sum_\sigma \int_{-W/2}^{W/2} \frac{1}{W} f(\varepsilon,\overline{\mu}_\sigma,\beta)\, d\varepsilon
\tag{7.5}
$$

$$
m = \sum_\sigma \overline{\sigma}\, n_\sigma = \sum_\sigma \overline{\sigma} \int_{-W/2}^{W} \frac{1}{W} f(\varepsilon,\overline{\mu}_\sigma,\beta)\, d\varepsilon
\tag{7.6}
$$

The DOS $D(\varepsilon)$, the electron numbers n_σ and n, the magnetisation m and the free energy F are expressed in units per atom here.

These equations have to be used to find the value of the magnetisation, which minimises the free energy for a given set of parameters. Parameters of the system are the on-site repulsion U, the bandwidth W, the total number of electrons n in the band, the external magnetic field B_0 and the temperature T. The magnetisation m can vary between $-m_{\text{max}}$ and $+m_{\text{max}}$, where

$$m_{\text{max}} = \min\{n, 2-n\} \tag{7.7}$$

is the maximal possible magnetisation, which is determined by the total number of electrons and electronic states in the band.

Solving (7.4) for the reduced chemical potentials $\bar{\mu}_\sigma$ yields:

$$\bar{\mu}_\sigma = k_B T \ln\left[\operatorname{csch}\left[\frac{W(2-n-\bar{\sigma}m)}{k_B T} \right] \sinh\left[\frac{W(n+\bar{\sigma}m)}{k_B T} \right] \right] \tag{7.8}$$

Here, $\operatorname{csch}(x) = \sinh(x)^{-1}$ is the hyperbolic cosecant. With (6.25), the first condition for the stable magnetisation value is:

$$0 = \left(\frac{\partial F}{\partial m} \right)_{B_0, T, n}$$

$$= -\mu_B B_0 - \frac{U}{2} n + k_B T \sum_\sigma \frac{\bar{\sigma}}{2} \ln\left[\operatorname{csch}\left[\frac{W(2-n-\bar{\sigma}m)}{k_B T} \right] \sinh\left[\frac{W(n+\bar{\sigma}m)}{k_B T} \right] \right] \tag{7.9}$$

With (6.26), the second condition is:

$$0 < \left(\frac{\partial^2 F}{\partial m^2} \right)_{B_0, T, n} = -\frac{U}{2} + \frac{W}{8} \sum_\sigma \bar{\sigma}\left(\coth\left[\frac{W(n+\bar{\sigma}m)}{4 k_B T} \right] - \coth\left[\frac{W(n-2+\bar{\sigma}m)}{4 k_B T} \right] \right) \tag{7.10}$$

The right hand side of (7.10) has been derived by differentiating the right hand side of (7.9) with respect to m. From this equation, the formula for the susceptibility can be derived:

$$\chi = 2\mu_B^2 \left(-U + \frac{W}{4} \sum_\sigma \bar{\sigma}\left(\coth\left[\frac{W(n+\bar{\sigma}m)}{4 k_B T} \right] - \coth\left[\frac{W(n-2+\bar{\sigma}m)}{4 k_B T} \right] \right) \right)^{-1} \tag{7.11}$$

The equations for finite temperatures are inappropriate for studying the system at zero temperature. The correct limiting process $T \to 0$ for these equations yields the equations

43

for the rectangular band at zero temperature given in chapter 5. The results found there can be integrated into the discussion here, where it is necessary.

7.2 General Properties of the Derivative of the Free Energy

The extrema of the free energy are the roots of equation (7.9). The roots corresponding to minima of the free energy represent a stable or metastable magnetic state of the system. The magnetisation enters equation (7.9) in an essentially non-algebraic way. A short discussion of the properties of $(\partial F/\partial m)_{T,B,n}$ as a function of m helps to find its roots of equation (7.9) and determine whether they represent a maximum or a minimum of the free energy. The free energy (7.2) is an analytical function of m in the range $-m_{max} < m < m_{max}$ and so are its derivatives. In the absence of an external magnetic field, $(\partial F/\partial m)_{T,B,n}$ is an odd function and therefore, $m = 0$ is a root of (7.9). Moreover, if $m = m_0$ is a root then $m = -m_0$ is also a root. From

$$\lim_{m \to \pm m_{max}} \left(\frac{\partial F}{\partial m}\right)_{B_0,T,n} = \pm\infty \tag{7.12}$$

it follows that the greatest and the smallest of the roots of (7.9) represent a maximum of the free energy and therefore, are stable magnetisation values.
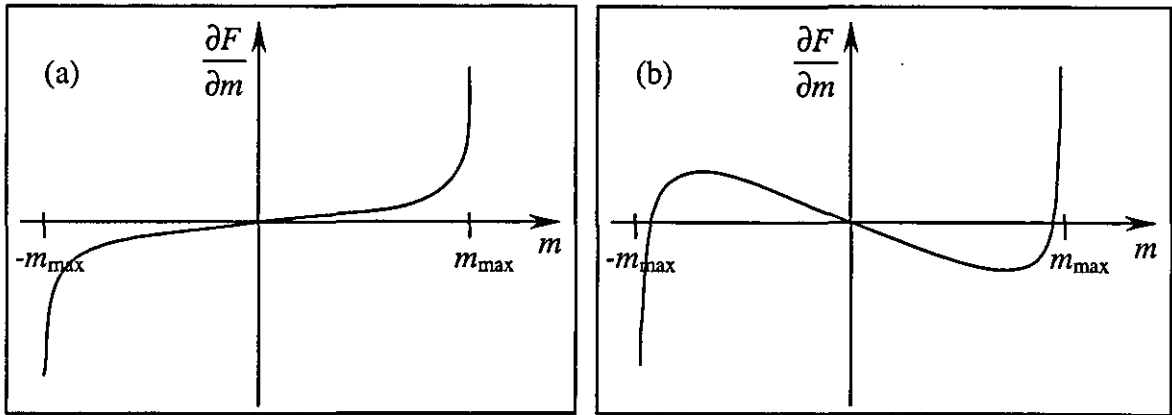
Fig. 7.1: Sketch of the derivative of the free energy for a rectangular DOS.

(a) The derivative has one root representing a minimum of the free energy. The system is paramagnetic.

(b) The derivative has three roots, of which the smallest and the largest represent minima of the free energy. The system is ferromagnetic.

The numerical investigation of (7.9) shows, that there are only two qualitatively different cases. In the first case, the equation (7.9) has only one root, which is then a minimum of

the free energy. For $B_0 = 0$, the root is $m = 0$. When B_0 is increased (decreased), the root is shifted continuously from zero to positive (negative) values. The system is paramagnetic.

In the second case, the equation (7.9) has three roots. For vanishing external field, one root is $m = 0$, which is a maximum of the free energy and represents an unstable paramagnetic state. The other two are $m = +m_0$ and $m = -m_0$ with $0 < m_0 < m_{max}$. These are the two, for $B_0 = 0$ degenerate minima of the free energy, which represent two ferromagnetic states with equal absolute magnetisation but opposite orientation. For a finite external field $B_0 > 0$, the degeneracy between the two ferromagnetic states is lifted. The three roots are shifted from the position for $B_0 = 0$. Since the magnetisation corresponding to the smallest root is unstable with respect to a rotation of the magnetisation direction, only the largest root represents a stable state.

Whether the system is paramagnetic or ferromagnetic depends on the system parameters. In general, the system is ferromagnetic for small bandwidth W and temperature T, large on-site Coulomb interaction U and an electron number n close to half-filling of the band. Conversely, the system is paramagnetic for an almost empty or filled band with large W and T, small U.

7.3 The Magnetisation

In the following, the consideration is restricted to a non-negative magnetisation, because of the symmetry of the system with respect to a simultaneous change of the direction of magnetisation and external field. Furthermore, only band fillings $n \leq 1$ are considered, since a band filling $n = n_1$ leads to the same results as a filling $n = 2 - n_1$ because of the symmetry between electrons and holes. If not mentioned explicitly, an external magnetic field is not considered. Furthermore, the model is invariant under a scale transformation of the energy. This implies that only the ratios between the parameters of the model, which are of dimension of energy, are of importance.

Firstly, the temperature-dependence of the magnetisation value $m(T)$ is studied in the absence of an external magnetic field. The behaviour of $m(T)$ is shown diagrammatically in Fig. 7.2.
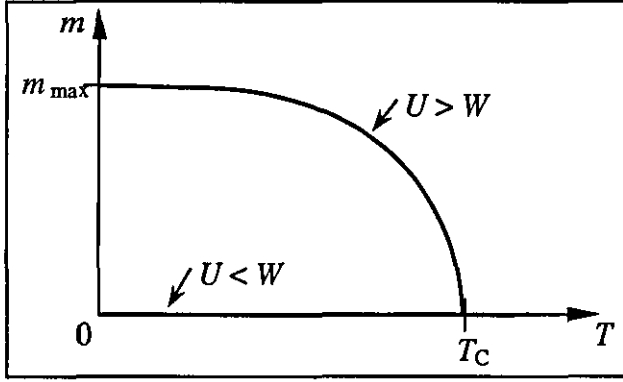
Fig. 7.2: The magnetisation m vs. temperature T in absence of an external field (schematic). For $U < W$, the system is paramagnetic at all temperatures. For $U > W$, the system is ferromagnetic for temperatures $T < T_C$ and paramagnetic for larger temperatures.

Two qualitatively different situations can be observed. For $U < W$, the system is paramagnetic at all temperatures:

$$m(T) = 0 \quad \forall\, T \quad for \quad U < W \tag{7.13}$$

For $U > W$, the system is ferromagnetic at low temperatures. The magnetisation decreases steadily from m_{max} at $T = 0$ with increasing temperature until the magnetisation vanishes at the Curie temperature T_C. Above T_C, the system is paramagnetic:

$$m(T) = \begin{cases} m_{max} & T = 0 \\ 0 < m(T) < m_{max} & for \quad 0 < T < T_c \quad for \quad U > W \\ 0 & T \geq T_c \end{cases} \tag{7.14}$$

Since the system is fully ferromagnetic at zero temperatures, there is an energy gap for excitations from the ground state. To change the magnetisation from $m = m_{max}$ at zero temperature by a small δm, the energy

$$\delta E \approx \left(\frac{\partial F}{\partial m}\right)_{B_0,T,n}\Bigg|_{T=0,m=m_{max}} \delta m \quad = \frac{W-U}{2}m_{max}\delta m \tag{7.15}$$

is needed. Hence, for an elementary magnetic excitation, where an electron changes from the majority to the minority spin band, a finite amount of energy $\delta \propto \dfrac{W-U}{2}m_{max}$ is needed. Therefore, the decrease of the magnetisation as a function of temperature $\Delta m(T)$

is proportional to $T^{3/2} \exp\left(\dfrac{U-W}{k_B T}m_{max}\right)$ for very low temperatures.

For temperatures close to the Curie temperature, the magnetisation is small. The free energy can be expanded in terms of m around $m = 0$:

$$F(m) = F_0 + \frac{\alpha_2}{2} m^2 + \frac{\alpha_4}{4} m^4 + o(m^6) \tag{7.16}$$

The coefficients are:

$$\alpha_2 = \left(\frac{\partial^2 F}{\partial m^2}\right)_{B_0,T,n}\Bigg|_{m=0} = -\frac{U}{2} + \frac{W}{4}\left(\coth\left[\frac{nW}{4k_BT}\right] + \coth\left[\frac{(2-n)W}{4k_BT}\right]\right) \tag{7.17}$$

$$\begin{aligned}
\alpha_4 &= \frac{1}{6}\left(\frac{\partial^4 F}{\partial m^4}\right)_{B_0,T,n}\Bigg|_{m=0} \\
&= \frac{W^3}{192(k_BT)^2}\left(\coth\left[\frac{nW}{4k_BT}\right]\operatorname{csch}\left[\frac{nW}{4k_BT}\right]^2 + \coth\left[\frac{(2-n)W}{4k_BT}\right]\operatorname{csch}\left[\frac{(2-n)W}{4k_BT}\right]^2\right)
\end{aligned} \tag{7.18}$$

The coefficient α_2 changes sign at the Curie temperature. The coefficient α_4 is positive for all $T > 0$. Hence, the transition at T_C is continuous, but $\lim\limits_{T\to T_C^-}\left(\dfrac{\partial m}{\partial T}\right) = -\infty$.

The decrease of the magnetisation with temperature and the Curie temperature depend on U, W and, via m_{max}, on n.

In Fig. 7.3, the magnetisation vs. temperature curves $m(T)$ for different values of the total number of electrons n in the band are compared. The behaviour is universal for all parameters with $W < U$ admitting a ferromagnetic state at low temperatures. The magnetisation m depends on the band filling n only via $m_{\text{max}} = \min\{n, 2-n\}$, due to the symmetry between electrons and holes in the band. Therefore, the dependence of the magnetisation is symmetric around the band filling $n = 1$, for which the magnetisation for a certain temperature is the highest compared to other band fillings. As the electron number is shifted from $n = 1$, the magnetisation decreases faster with temperature and the Curie temperature is reached earlier. In the limit of vanishing or complete band filling, i.e. $n = 0$ or $n = 2$, the magnetisation vanishes. In order to illustrate this dependence, the magnetisation is plotted in Fig. 7.4 as a function of both band filling and temperature. In section 7.5, an investigation of the Curie temperature will show that in this limit not only the maximum magnetisation goes to zero, but also the Curie temperature.
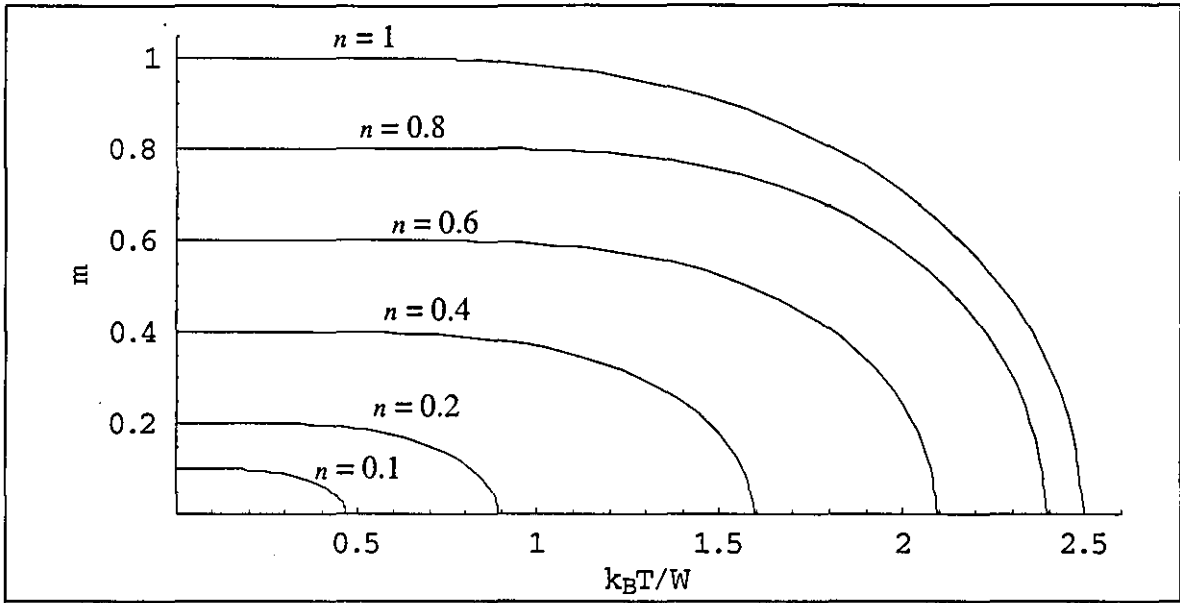
Fig. 7.3: The magnetisation m vs. temperature T for $U/W = 10$ and different band fillings n.
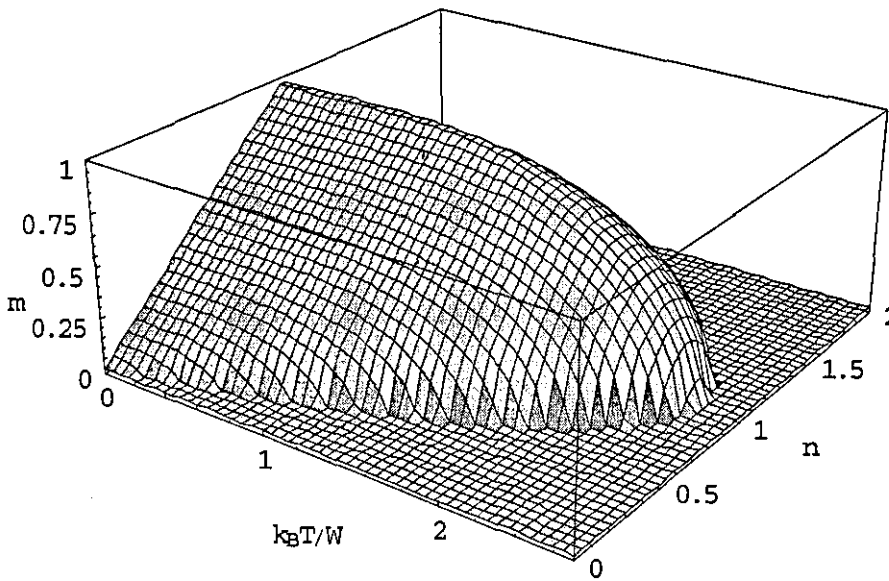

Fig. 7.4: The magnetisation m as a function of the band filling n and the temperature T for $U/W = 10$.

The dependence of the magnetisation as a function of temperature $m(T)$ on the on-site repulsion U is shown in Fig. 7.5. The magnetisation as a function of both temperature and on-site repulsion is shown in Fig. 7.6. At zero temperature, the magnetisation as a function of the on-site repulsion is the step function (5.14). For $U < W$, the magnetisation is zero for all temperatures. For $U > W$, the magnetisation is finite for temperatures smaller than the Curie temperature. In this temperature range, the magnetisation is larger for a larger on-site repulsion. For U slightly larger than W, the Curie temperature increases rapidly. For $U \gg W$, the Curie temperature increases linearly with increasing U.
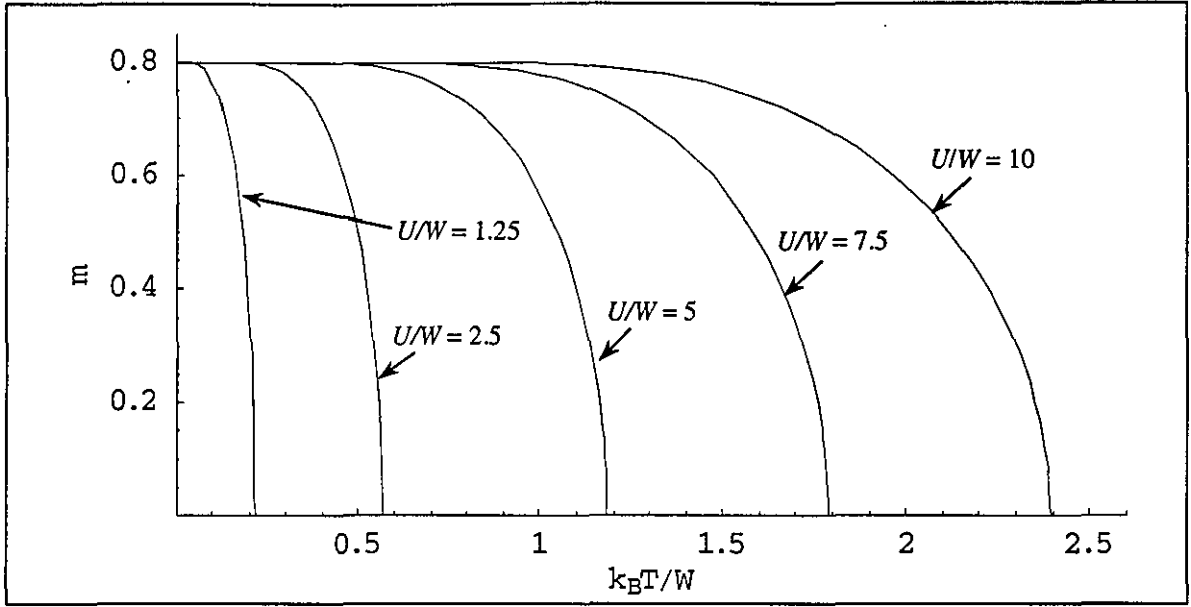
Fig. 7.5: The magnetisation m as a function of temperature T for $n = 0.8$ and different on-site repulsion U.
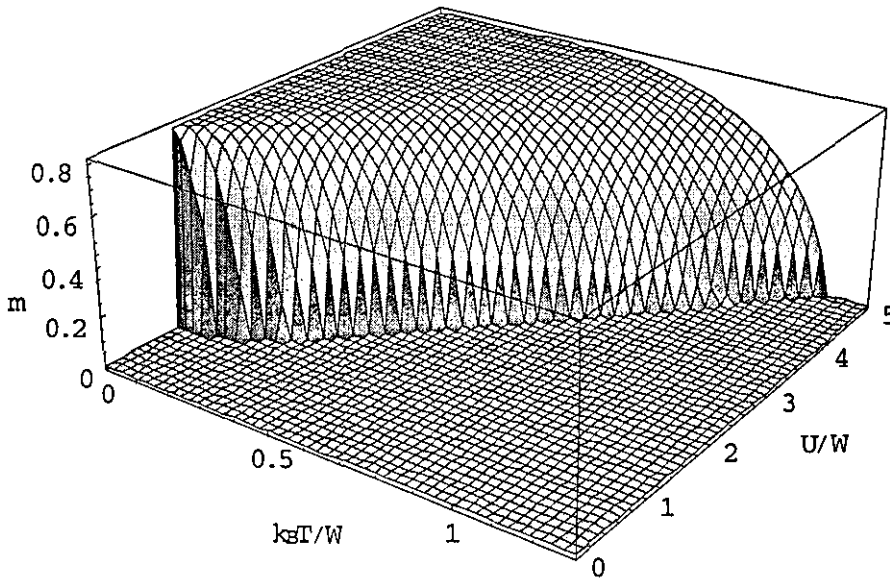
Fig. 7.6: The magnetisation m as a function of temperature T and on-site repulsion U for $n = 0.8$.

Since only the ratios of the energies are of importance, the dependence of the magnetisation on the bandwidth can be obtained from the dependence of the magnetisation on the on-site repulsion. Therefore, the dependence of the magnetisation on the bandwidth will only be briefly discussed.
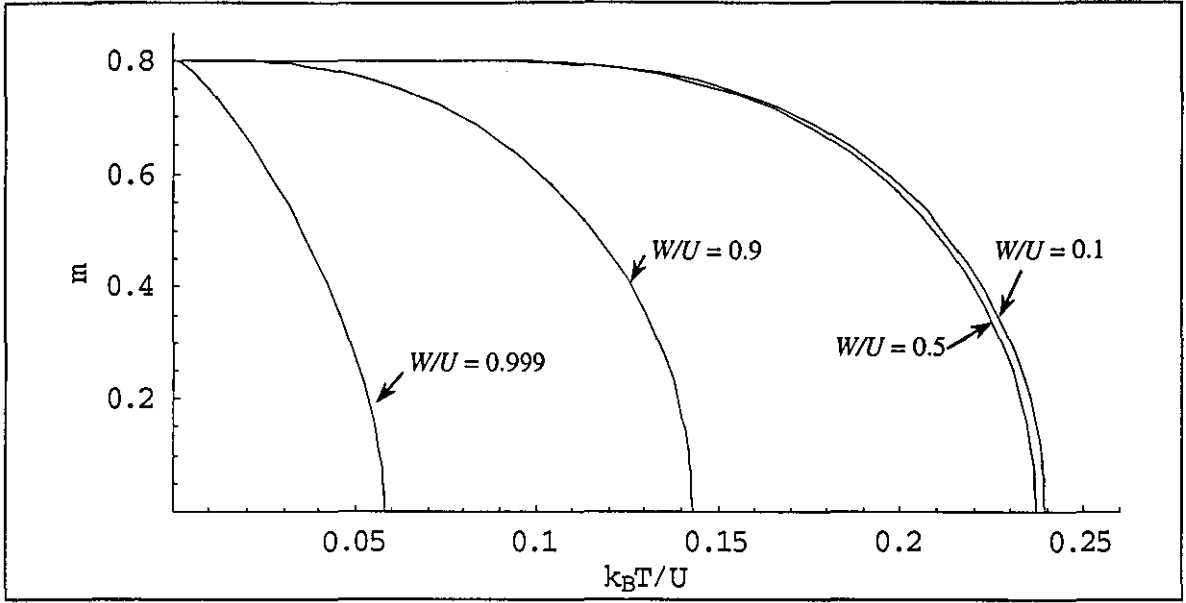
Fig. 7.7: The magnetisation m as a function of temperature T for $n = 0.8$ and different bandwidths W.
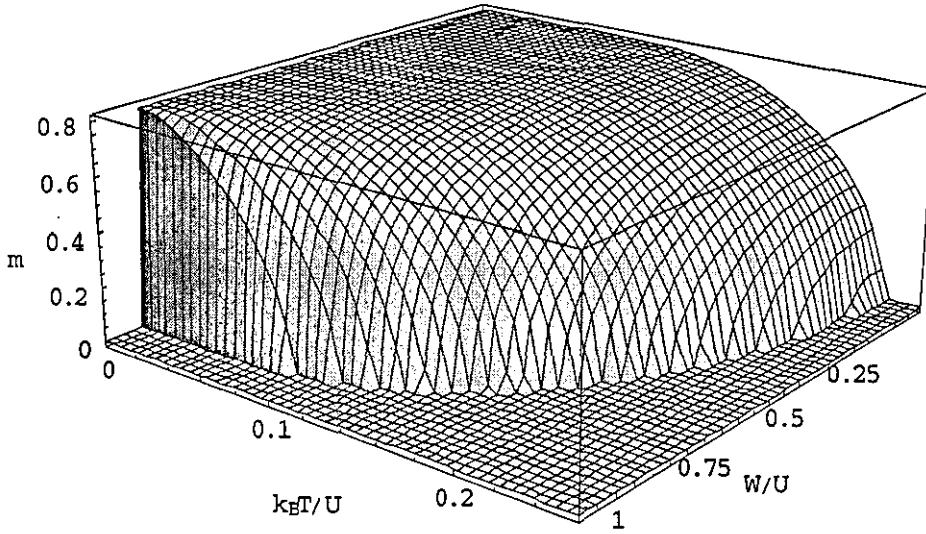
Fig. 7.8: The magnetisation m as a function of temperature T and bandwidth W for $n = 0.8$.

In Fig. 7.7, the magnetisation as a function of the temperature $m(T)$ is plotted for different bandwidths W. In addition the magnetisation as a function of both the temperature and the bandwidth is plotted in Fig. 7.8. As long as $W \ll U$, the dependence of the magnetisation curve $m(T)$ on the width of the band W is weak. However, for a bandwidth W, which is comparable to the on-site repulsion U, the dependence becomes crucial. As W approaches U from below, the magnetisation decreases much faster with temperature and the Curie temperature drops rapidly.

Finally, the magnetisation in the presence of an external magnetic field B_0 is studied.
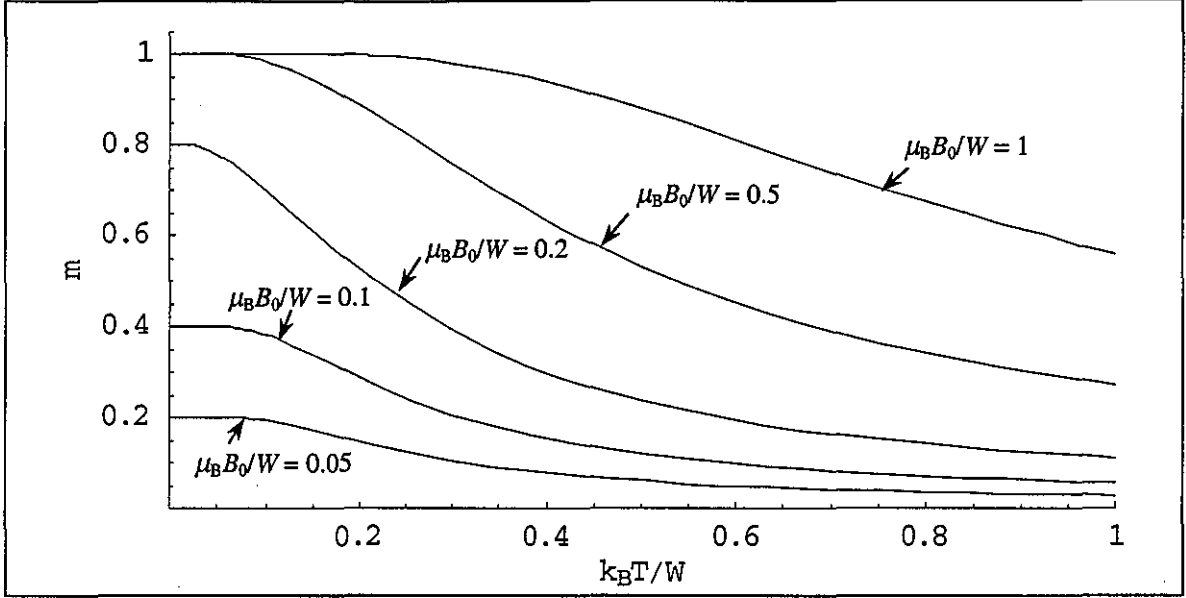
Fig. 7.9: The magnetisation m as a function of temperature T for and different external fields B_0. Parameters: $n = 1$ and $U/W = 0.5$. The system is paramagnetic at all temperatures.
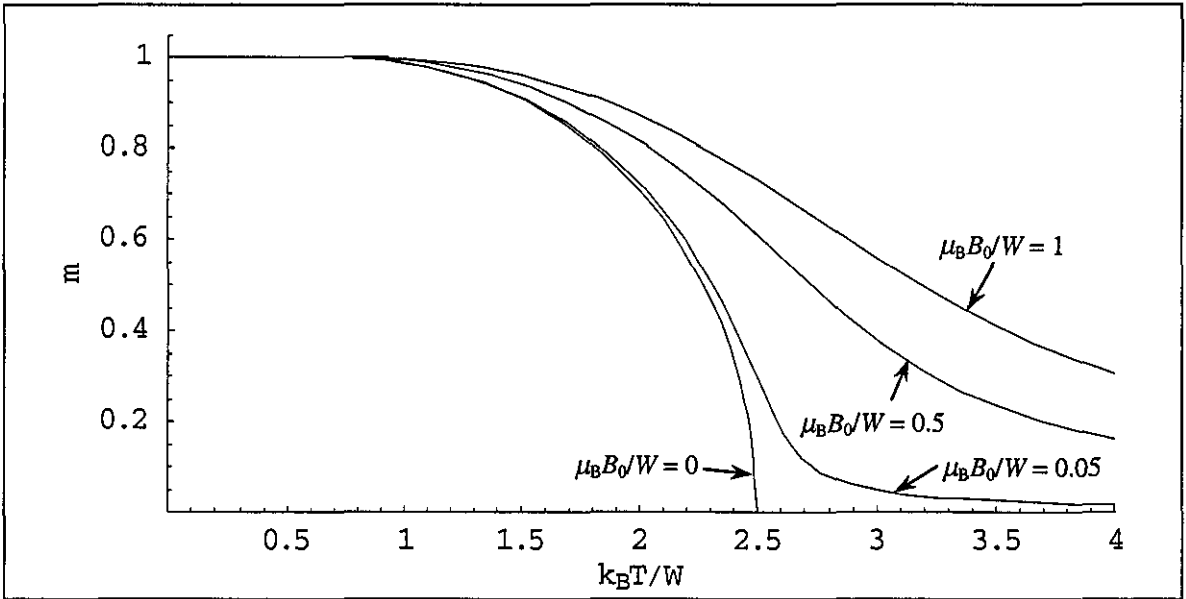
Fig. 7.10: The magnetisation m as a function of temperature T for different external fields B_0. Parameters: $U/W = 10$, $n = 1$. The system is ferromagnetic below the Curie temperature $k_B T_C/W \approx 2.5$.

The dependence is illustrated in Fig. 7.9 for $U < W$, where the system is paramagnetic at all temperatures. The external magnetic field causes a non-vanishing magnetisation. For a given external field, the magnetisation is larger for lower temperatures. If the external field is strong enough, saturation of the magnetisation occurs and the magnetisation does not increase noticeably with increasing field any more.

51

In Fig. 7.10, the dependence of the magnetisation on an external field is illustrated for $U > W$, where the system is ferromagnetic at low temperatures. A non-vanishing external field causes a non-vanishing magnetisation also in the paramagnetic phase at temperatures above the Curie temperature. At low temperatures, where the magnetisation is almost maximal, a non-vanishing external field changes the magnetisation only slightly. The change of the magnetisation by the external field is maximal for temperatures around the Curie temperature.

7.4 The Reduced Magnetisation

From the temperature dependence of the magnetisation, one can calculate the reduced magnetisation $\bar{m} = m/m_{max}$ as a function of the reduced temperature $\bar{T} = T/T_C$ for parameters with $U > W$, which permit a ferromagnetic state at low temperatures. The behaviour of $\bar{m}(\bar{T})$ is similar for a wide range of parameters. Firstly, the influence of the on-site repulsion U and the width W of the band will be considered.
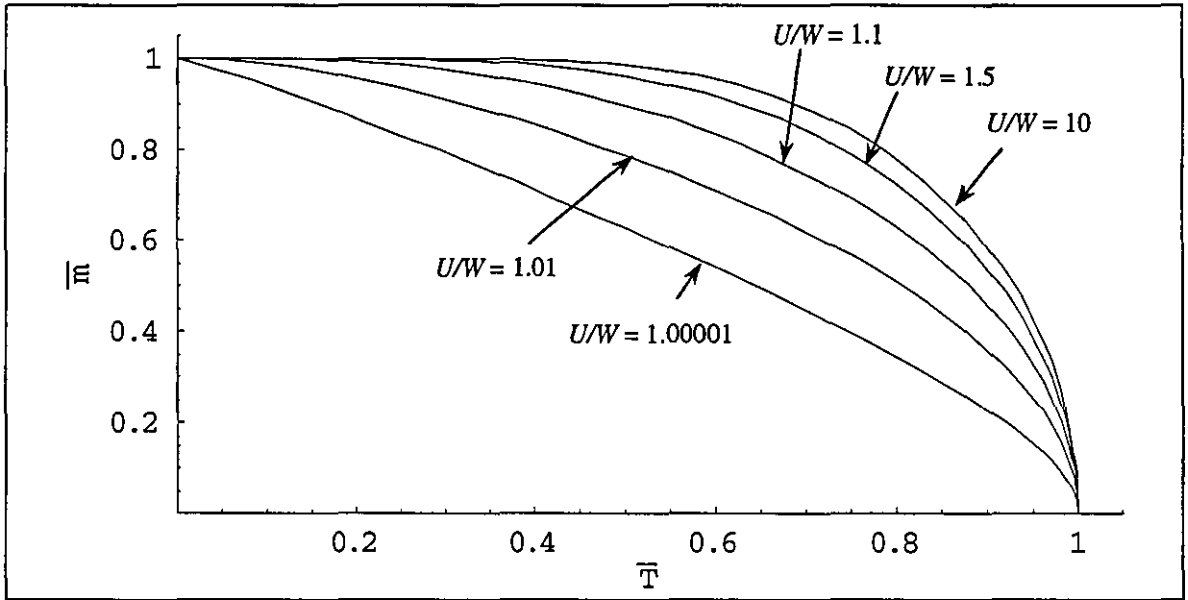
Fig. 7.11: The reduced magnetisation $\bar{m}$ as a function of the reduced temperature $\bar{T}$ for different ratios U/W and $n = 0.8$.

As seen in Fig. 7.11, the curves $\bar{m}(\bar{T})$ for larger ratios U/W lie above those for smaller ratios. For $1 < U/W \le 1.00001$, i.e. for U very close to W, the reduced magnetisation $\bar{m}(\bar{T})$ decreases almost linearly accept for $\bar{T}$ close to zero or unity. For larger U/W, the reduced

magnetisation curve becomes rapidly more convex. For $U \gg W$, the graphs for the reduced magnetisation against the reduced temperature are almost indistinguishable.
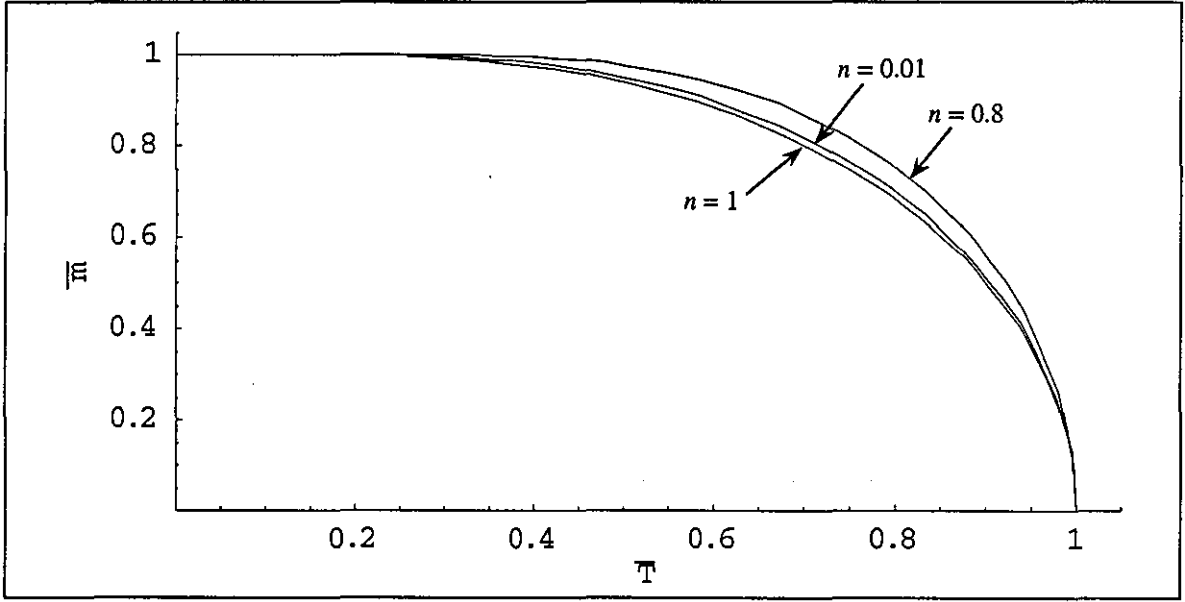

Fig. 7.12: The reduced magnetisation $\overline{m}$ as a function of the reduced temperature $\overline{T}$ for different n and U/W=2.

The influence of the total number of electrons n on the shape of the reduced magnetisation as a function of the reduced temperature is very small. Fig. 7.12 illustrates the dependence. The reduced magnetisation for $n = 1$ and $n \ll 1$ is slightly smaller than for intermediate values of n.

For large $U \gg W$, the behaviour of the reduced magnetisation is very similar to that derived from the Molecular Field Approximation for a ferromagnetic Heisenberg Hamiltonian with $S = \frac{1}{2}$, which is given by:

$$\overline{m}(\overline{T}) = \text{Root}\left[\overline{m} = \tanh\left(\frac{\overline{m}}{\overline{T}}\right)\right] \tag{7.19}$$

This seems reasonable, because in the limit $W \to 0$, the Heisenberg model and the single band Stoner model differ in the mean field approximation only in the statistics used. Whereas in the Heisenberg model, the spins are considered distinguishable particles and therefore, Boltzmann statistics is used, Fermi statistics is used for the electrons in the Stoner model.
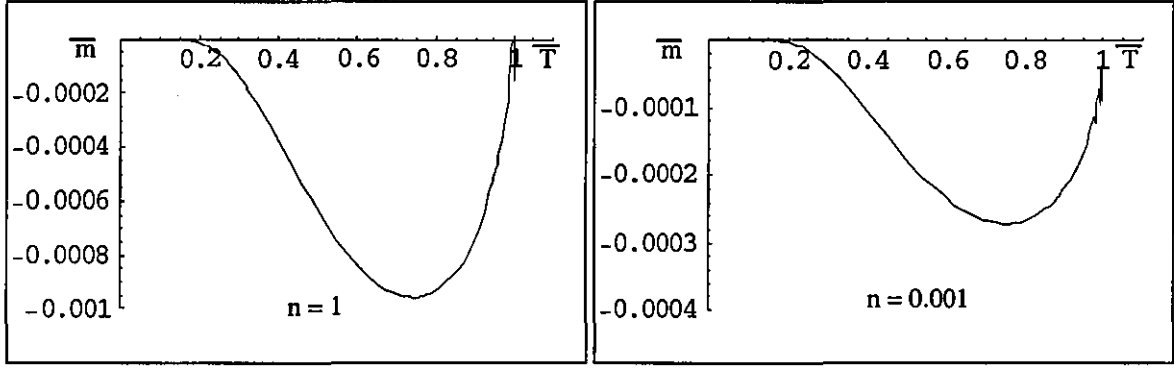
Fig. 7.13: The deviation of the reduced magnetisation $\Delta\overline{m}(\overline{T})$ of the Stoner model from the one derived from the Heisenberg model (7.19) for $U/W = 10$.

The roughness of the graphs is due to numerical inaccuracies.

In particular for $n = 1$ and $n \ll 1$, the graphs $\overline{m}(\overline{T})$ of the Stoner model differ only very little from the reduced magnetisation defined by (7.19) as is illustrated in Fig. 7.13. For intermediate values of n or smaller U/W, the deviation is larger.

7.5 The Curie Temperature

If the on-site repulsion U is larger than the width of the band W, the system is ferromagnetic at low temperatures and paramagnetic at high temperatures. In this model, the transition is continuous and takes place at the Curie temperature T_C, which depends on the system parameters U, W and n. Below the Curie temperature, the paramagnetic state is unstable. When the temperature is increased above the Curie temperature, the paramagnetic state becomes stable. This is accompanied by a sign change of $\left(\partial^2 F/\partial m^2\right)_{B_0, T, n}$ for $m = 0$ at $T = T_C$. Therefore, the Curie temperature can be calculated by solving the equation

$$0 = \left(\frac{\partial^2 F}{\partial m^2}\right)_{B_0, T, n}\Bigg|_{m=0, T=T_C} = -\frac{U}{2} + \frac{W}{4}\left(\coth\left[\frac{(2-n)W}{4k_B T_C}\right] + \coth\left[\frac{nW}{4k_B T_C}\right]\right) \tag{7.20}$$

for T_C. This equation has a real and non-negative solution only for $U \geq W$. This is consistent with the fact that for $U < W$ the paramagnetic state is stable at all temperatures and there is no paramagnetic-to-ferromagnetic transition and no Curie temperature.

There is no exact general expression for the solution of (7.20) in terms of standard functions. Therefore, the case for $n = 1$, the limit $n \to 0$ and $W \to 0$ will be considered first, where an analytical expression can be found. Then an approximate expression will be

developed for all values of n. This expression will then be compared with the values of T_C obtained by solving (7.20) numerically.

For $n = 1$, the solving of equation (7.20) yields for the Curie temperature:

$$T_C(n = 1) = \frac{W}{4 \operatorname{arccoth}\left[\dfrac{U}{W}\right]} \approx \frac{U}{4} \quad \text{for} \ U \gg W \tag{7.21}$$
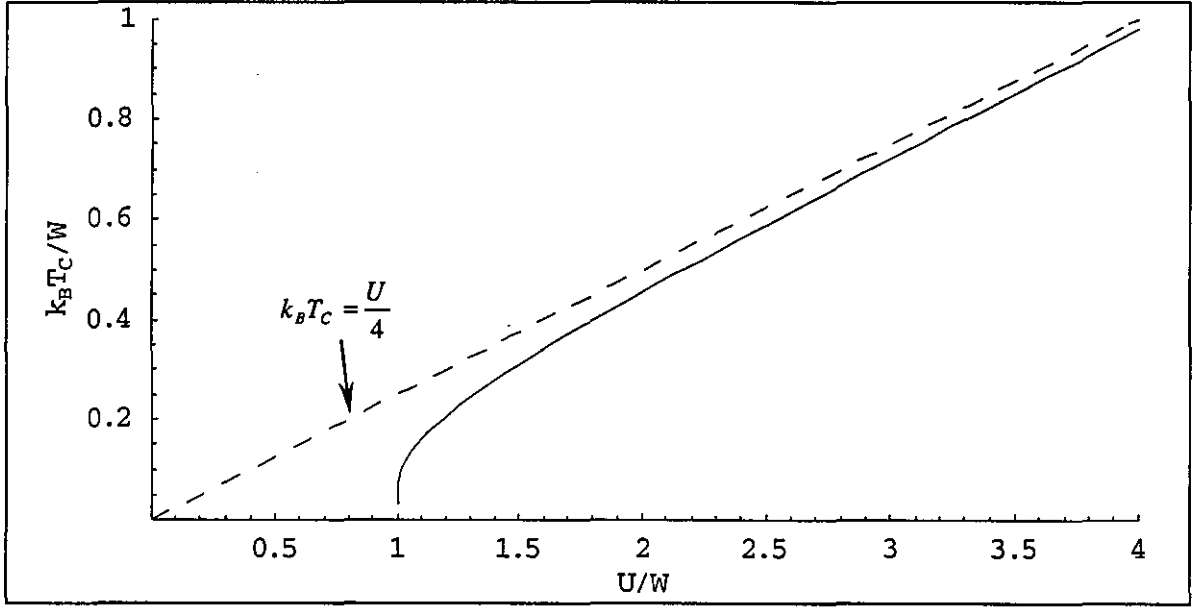
This dependence is illustrated in Fig. 7.14.

Fig. 7.14: The Curie temperature T_C (solid line) for a total number of electrons $n = 1$.

For $U \gg W$, the Curie temperature can be approximated by $k_B T_C \approx U / 4$ (dashed line).

For $U \gg W$, the Curie temperature behaves asymptotically as $U/4$. For $U \to W$ from above, the Curie temperature goes to zero.

For calculating the Curie temperature for small n, the properties of the hyperbolic cotangent can be employed to approximate (7.20). As observed in the numerical calculations of the magnetisation, the Curie temperature $k_B T_C$ is very small compared to the width W of the band for small n. Thus, the second term in (7.20) can be approximated by:

$$\coth\left[\frac{(2-n)W}{4 k_B T_C}\right] \approx \coth\left[\frac{W}{2 k_B T_C}\right] \approx 1 \quad \text{for} \ k_B T_C \ll W \ \& \ n \ll 1 \tag{7.22}$$

The third term in (7.20) can not be approximated in this way, since the argument of the hyperbolic cotangent $n\dfrac{W}{k_B T_C}$ might not be much larger than unity. Therefore for small n, equation (7.20) is approximated by:

$$0 \approx -\frac{U}{2} + \frac{W}{4}\left(1 + \coth\left[\frac{nW}{4k_B T_C}\right]\right) \qquad for \quad k_B T_C \ll W \ \& \ n \ll 1 \tag{7.23}$$

This yields the Curie temperature:

$$k_B T_C \approx \frac{nW}{4\operatorname{arccoth}\left[\dfrac{2U-W}{W}\right]} \qquad for \quad n \ll 1$$

$$\approx 2n\frac{U}{4} \qquad\qquad for \quad U \gg W \ \& \ n \ll 1 \tag{7.24}$$

The Curie temperature calculated by (7.24) is shown in Fig. 7.15.
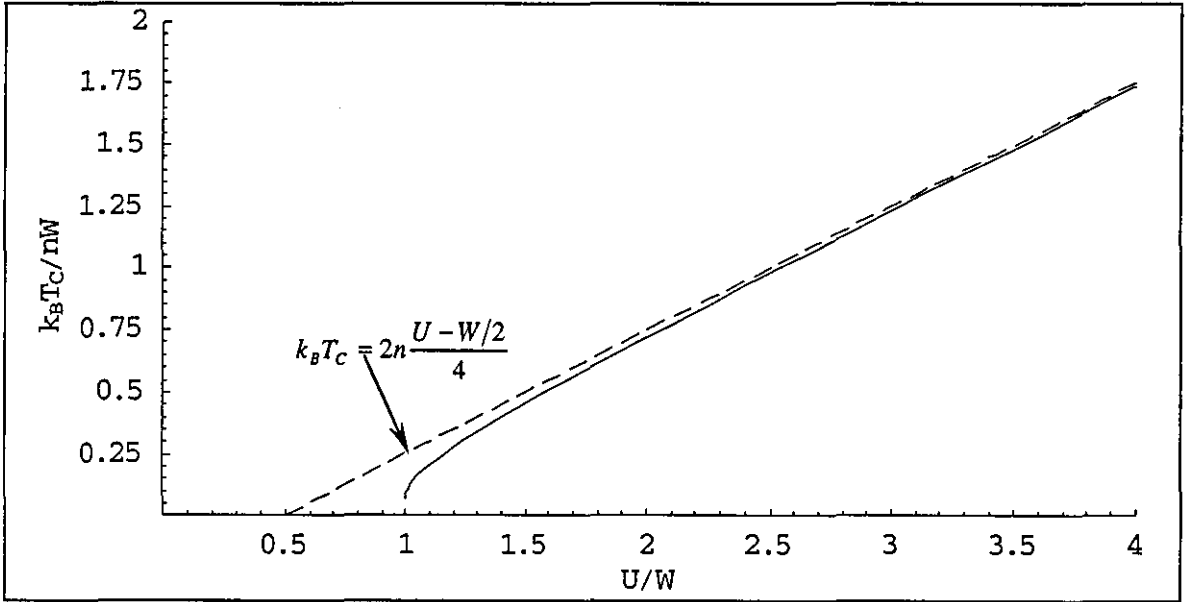
Fig. 7.15: The Curie temperature T_C (solid line) for a total number of electrons $n \ll 1$ calculated by (7.24).

The behaviour of T_C for $n \ll 1$ is similar to the case $n = 1$. For $U \to W$ from above, the Curie temperature goes to zero. For $U \gg W$, the Curie temperature can be approximated by $2n\,U/4$. For $n \le 0.1$, the values for T_C calculated by (7.24) are in such good agreement with the ones calculated by the full equation (7.20), that the difference would not be visible in Fig. 7.15. For an almost completely filled band with $2 - n \ll 1$, a similar analysis yields the results as for $n \ll 1$ by substituting n by $2 - n$.

For any band filling, the Curie temperature can be computed in the limit of a vanishing W. With

$$0 = \lim_{W \to 0} \left(\frac{\partial^2 F}{\partial m^2} \right)_{B_0, T, n} \bigg|_{m=0, T=T_C} = -\frac{U}{2} + \frac{2 \, k_B T_C}{n(2-n)}$$ (7.25)

it follows that:

$$k_B T_C = n(2-n) \frac{U}{4} \quad \text{for} \quad W \to 0$$ (7.26)

This result represents also the asymptotic behaviour for $U \gg W$. In this limit, it confirms the findings for $n = 1$ and $n \ll 1$.

The results for the Curie temperature for $n = 1$ and $n \ll 1$ can be used to obtain an approximate expression for all values of n. This formula must be symmetric with respect to n around $n = 1$. Furthermore, it must be identical with (7.21) for $n = 1$ and for $U \gg W$, it must go to (7.26). The formula

$$k_B T_C = n(2-n) \frac{W}{4 \, \text{arccoth} \left[\dfrac{U}{W} \right]}$$ (7.27)

satisfies these conditions. In Fig. 7.16, the Curie temperature calculated using this formula is compared with the values calculated by solving (7.20) numerically.
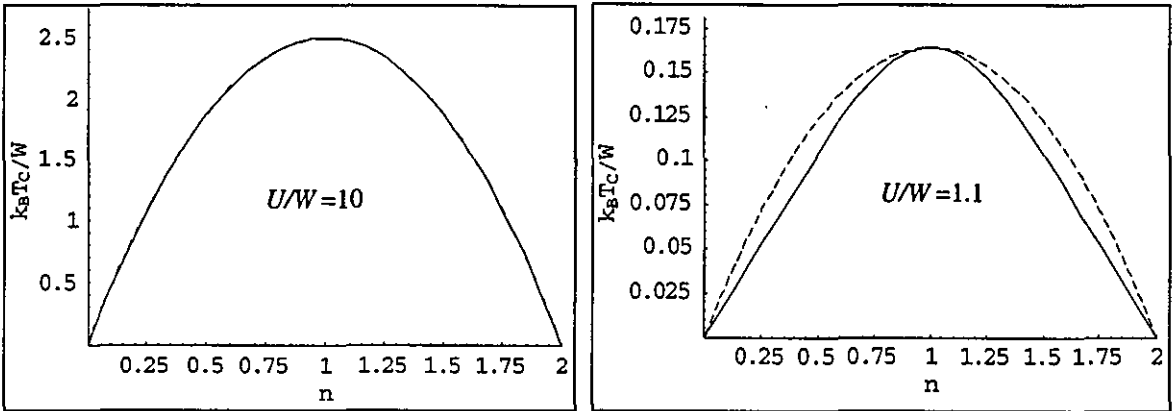

Fig. 7.16: The Curie temperature T_C as a function of the total number of electrons n.
Dashed line: interpolation formula (7.27). Solid line: exact formula (7.20) numerically solved.

The deviation of the values calculated by (7.27) from the ones obtained by solving (7.20) numerically is only noticeable for U close to W and small m_{max}. For $U \gg W$, the

difference is negligible for all n. Only for $(U - W)/W \ll 1$ and $m_{max} \ll 1$, the relative difference amounts to values up to 50%.

7.6 The Susceptibility

After the magnetisation is computed, the susceptibility can be simply calculated using (7.11). For $U < W$ at all temperatures or for $U > W$ and $T > T_C$, the system is paramagnetic and the magnetisation vanishes in the absence of an external magnetic field. Formula (7.11) then yields the zero field susceptibility in the paramagnetic phase:

$$\chi(T) = \mu_B^2 \left(-\frac{U}{2} + \frac{W}{4} \operatorname{csch}\left[\frac{(2-n)W}{4 k_B T} \right] \operatorname{csch}\left[\frac{nW}{4 k_B T} \right] \sinh\left[\frac{W}{4 k_B T} \right] \right)^{-1} \quad \text{for } m = 0 \quad (7.28)$$

In 7.17, the zero field susceptibility is shown as a function of temperature for different values of the on-site repulsion $U < W$. The system is paramagnetic at all temperatures. At very low temperatures, the susceptibility as a function of temperature is almost constant, since the free energy is dominated by the internal energy. For higher temperatures, where the entropy dominates the free energy, the susceptibility decreases faster with increasing temperature. In particular at low temperatures, the susceptibility is enhanced for $U > 0$ compared to $U = 0$. The larger the on-site repulsion, the larger is the zero field susceptibility. As U reaches W, the susceptibility goes to infinity at zero temperatures.
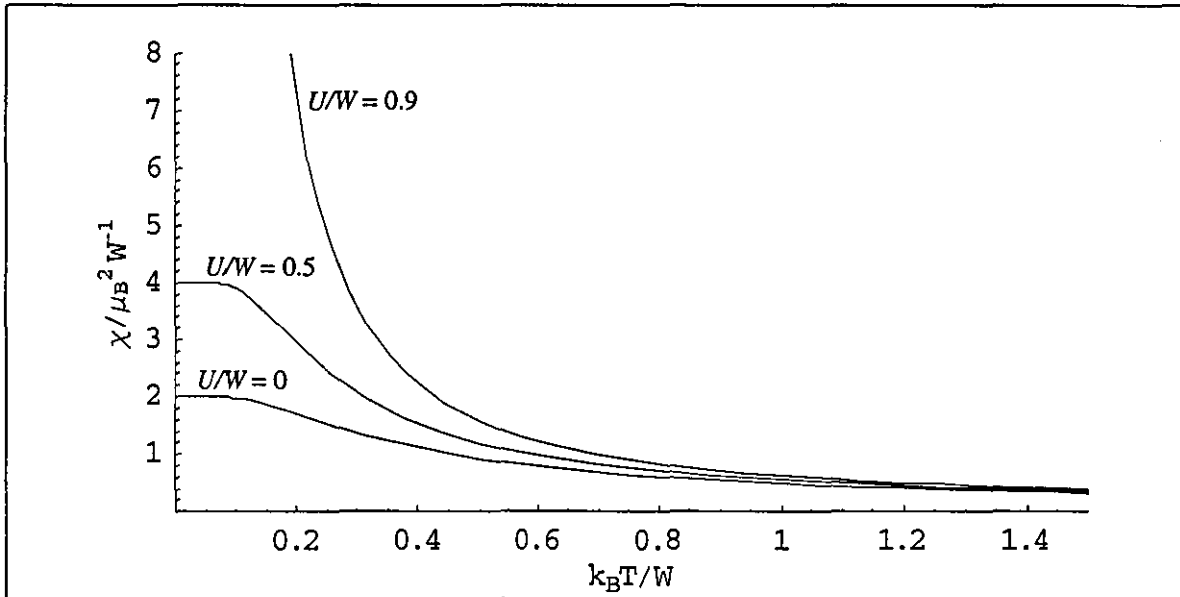
7.17: The zero field susceptibility χ vs. temperature T for different on-site repulsion $U < W$ and $n = 1$

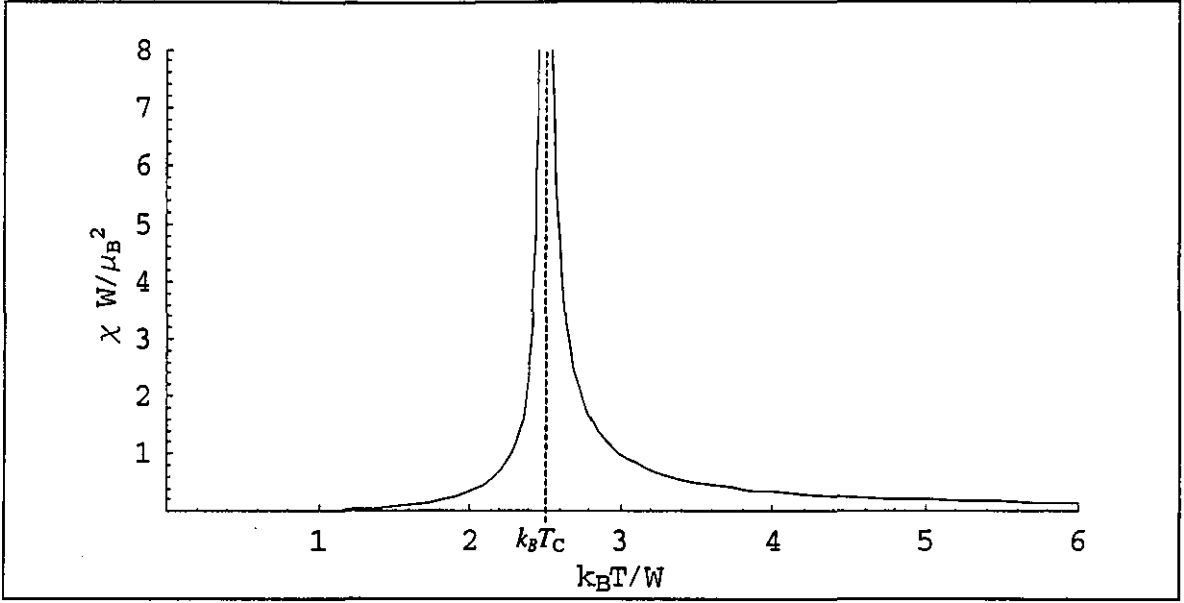The system is paramagnetic at all temperatures.

58

Fig. 7.18: the zero field susceptibility χ vs. temperature T for $n = 1$, and $U/W = 10$.

The system is ferromagnetic below the Curie temperature $k_B T_C \approx 2.5$ and paramagnetic above.
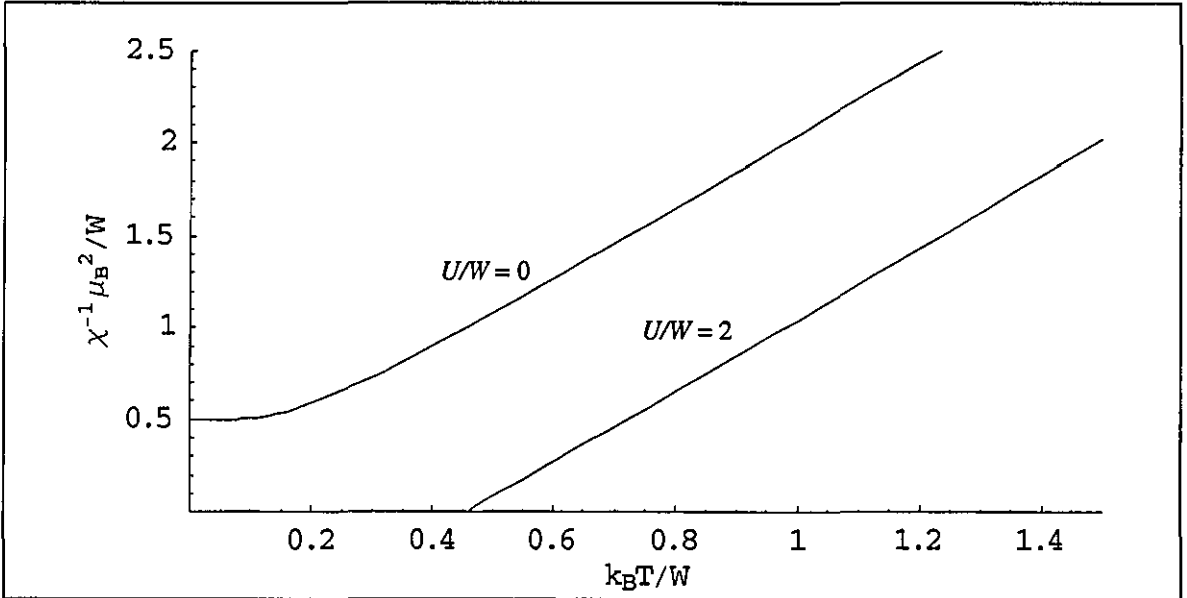

Fig. 7.19: the inverse high-temperature zero-field susceptibility χ^{-1} vs. temperature T for $n = 1$.

For $U = 0$, the system is paramagnetic at all temperatures.

For $U/W = 2$, the system is ferromagnetic below $k_B T_C \approx 0.455$.

In Fig. 7.18, the susceptibility is shown for the case $U > W$, where the system is ferromagnetic at temperatures below T_C and paramagnetic above. The susceptibility is strongly enhanced for temperatures around the Curie temperature. The susceptibility has a pole at $T = T_c$. This marks the ferromagnetic-to-paramagnetic phase transition. At very low temperatures, the susceptibility is small and reaches zero for $T = 0$, because the

59

magnetisation is saturated already in the absence of an external field. For very high temperatures, where the entropy part of the free energy strongly disfavours a non-zero magnetisation, the susceptibility is very small, too.

The inverse zero field susceptibility χ^{-1} as a function of temperature is shown in Fig. 7.19. For $U < W$, the inverse susceptibility is almost constant at low temperatures. With increasing temperature, the inverse susceptibility increases. At high temperatures, the inverse susceptibility increases linearly with temperature. For $U > W$, the inverse susceptibility is negative for temperatures $T < T_C$. At temperatures above T_C, the inverse susceptibility increases linearly, but a shift can be observed towards higher temperatures in comparison to the case of $U = 0$.

The high temperature susceptibility in this model looks very much like the one calculated from the Heisenberg model (2.2). For example, the linear dependence of the inverse susceptibility on the temperature suggests that the susceptibility is inversely proportional to the temperature. From the limit

$$\lim_{T \to \infty} k_B T \cdot \chi(T) = \mu_B^2 \frac{n(2-n)}{2} \tag{7.29}$$

it follows that at high temperatures, the susceptibility can be approximated by:

$$\chi(T) \approx \mu_B^2 \frac{n(2-n)}{2 k_B T} \tag{7.30}$$

This approximation can be improved by calculating:

$$\lim_{T \to \infty} \left(\chi^{-1}(T) - \frac{2 k_B T}{\mu_B^2 n(2-n)} \right) = -\frac{U}{2\mu_B^2} \tag{7.31}$$

From this, a shift of the temperature in the denominator of the right hand side of (7.30) can be calculated:

$$T_{Shift} = -\frac{U}{2\mu_B^2} \bigg/ \frac{2k_B}{\mu_B^2 n(2-n)} = -n(2-n)\frac{U}{4 k_B} \tag{7.32}$$

Therefore, the approximation becomes:

$$\chi(T) \approx \mu_B^2 \frac{n(2-n)}{2 k_B (T - T_P)} \qquad \text{with } T_p = -T_{shift} = n(2-n)\frac{U}{4 k_B} \tag{7.33}$$

This approximation is correct as far as both the difference between the exact formula and the approximation and the difference between their reciprocal values go to zero as $T \to \infty$. For $U \gg W$, the temperature shift T_p is almost identical to the Curie temperature T_C. Furthermore, for $n = 1$ and setting $T_p := T_C$, the formula (7.33) is identical to (2.2) assuming a spin $S = \frac{1}{2}$. A reason for the similarity between both models is that at very high temperatures, the system behaviour is dominated by entropy.

7.7 Discussion

The mean field approximation has been used to study the finite temperature properties of the Stoner model for a single band with rectangular density of states. Expressions have been derived for the free energy and its derivatives, the magnetisation and the susceptibility. The magnetisation and the susceptibility have been calculated for various sets of parameters, and the dependence of the magnetic properties on the system parameters has been discussed.

Assuming a rectangular density of states permits a large part of the calculations to be carried out analytically, which facilitated the discussion. Moreover, a rectangular shape can be seen as a first approximation for more complicated band shapes and is therefore, in this sense, quite general. Small deviations of the DOS shape from a rectangular form do not affect the results noticeably as shown by numerical investigations, which have been carried out.

The model can be used to describe the magnetic behaviour of a paramagnet. For a bandwidth larger than the on-site repulsion, the system is paramagnetic at all temperatures. At high temperatures, the magnetic susceptibility follows a Curie law. Near zero temperature, the susceptibility is almost constant as predicted by the Pauli theory of spin-paramagnetism, but may be enhanced by the on-site repulsion.

Furthermore, the model can describe a strong ferromagnet. For a bandwidth smaller than the on-site repulsion, the magnetisation is maximal at zero temperature. The maximum magnetisation, which depends on the band filling, can take any real value between zero and half the number of states in the band. By the dependence of the maximum magnetisation on the filling of the band, the values of the zero-temperature magnetisation in transition metals and alloys can be explained. At finite temperatures, the magnetisation decreases with increasing temperature and vanishes at the Curie temperature. Above the Curie

temperature, the system is paramagnetic. The susceptibility is low at low temperatures where the magnetisation is almost maximal. At the Curie temperature, the susceptibility is singular as expected for the ferromagnetic-to-paramagnetic phase transition. At high temperatures, the susceptibility follows a Curie-Weiss law.

8 The Coupling of Magnetisation and Lattice

8.1 Introduction

So far, the magnetic degrees of freedom in the model investigated here, namely spatially uniform magnetisation m, has been considered only. For the derivation of the Stoner model, the perfect periodicity of the crystal lattice has been assumed. For the study of the Stoner model at finite temperatures, the nuclear lattice has been seen as a fixed, rigid, immobile array of ions. This is only an approximation for the actual ionic configuration. In a crystal, the electron configuration is affected by the ions moving around their equilibrium positions, which in turn depend on the electronic structure.

In many magnetic materials, experiments show that the interaction between lattice and magnetic degrees of freedom is crucial for their magnetic and mechanic properties. A group of materials exhibiting a strong interaction of magnetic and lattice degrees of freedom are Invar alloys. These materials are characterised by a low thermal expansion in a wide temperature range around room temperature [21]. Furthermore, Invar materials show a large forced volume magnetostriction and a substantial pressure dependence of the magnetisation and the Curie temperature. The unusual thermal expansion making these materials interesting for many applications, such as precision instruments or seismographic devices, was first found by Guillaume [20] in 1897 in ferromagnetic iron-nickel alloys with compositions close to the classic Invar alloy $Fe_{65}Ni_{35}$. Later, Invar anomalies where observed in other ferromagnetic materials, e.g. in ordered and disordered Fe_3Pt, and in antiferromagnetic materials.

One way of introducing an interaction of the magnetisation and lattice degrees of freedom into the Stoner model is to consider the dependence of the one-electron energies on the state of the lattice. Via such a coupling, the system parameters determining the electronic behaviour may become temperature-dependent. Furthermore, fluctuations of the lattice may cause fluctuations of the system parameters.

In the following, the study will be restricted to the case of a rectangular density of states, which is fully characterised by its bandwidth W. The interaction of lattice and magnetic degrees of freedom will be incorporated into the model via dependence of the bandwidth on the lattice parameter. The effects of local variations of the lattice parameter are studied by introducing a local bandwidth and treating the variations as fluctuations.

8.2 The Lattice Parameter and the Electronic States

To study the interaction between the lattice degrees of freedom and the magnetisation, the possible dependence of the parameters in Hamiltonian (4.4) on the lattice parameter will be considered in this section. The inter-atomic distance or lattice parameter is chosen to describe the relative position and the dynamics of the ion cores. The emphasis is on finding a simple description reflecting the correct general behaviour rather than exact formulas.

From the derivation of the Stoner model in chapter 3, the on-site repulsion U is the matrix element of the Coulomb interaction between electrons of opposite spin on the same atom. Therefore, it may be regarded as independent of the location of the atoms. However, in a generalisation of the Stoner model, the on-site repulsion can be seen as the linear coefficient of an expansion of the one-electron energies in terms of the magnetisation. In this case, the on-site repulsion might as well depend on the lattice configuration, but here it will be regarded as independent.

In a complex band structure with more than one band, the total number of electrons n in a band may depend on the lattice configuration. However, only a single independent band is considered here and particle exchange with other bands or the environment is neglected. Therefore, the total number of electrons is regarded as constant and independent of the lattice configuration.

In contrast, the one-electron energies and the band structure clearly depend on the relative position of the atoms with respect to each other. If the atoms are sufficiently far away from each other, the one-electron states of the band are degenerate and their energies are identical to the energy levels of the isolated atom. Conversely, bringing the atoms close together results in a broadening of the atomic energy levels to a band.

Here, only a simple approximation of the bandwidth on the inter-atomic distance is desired. The d-bands in transition metals and their alloys are narrow. In the view of the Stoner criterion, this favours the occurrence of ferromagnetism. For a narrow band, a tight-binding model may be used to derive the dependence of the width of the band on the lattice parameter. In the tight-binding approximation for a single band, the bandwidth is proportional to the overlap integral [29]

$$W \propto \int dr \, \phi^*(r) \, \Delta V(r) \, \phi(r + R) \tag{8.1}$$

with the tight binding atomic wave function $\phi(\mathbf{r})$ of the atom at the origin, the vector $\mathbf{R}$ joining nearest-neighbour atoms and $\Delta V(\mathbf{r})$ comprising corrections to the atomic potential to produce the full periodic potential of the crystal.

The overlap integral (8.1) depends on the distance $|\mathbf{R}|$ between neighbouring atoms in the crystal. At sufficiently large distances from the origin, the atomic wave function falls of exponentially with the distance r from the nucleus:

$$\phi(\mathbf{r}) \propto \exp\left(-\alpha |\mathbf{r}|\right) \quad , (\alpha > 0) \tag{8.2}$$

In the tight-binding model, the next-neighbour separation is large enough to use this approximation for the overlap integral. With the lattice parameter a proportional to the next-neighbour separation $|\mathbf{R}|$, the overlap integral can be roughly estimated as being proportional to $\exp(-\beta a)$. From this, it follows that

$$W \approx W_0 \exp\left(-\beta a\right) \quad , (\beta > 0) \tag{8.3}$$

for distances a from the nucleus.

8.3 The Lattice-Parameter Dependence of Magnetisation and Curie Temperature

With the electronic structure depending on the location of the ion cores in the crystal, the magnetisation of the crystal may change by a change of the lattice parameter. The results for the magnetisation of a rectangular band in chapter 5 can be used to estimate the dependence of the magnetisation on the lattice parameter at zero temperature. Assuming a single band with a rectangular DOS (5.1), the magnetisation at zero temperature is either zero or maximal depending on whether the bandwidth W is larger or smaller than the on-site repulsion U:

$$m = \begin{cases} \pm m_{max} & for \quad W < U \\ 0 & for \quad W > U \end{cases} \tag{8.4}$$

With a dependence (8.3) of the bandwidth on the lattice parameter a, the magnetisation as a function of the lattice parameter is then:

$$m(a) = \begin{cases} \pm m_{max} & for \quad a > a_m \\ 0 & for \quad a < a_m \end{cases} \tag{8.5}$$

Here,

$$a_m = -\beta^{-1} \ln(U/W_0) \tag{8.6}$$

is the lattice parameter, where the on-site repulsion and the bandwidth become equal. This distance can be used to rewrite (8.3) as:

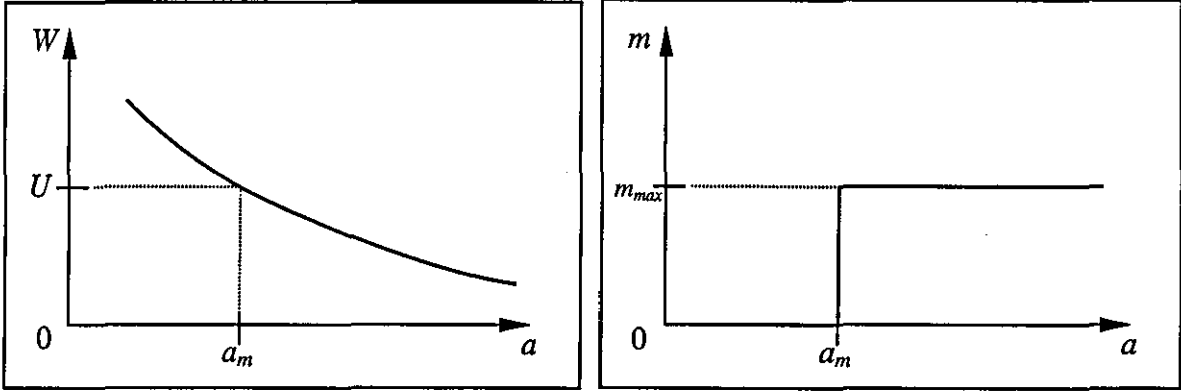$$W = U \exp(-\beta(a - a_m)) \quad , (\beta > 0) \tag{8.7}$$

Fig. 8.1: The bandwidth W and the magnetisation m as functions of the lattice parameter a at $T = 0$.

The dependence of W and m on the lattice parameter at zero temperature is illustrated in Fig. 8.1. If the atoms of the crystal are far apart, the gain in Coulomb energy is larger than the loss in kinetic energy by increasing the magnetisation. The magnetisation is maximal. If the lattice constant is smaller than a_m, the cost in kinetic energy for a finite magnetisation becomes too large and the magnetisation goes to zero. For a rectangular density of states, the change of magnetisation is discontinuous.

For a different DOS with a more complicated dependence of its shape on the lattice parameter, the dependence of the magnetisation may be more complicated. However, as long as the bandwidth becomes very large for small lattice parameters, the system is paramagnetic for small lattice parameters. With a bandwidth going to zero, as should be expected for a realistic DOS, the system becomes ferromagnetic for sufficiently large lattice parameters within the framework of Stoner theory.

For very large lattice parameters, the single band Stoner model predicts a ferromagnetic state for all materials at zero temperature. This is not consistent with experimental findings. However, for very large lattice parameters, the mobility of the electrons in the band goes to zero and the electrons of the solid become localised on the atoms. Hence, the

Stoner model is inapplicable and a model of localised moments must be used to calculate the magnetic state.

In order to study the dependence of the magnetisation on the lattice parameter at finite temperatures, the results for the rectangular DOS in chapter 7 can be used. The dependence (8.7) of the bandwidth is inserted into the conditions (7.9) and (7.10), which determine the magnetisation of the system. The resulting magnetisation, as a function of the lattice parameter, is shown in Fig. 8.2 for a set of temperatures.
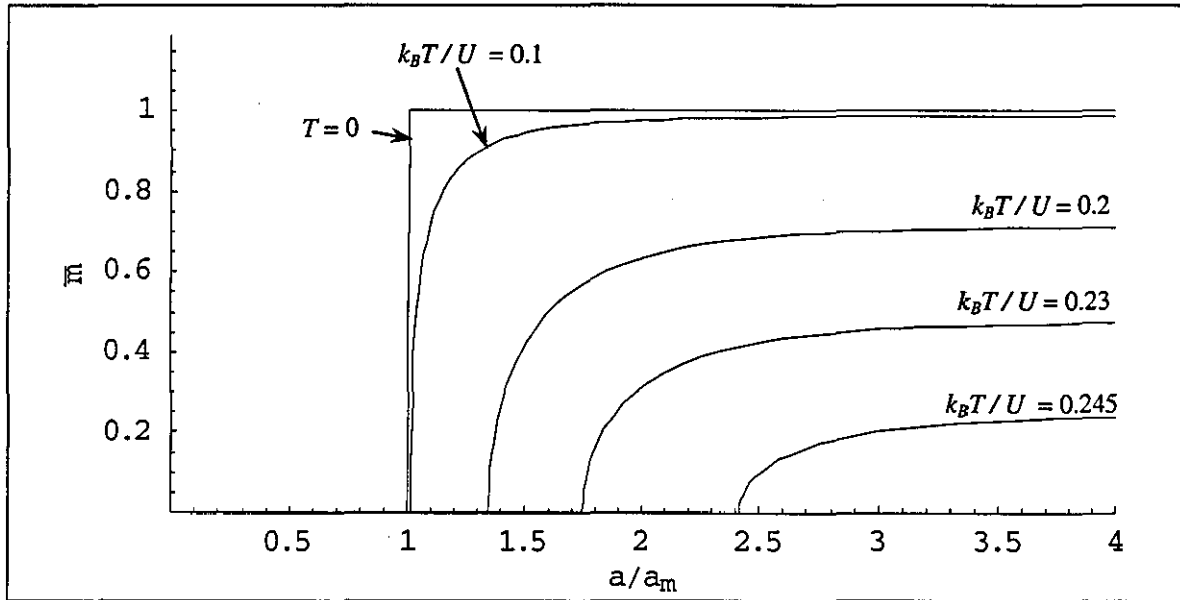
Fig. 8.2: The dependence of the reduced magnetisation $\overline{m}$ on the lattice parameter a (for $n = 1$ and $\beta = 1$).

For $a < a_m$, the magnetisation is zero for all temperatures. For $a > a_m$, the magnetisation is maximal at zero temperatures. At low temperatures, the magnetisation is only noticeably decreased for lattice parameters close to a_m. For higher temperatures, the magnetisation is manifestly decreased for all lattice parameters. The minimal lattice parameter with a non-zero magnetisation $a_{min}(T) = \min\{a \mid m(T,a) \neq 0\}$ increases faster with increasing temperature. The transition from $m(T,a) = 0$ to $m(T,a) > 0$ at $a = a_{min}(T)$ is continuous at finite temperatures in contrast to the transition at $T = 0$. Above the maximum Curie temperature $T_{Cmax} = \max\{T_C(a)\}$, the magnetisation is zero for all lattice parameters.

Since the bandwidth goes to zero for large lattice parameters and the Curie temperature T_C is highest for minimal bandwidth, the maximum Curie temperature is (using (7.26)):
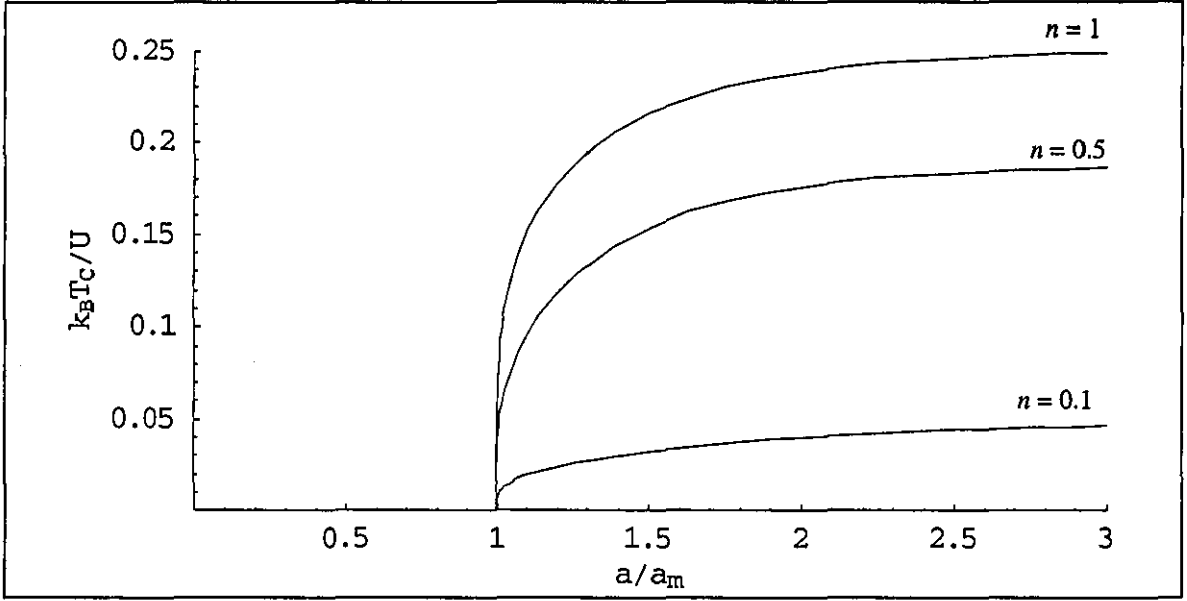
$$k_B T_{C\max} = n(2-n)\frac{U}{4} \tag{8.8}$$

Fig. 8.3: the dependence of Curie temperature T_C on the lattice parameter a for different band fillings n.

The dependence of the Curie temperature on the lattice parameter is shown in Fig. 8.3. For $a < a_m$, the system is paramagnetic at all temperatures and the Curie temperature is not defined. For a close to a_m, the Curie temperature increases rapidly with increasing lattice parameter. For large lattice parameters, the Curie temperature goes to $T_{C\max}$.

8.4 The Pressure Dependence of Magnetisation and Curie Temperature

In a solid, the application of external pressure changes the lattice parameter. For small external pressure, the lattice parameter a depends linearly on the external pressure p_0:

$$a(p_0) = a_0 - \eta\, p_0 \tag{8.9}$$

Here, $a_0 = a(p_0 = 0)$ is the lattice parameter in the absence of external pressure and:

$$\eta = -\left.\frac{da}{dp_0}\right|_{p_0=0} \tag{8.10}$$

The pressure dependence of the magnetisation and Curie temperature follows from the dependence on the lattice parameter. Assuming (8.9) for the lattice parameter and (8.7) for

the bandwidth of a rectangular DOS, the pressure dependence follows straightforwardly from the previous section.
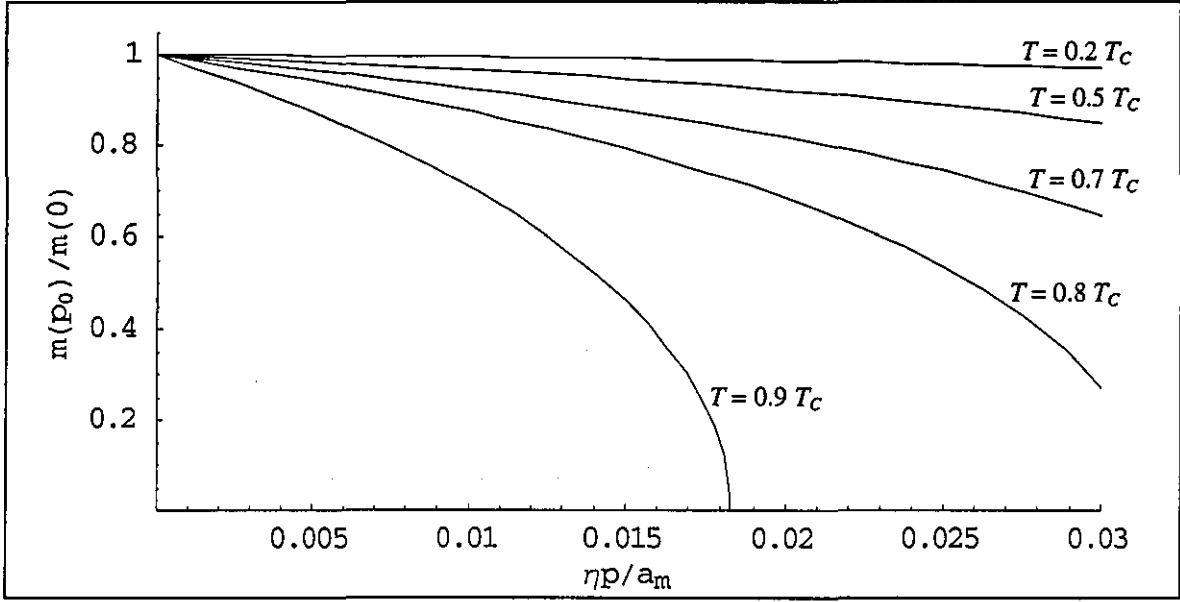

Fig. 8.4: The dependence of magnetisation m on external pressure p_0 at different temperatures T.
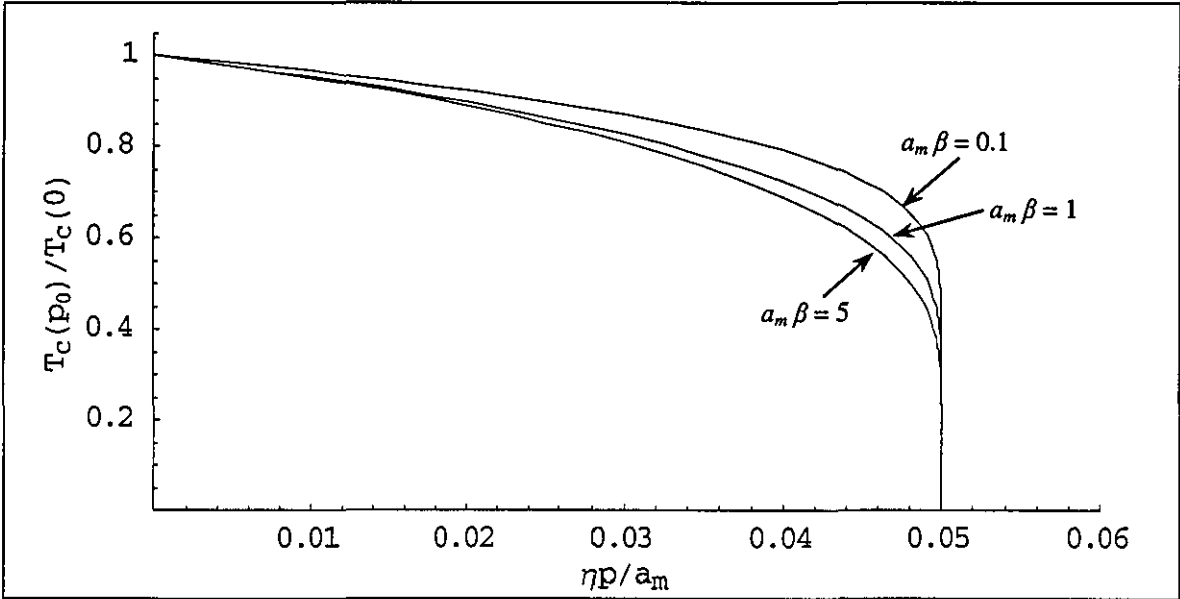Parameters: $a_0/a_m = 1.05$, $a_m\beta = 1$, $n = 0.8$, $k_B T_C/U = 0.12$.

Fig. 8.5: The dependence of the Curie temperature T_C on external pressure p_0.
Parameters: $a_0/a_m = 1.05$, $n = 0.8$, $k_B T_C/U = 0.12$.

The response of the magnetisation to external pressure in the model is shown in Fig. 8.4. The magnetisation decreases with increasing pressure. For low temperatures, the relative decrease in magnetisation is low and almost linear for low pressures. For higher temperatures, the relative decrease in magnetisation is higher and the critical pressure

needed to bring the magnetisation to zero is lower. However, for a pressure large enough to compress the lattice parameter below a_m, the magnetisation is zero for all temperatures. Close to the critical pressure, the dependence of the magnetisation on pressure is non-linear.

The dependence of the Curie temperature on external pressure is shown in Fig. 8.5. At low external pressure, the Curie temperature decreases slowly and almost linearly with increasing pressure. Close to the value of external pressure p_0, where $a(p_0) = a_m$, the Curie temperature decreases faster with temperature and reaches zero for $p_0(a = a_m)$. For higher pressures, the system is paramagnetic at all temperatures and the Curie temperature is not defined.

8.5 Lattice Vibrations

At finite temperatures, the perfect periodicity of the lattice is disturbed by lattice vibrations. The distance between neighbouring ions may be elongated or shortened compared to the lattice parameter of the crystal due to the lattice vibrations. The deviations from the perfect periodicity complicate the description of electronic states. The band picture of the electrons has to be corrected by including the interaction of electrons with lattice vibrations.

At low temperatures, where mainly acoustic long-wavelength phonons are present, the inter-ionic distance varies slowly in space [28]. Compared to electronic time scales, they also vary slowly in time. Therefore, it seems reasonable to divide the whole solid into regions, where the inter-atomic distance is almost constant. Within these regions, the periodicity is mainly preserved and the electronic states may be regarded as states in a local band. Furthermore, a local lattice parameter a_l equal to the local average of the inter-ionic distance can be associated with the region. The width of the local band depends on the local lattice parameter.

The whole crystal then is composed of an ensemble of regions with a local lattice parameter. The statistical distribution of these regions in the crystal can be estimated using the elastic energy associated with the deformation. In the harmonic approximation, the energy V needed to change the inter-ionic distance x from the equilibrium position x_0 is [28]:

$$V(x) = \frac{\kappa}{2}(x - x_0)^2 \tag{8.11}$$

where κ is the elastic constant associated with the deformation.

In classical statistics, the probability p for an inter-ionic distance x is then a Gauss distribution [33]:

$$p(x) = \left(Tr \exp\left\{ -\frac{V(x)}{k_B T} \right\} \right)^{-1} \exp\left\{ -\frac{V(x)}{k_B T} \right\} = \sqrt{\frac{\kappa}{2\pi k_B T}} \exp\left\{ -\frac{\kappa(x - x_0)^2}{2 k_B T} \right\} \tag{8.12}$$

With the global lattice parameter a_0 as the equilibrium distance, the probability of a region in the crystal having a local lattice parameter $a_l = x$ is then:

$$p(a_l) = \sqrt{\frac{\kappa}{2\pi k_B T}} \exp\left\{ -\frac{\kappa(a_l - a_0)^2}{2 k_B T} \right\} \tag{8.13}$$

This step includes fluctuations of the lattice parameter into the model.

With a probability (8.12) of a region having a local lattice parameter, one can calculate the average magnetisation of the whole solid from the local magnetisation, which depends on the local lattice parameter. The limiting case of one well-defined lattice parameter in the whole crystal and a temperature dependent magnetisation has been treated in chapter 7. The opposite limiting case is a local magnetisation

$$m_l(a_l, T) = \begin{cases} m_{max} & for \quad a_l > a_m \\ 0 & for \quad a_l < a_m \end{cases} \quad for\ all\ T \tag{8.14}$$

and a distribution (8.12) of the lattice parameter. The average magnetisation is then

$$
m(T) = \int_{-\infty}^{\infty} p(a_l)\, m_l(a_l, T)\, da_l = m_{max} \int_{-\infty}^{a_m} \sqrt{\frac{\kappa}{2\pi k_B T}} \exp\left\{ -\frac{\kappa(a_l - a_0)^2}{2 k_B T} \right\} da_l
$$

$$
= \frac{m_{max}}{2} \left(1 + erf\left[\sqrt{\frac{\kappa}{2 k_B T}}(a_0 - a_m) \right] \right) \tag{8.15}
$$

with the error function $erf(z) := \frac{2}{\sqrt{\pi}} \int_0^z e^{-t^2} dt$.

For $a_0 > a_m$, the result is shown in Fig. 8.6. The system is fully ferromagnetic at zero temperature. For very low temperatures, the lattice vibrations do not noticeably decrease the magnetisation. Indeed, all coefficients of a power expansion in terms of T around

$T = 0$ are zero. With increasing temperature, the change of magnetisation becomes more rapid. At the temperature

$$T_{2/3} := \frac{\kappa}{3k_B}(a_0 - a_m)^2 \qquad (8.16)$$

the magnetisation is still 96% of the maximum magnetisation, but the slope of the magnetisation vs. temperature curve reaches its maximum. For larger temperatures, the decrease in magnetisation becomes smaller and the magnetisation goes asymptotically to $m_{max}/2$ for $T \rightarrow \infty$.
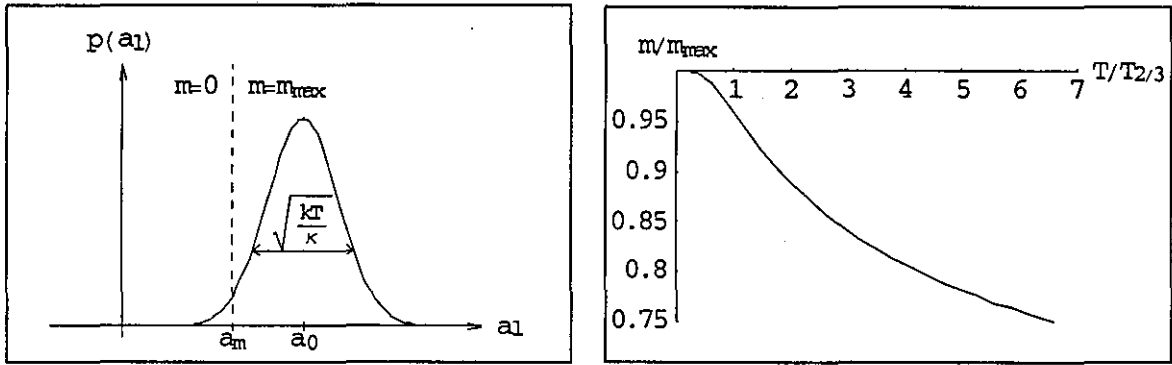

Fig. 8.6: The distribution of the local lattice parameter $p(a_l)$ (schematic) and the magnetisation m as a function of temperature T.

However, for high temperatures, the local magnetisation can not be regarded as constant with temperature. With a dependence of the magnetisation on the local lattice parameter as discussed in section 8.3 for the rectangular band and a distribution (8.13) of the local lattice parameter, the average magnetisation can be calculated taking into account both effects. The average magnetisation is then calculated by

$$m(T) = \int_{-\infty}^{\infty} p(a_l) m_l(a_l, T) \, da_l \qquad (8.17)$$

with a local magnetisation, which depends on temperature as calculated in section 7.3 in contrast to the simple dependence presented by (8.14).

The resulting reduced magnetisation is shown in Fig. 8.7 for different values of κ. In the case of absent magneto-elastic coupling, the bandwidth is independent of the lattice parameter. This case is equivalent to the limit $\kappa \rightarrow \infty$, where the case of a constant lattice parameter throughout the solid at all temperatures is recovered. In this limit, the Curie temperature T_C is well defined and can be used to calculate the reduced temperature

$\bar{T} = T/T_C$. The limit $\kappa \to 0$ corresponds to a temperature dependence (8.15) of the magnetisation.

For $0 < \kappa < \infty$, the resultant average magnetisation is shown in Fig. 8.7. At low temperatures, the magnetisation falls off faster with increasing temperature for a softer lattice, i.e. smaller κ. However, above a temperature closely below the Curie temperature, the magnetisation is larger for smaller κ. For finite κ, there is a tail of non-zero magnetisation above the Curie temperature. The temperature range of visible non-zero magnetisation becomes larger with decreasing κ.
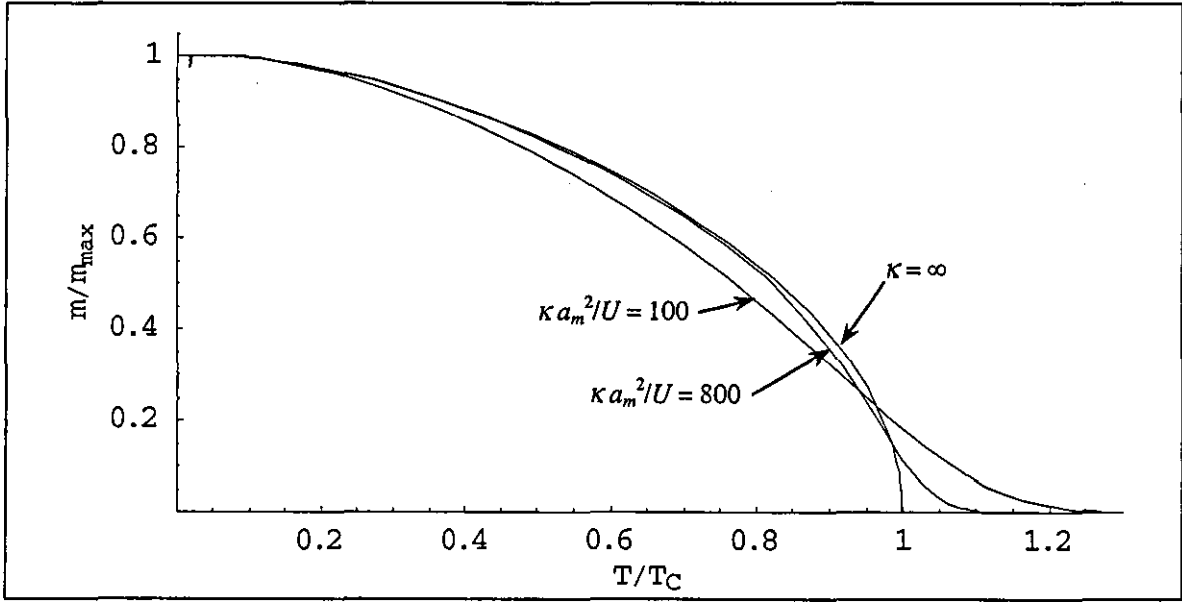
Fig. 8.7: The magnetisation m as a function of the temperature T for different elastic constants κ. Parameters: $a_0/a_m = 1.05$, $a_m\beta = 1$, $n = 1$, $k_B T_C/U = 0.13$.

For a soft lattice, the reduced magnetisation is similar to the curves of Invar materials. In comparison with most other ferromagnetic transition metals and alloys, the magnetisation of Invar compounds decreases much faster with increasing temperature. Furthermore, they show a pronounced tail of non-zero magnetisation above the Curie temperature. It is believed that these deviations from the behaviour shown by FeNi alloys with different composition occur due to the large magneto-elastic coupling present in Invar alloys.

In order to compare the model with experimental data, a reasonable range of parameters has to be chosen. For the transition metals Fe and Ni, the width of the d-band is approximately 5eV. The effective on-site repulsion U is of the same order of magnitude, but difficult to estimate. To achieve a ferromagnetic ground state, the on-site repulsion is assumed slightly larger than the bandwidth. For $Fe_{65}Ni_{35}$ Invar alloy, the saturation magnetisation at zero temperature is about $2\mu_B$ per atom, which is consistent with a filling

of the d-band states of approximately 80%. The possible dependence of the bandwidth on the lattice parameter and the rigidity of the lattice are more difficult to estimate.
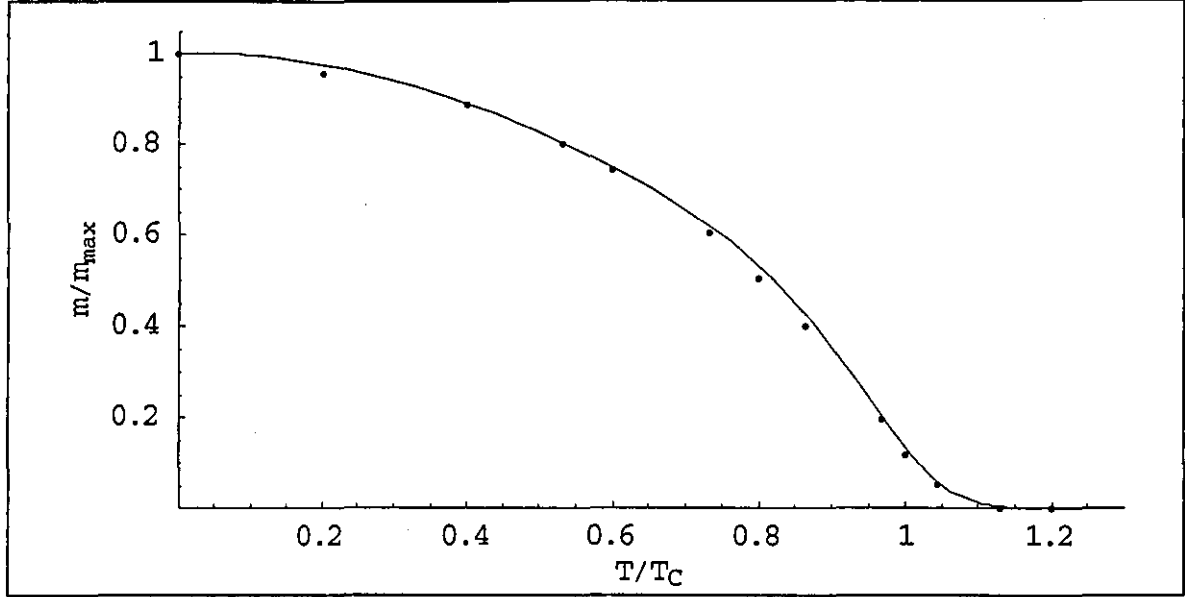

Fig. 8.8: Comparison of reduced magnetisation m/m_{max} as function of reduced temperature T/T_C of the model (line) to experimental data of $Fe_{65}Ni_{35}$ (dots) [21].

In Fig. 8.8, the measured reduced magnetisation of $Fe_{65}Ni_{35}$ Invar alloy [21] is compared to the reduced magnetisation calculated using (8.17) for an adjusted set of parameters. The parameters chosen are: $n = 1.8$, $U = 5.13eV$, $a_0/a_m = 1.02567$, $\beta\, a_m = 1$ and $\kappa\, a_m^2 = 2800$. This yields a bandwidth $W(a_0) = 5eV$ and a Curie temperature $T_C = 0.136eV$, which is too large compared to the Curie temperature $T_C = 0.045eV$ [21] observed in $Fe_{65}Ni_{35}$, as typical for the Stoner model. However, concerning the simplicity of the model used, the curves of the reduced magnetisation vs. reduced temperature are in excellent agreement.

8.6 Periodic Lattice Distortions

The model used to study the dependence of the magnetisation on the lattice parameter may not only be used to describe systems in thermal equilibrium, but also certain situations, where the system is not in its equilibrium state. In a crystal at zero temperature, each nucleus in the crystal is located at its equilibrium position and the lattice can be seen as having the perfect periodicity of the lattice parameter. However, the crystal may be shifted away from equilibrium by the creation of a single phonon, for example by inelastic scattering of a neutron at a nucleus. Due to the much smaller time scales of their dynamics, the electrons may have adjusted to the new positions of the nuclei, before the phonon

decays and the lattice finds back to its equilibrium. Furthermore, there may be situations, where a static distortion of the lattice occurs.

Consider a lattice, which is distorted by a sinusoidal modulation of the inter-ionic distance:

$$a(\mathbf{r}) = a_0 + A\sin(\mathbf{k} \cdot \mathbf{r}) \qquad (A > 0, \mathbf{k} \neq 0) \tag{8.18}$$

Here, a_0 is the inter-ionic distance in absence of the distortion, i.e. the lattice parameter, A the amplitude and $\mathbf{k}$ the wave vector of the distortion. The whole crystal may then be seen as composed of many small regions with a local lattice parameter $a_l = a(\mathbf{r})$. The width $W(\mathbf{r})$ of the local electron band with rectangular DOS in a region around $\mathbf{r}$ is assumed to depend on the local lattice parameter:

$$W_l(\mathbf{r}) = W_0 \exp[-\beta\, a(\mathbf{r})] \tag{8.19}$$

At zero temperature, the magnetisation of each region is then:

$$m_l(\mathbf{r}) = \begin{cases} \pm m_{max} & for \quad a(\mathbf{r}) > a_m \\ 0 & for \quad a(\mathbf{r}) < a_m \end{cases} \tag{8.20}$$

where $a_m := -\beta^{-1}\ln(U/W_0)$ is the lattice parameter, at which the bandwidth and the on-site repulsion are equal. The resulting average magnetisation then can be calculated by integrating over the whole volume V of the crystal:

$$m = \frac{1}{V}\int_V m_l(\mathbf{r})\, d\mathbf{r} \tag{8.21}$$

Without any distortions, the average magnetisation is either zero or maximal:

$$m = \begin{cases} m_{max} & for \quad a_0 > a_m \\ 0 & for \quad a_0 < a_m \end{cases} \tag{8.22}$$

This does not have to be the case for a finite distortion. With $z := \mathbf{k} \cdot \mathbf{r}$ and

$$m_l(z) = \begin{cases} m_{max} & for \quad a_0 - a_m + A\sin(z) > 0 \\ 0 & for \quad a_0 - a_m + A\sin(z) < 0 \end{cases} \tag{8.23}$$

one obtains:

$$m = \frac{1}{V}\int_V m_l(\mathbf{r})\,d\mathbf{r} = \frac{1}{V}\int_V m_l(a(\mathbf{r}))\,d\mathbf{r} = \frac{1}{2\pi}\int_0^{2\pi} m_l(a(z))\,dz = \frac{1}{2\pi}\int_0^{2\pi} m_l(z)\,dz$$

$$= m_{max}\begin{cases} 1 & for \quad (a_0 - a_m) > A \\ \dfrac{1}{\pi}\arccos\left(\dfrac{a_m - a_0}{A}\right) & for \quad A > (a_0 - a_m) > -A \\ 0 & for \quad -A > (a_0 - a_m) \end{cases} \qquad (8.24)$$
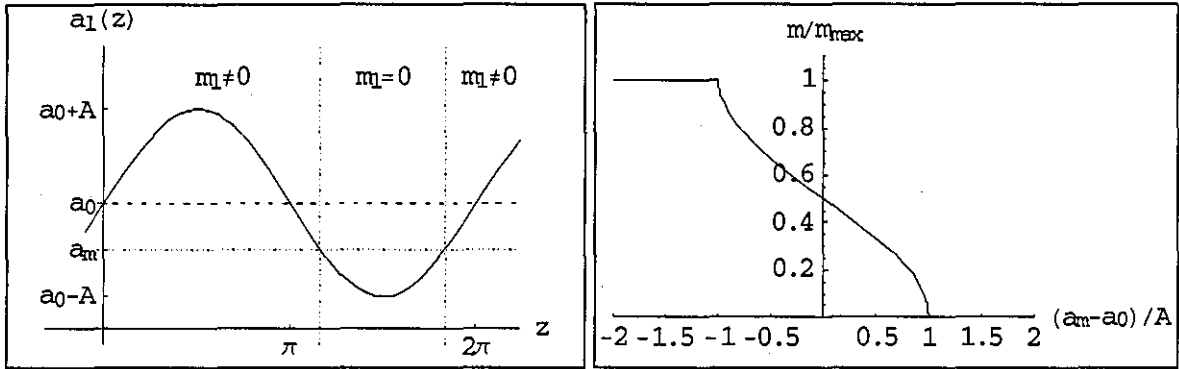
The result is shown in Fig. 8.9.

Fig. 8.9: The local lattice parameter $a_l(z)$ and the average magnetisation m.

The average magnetisation depends on the ratio of the difference $(a_m - a_0)$ and the amplitude A of the distortion. If $(a_m - a_0) > A$, the magnetisation is not affected by the distortion, since all regions have a local lattice parameter smaller than a_m and therefore the average magnetisation remains zero. For $(a_0 - a_m) > A$, the local lattice parameter is larger than a_m throughout the crystal and the average magnetisation is maximal. Only if a_m and a_0 are close enough, i.e. $|a_0 - a_m| < A$, the lattice parameter is in some regions larger than a_m and smaller in others. Consequently, the average magnetisation takes a value between zero and maximum magnetisation in contrast to the magnetisation in absence of distortions.

8.7   Coupling of Lattice Parameter and Magnetisation

So far, only the dependence of the magnetisation on the lattice parameter has been studied. Now, the dependence of lattice parameter on the magnetisation will be taken into consideration, too. The origin of the inter-ionic potential, which defines the equilibrium distance between neighbouring ions, is the interplay between the Coulomb repulsion

between the ions and the gain in electronic energy by forming partially filled electron bands.

A large part of the cohesive energy of the crystal comes from the electrons in the conduction band. The part E_C of the cohesive energy from the conduction electrons may be approximated near its equilibrium position by a harmonic potential:

$$E_C(x) = \frac{\xi}{2} x^2 \tag{8.25}$$

Here,

$$x := a - a_{0C} \tag{8.26}$$

is the deviation of the inter-ionic distance a from the equilibrium position a_{0C} of E_C and ξ the elastic constant of the harmonic approximation of E_C. For simplicity, it is assumed that further contributions to the inter-ionic potential, which are not due to the rectangular band, are included in E_C. With (5.12) and (8.3), the energy of the rectangular band at zero temperature is:

$$E_R(x,m) = \frac{W_0 \exp[-\beta x]}{4}(n^2 - 2n + m^2) + \frac{U}{4}(n^2 - m^2) \tag{8.27}$$

It depends on the magnetisation m, which can take values between $-m_{max}$ and m_{max} with $m_{max} = \min\{n, 2-n\}$.

The total energy is the sum of both contributions:

$$\begin{aligned} E(x,m) &= E_C(x) + E_R(x,m) \\ &= \frac{\xi}{2} x^2 + \frac{W_0 \exp[-\beta x]}{4}(n^2 - 2n + m^2) + \frac{U}{4}(n^2 - m^2) \end{aligned} \tag{8.28}$$

The total energy becomes unstable for negative x with sufficient magnitude. Since (8.28) is only a reasonable approximation for small $|x|$, the considerations will be restricted to these values of x.

In equilibrium, the energy is a minimum of both m and x. Let m_0 and x_0 denote the values of m and x, for which the total energy is minimal. The minimum value x_0 must satisfy

$$0 = \frac{\partial E}{\partial x}\bigg|_{x=x_0} = \xi x_0 - \frac{\beta}{4} W_0 \exp[-\beta x_0](n^2 - 2n + m^2) \tag{8.29}$$

and:

$$0 < \frac{\partial^2 E}{\partial x^2}\bigg|_{x=x_0} = \xi + \frac{\beta^2}{4} W_0 \exp\left[-\beta x_0\right](n^2 - 2n + m^2) \tag{8.30}$$

This yields:

$$x_0 = \frac{1}{\beta} \text{product} \log\left[\frac{\beta^2 W_0(n^2 - 2n + m^2)}{4\xi}\right] \tag{8.31}$$

where $\text{product} \log[z]$ is the principal solution for $z = w\, e^w$.

For all choices of parameters, x_0 is negative. For a fixed set of parameters, x_0 is smaller for magnetisation values with smaller magnitude. Therefore, as a guideline, a paramagnetic state has lower volume than a ferromagnetic state. For the magnetisation, it is sufficient to restrict the calculation to $n \leq 1$, since for $2 - n$, one obtains the same results as for n. For $n \leq 1$, the maximum magnetisation is $m_{\max} = n$ and therefore:

$$m_0 = \begin{cases} n & for & U > W_0 \exp\left[-\beta x\right] \\ 0 & for & U < W_0 \exp\left[-\beta x\right] \end{cases} \tag{8.32}$$

The total energy landscape for various parameters is shown in Fig. 8.10. The system shows a surprisingly rich behaviour. For $W_0 > U$, $W_0 \exp\left[-\beta x\right] > U$ for all m and therefore, the system is paramagnetic:

$$\left.\begin{aligned} m_0 &= 0 \\ x_0 &= \frac{1}{\beta} \text{product} \log\left[\frac{\beta^2 W_0(n^2 - 2n)}{4\xi}\right] \end{aligned}\right\} \quad for\, W_0 > U \tag{8.33}$$

For $W_0 \ll U$, the system is fully magnetic:

$$\left.\begin{aligned} m_0 &= \pm m_{\max} \\ x_0 &= \frac{1}{\beta} \text{product} \log\left[\frac{\beta^2 W_0(2n^2 - 2n)}{4\xi}\right] \end{aligned}\right\} \quad for\, W_0 \ll U \tag{8.34}$$

For W_0 smaller, but close to U, there may exist both a stable paramagnetic state with low lattice parameter and a stable fully ferromagnetic state with higher lattice parameter:

$$\left.\begin{aligned} m_{0\,ferro} &= \pm m_{\max} \\ x_{0\,ferro} &= \frac{1}{\beta} \text{product} \log\left[\frac{\beta^2 W_0(2n^2 - 2n)}{4\xi}\right] \end{aligned}\right\} \quad \text{and}$$

$$\left.\begin{aligned} m_{0\,para} &= \pm m_{\max} \\ x_{0\,para} &= \frac{1}{\beta} \text{product} \log\left[\frac{\beta^2 W_0(n^2 - 2n)}{4\xi}\right] \end{aligned}\right\} \tag{8.35}$$

78

The energy difference between both states depends on the system parameters. However, the energy barrier between the two states may be very small. Hence, the activation energy needed to transform parts of the system from the ground state to the meta-stable state may be accessible for thermal excitations.
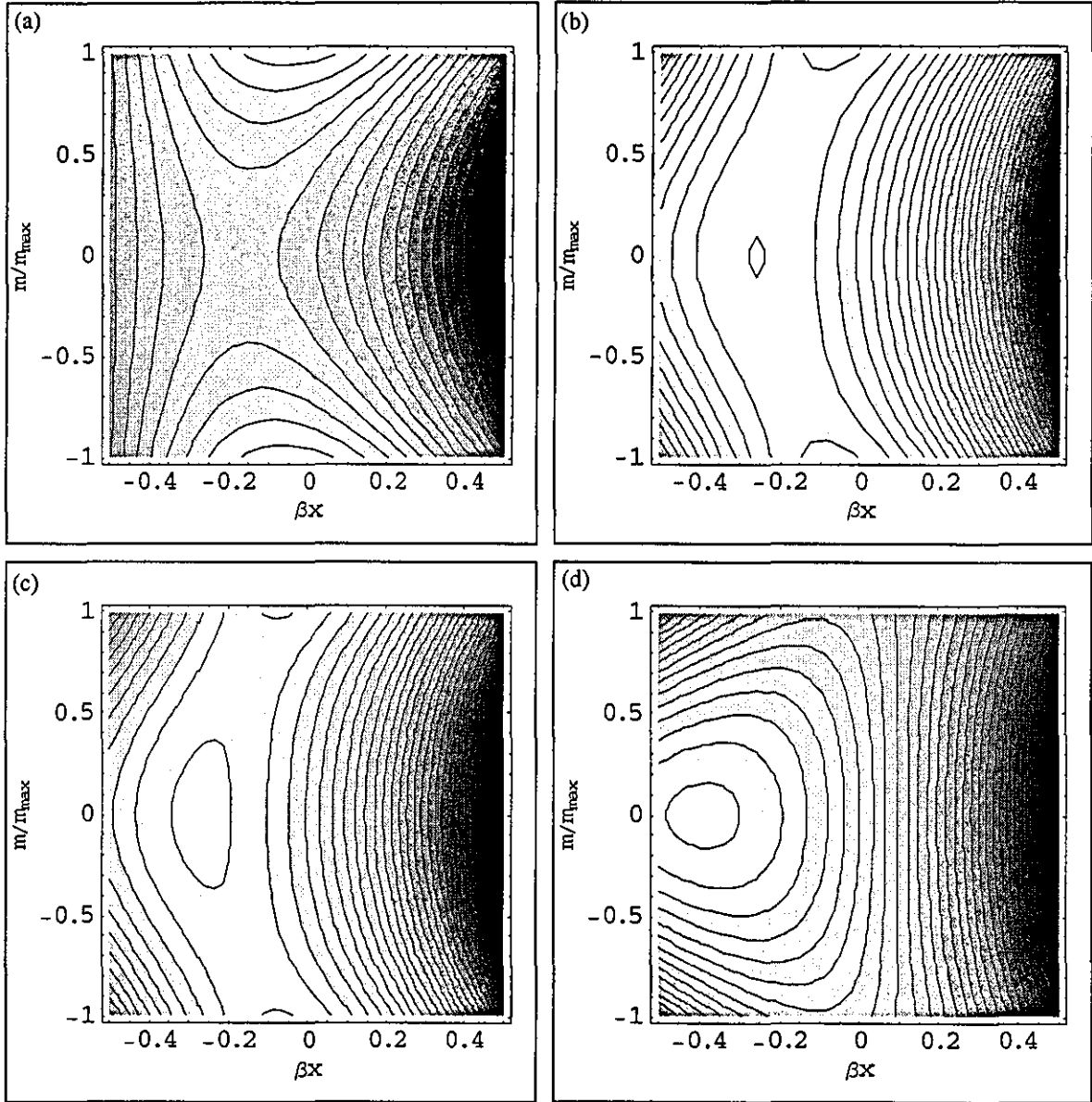

Fig. 8.10: The total energy E as a function of magnetisation m and deviation x.

Darker areas represent higher values of E. Parameters: $n = 0.8$, $\xi / U\beta^2 = 1$.

(a) $W_0/U = 0.6$: The minima of the energy are at $(m / m_{max} = \pm 1, \beta x = -0.05)$. The system is ferromagnetic.

(b) $W_0/U = 0.8386$: Besides the minima at $(\pm 1, -0.072)$ a local minimum at $(0, -0.261)$ with slightly higher energy occurs.

(c) $W_0/U = 0.854$: The minimum at $(0, -0.268)$ has lower energy than the local minima at $(\pm 1, -0.074)$.

(d) $W_0/U = 1.1$: There is only one minimum, namely at $(0, -0.39)$. The system is paramagnetic.

Assuming a ferromagnetic ground state and that with increasing temperature the total energy landscape is not deformed very much from its $T = 0$ form, thermal excitations may lead not only to a reduction of the magnetisation, but also to a volume reduction. For the case of another paramagnetic low-volume state being close in energy to the ferromagnetic one, the volume reduction may become significant.

For zero temperature, total-energy contours exhibiting both a high-volume high-moment (HS) and low-volume low-moment (LS) state have been calculated, for example, by Morruzzi [40] for ordered Fe_3Ni as a model for $Fe_{65}Ni_{35}$ Invar and by Schröter and Entel [41] for ordered Fe_3Pt. The theoretical calculations predicting the occurrence of the HS and LS states support the phenomenological two-state model of Weiss [42]. This early model seeks to explain the low or negative thermal expansion of Invar materials. It is based on the volume reduction due to the thermal excitation from the HS state to the LS state. However, experimental evidence for the existence of the two states has not been forthcoming. Furthermore, neutron diffraction experiments on $Fe_{65}Ni_{35}$ [43] question models invoking the thermal population of two states with a different number of e_g and t_{2g} sub-band carriers. This objection does not apply to the simple model presented here. Only one single band is considered with a fixed the number of electrons. No electrons are exchanged with other bands in the solid or the environment and therefore, the distribution of the electrons among different bands in the solid does not change. Furthermore, the model has the property that x_0 is smaller for smaller $|m|$ even without two pronounced minima of the total energy. This effect may give a negative magnetic contribution to the thermal expansion in the ferromagnetic regime within such a model.

8.8 Thermal Expansion and Magnetostriction

In the last section, the dependence of the total energy on both magnetisation and lattice parameter suggested a negative contribution from the coupling of the magnetisation to the thermal expansion. In this section, an example will be presented of a calculation of the lattice parameter and the magnetisation for finite temperatures based on the Stoner model.

In most solids, the thermal expansion can be roughly described by the Debye approximation [29]. In this approximation, the specific heat per atom is:

$$c_v = 9k_B \left(\frac{T}{\Theta_D} \right)^3 \int_0^{\Theta_D/T} \frac{x^4 e^x}{\left(e^x - 1 \right)^2} dx \qquad (8.36)$$

The Debye temperature Θ_D can be obtained from experimental data. The linear thermal expansion coefficient

$$\alpha = \frac{1}{l}\left(\frac{\partial l}{\partial T}\right)_p \tag{8.37}$$

as the relative change of length l of the crystal with temperature T at constant pressure p, is proportional to the specific heat c_v:

$$\alpha = \frac{\gamma}{3B}c_v \tag{8.38}$$

The overall Grüneisen parameter γ describes the volume dependence of phonon frequencies and the Bulk modulus B is the inverse compressibility. Within the Debye approximation, γ is independent of temperature. The bulk modulus is only weakly temperature dependent [29]. If the temperature dependence of the bulk modulus is neglected, one obtains for the lattice parameter:

$$a(T) = a_0\left(1 + \int_0^T \alpha(T')dT'\right) = a_0\left(1 + \frac{\gamma}{3B}\int_0^T c_v(T')dT'\right) \tag{8.39}$$

The weak temperature dependence of the bulk modulus implies a weak temperature dependence of the elastic constant describing the change of the lattice parameter by application of pressure.

Now the results of the Debye model will be used to develop a model of thermal expansion incorporating the effects of a narrow band, which may be polarised at low temperatures. The narrow band will be again described by the rectangular band. The part of the free energy, which does not originate from the rectangular band, is approximated by a harmonic potential with a temperature-dependent equilibrium distance:

$$F_C(x) = \frac{\xi}{2}(x - \delta(T))^2 \tag{8.40}$$

Here,

$$x := a - a_{0C} \tag{8.41}$$

is the deviation of the inter-ionic distance a from the equilibrium position a_{0C} of F_C at $T = 0$ and ξ the elastic constant of the harmonic approximation of F_C. The shift of the equilibrium position with temperature $\delta(T)$ is chosen to reproduce a temperature

dependence of the lattice parameter according to (8.39), if the rectangular band is neglected:

$$\delta(T) = \alpha_\infty a_{0C} \, 3 \int_0^T D(T'/\Theta_D) \, dT' \tag{8.42}$$

with

$$D(t) := t^3 \int_0^{1/t} \frac{x^4 e^x}{(e^x - 1)^2} \, dx \tag{8.43}$$

The parameters of the shift $\delta(T)$ are the high-temperature thermal expansion coefficient α_∞ and the Debye temperature Θ_D. With these parameters and a_{0C}, a reference length for the thermal expansion can be defined as:

$$x_0 := \alpha_\infty \Theta_D \, a_{0C} \tag{8.44}$$

This distance is roughly the total length change of the lattice parameter caused by raising the temperature by the amount of the Debye temperature.

Assuming a deviation dependence of the bandwidth

$$W(x) = W_0 \exp\left[-\beta x^2\right] \tag{8.45}$$

and using (7.2) to (7.6), (7.8) and (8.3), the free energy F_R of the rectangular band can be expressed in terms of the magnetisation m and the deviation x. By help of [38], an analytical expression can be found for $F_R(W(x), m)$, which can be used to find analytical expressions for the derivatives of F_R [44].

The free energy of the whole system is the sum of both contributions:

$$F(x, m) = F_C(x) + F_R(W(x), m) \tag{8.46}$$

The equilibrium values of the magnetisation and the deviation minimise the free energy. Therefore, they satisfy:

$$\left.\begin{array}{l} 0 = \left(\dfrac{\partial F}{\partial x}\right)_{m,n,T,B_0} = \xi(x - \delta(T)) + \left(\dfrac{\partial F_R}{\partial x}\right)_{m,n,T,B_0} \\[4mm] 0 = \left(\dfrac{\partial F}{\partial m}\right)_{x,n,T,B_0} = \left(\dfrac{\partial F_R}{\partial m}\right)_{x,n,T,B_0} \end{array}\right\} \tag{8.47}$$

In actual calculations, the minimum values will be obtained by solving these coupled equations numerically. The stability of the solutions is analysed by calculating the matrix of the second derivatives and checking if it is positive definite.
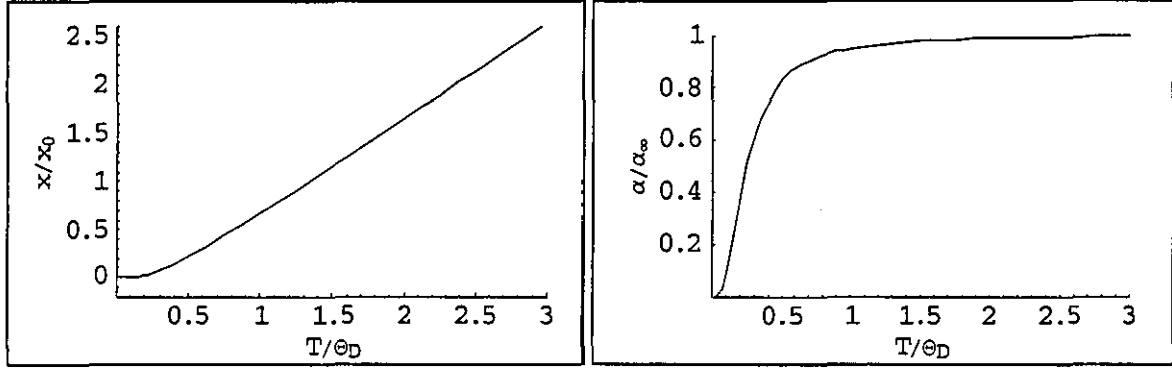

Fig. 8.11: The deviation x and the thermal expansion α as functions of temperature T for a distance-independent bandwidth.

For a rectangular band with distance-independent bandwidth, i.e. $\beta = 0$, the behaviour of the model is shown in Fig. 8.11. The deviation is independent of the magnetic state of the system. Moreover, it is identical to the case without rectangular band. The contribution of the rectangular band merely shifts the free energy of the system uniformly for a given magnetisation. Therefore, this contribution does not alter the x-values of the minima of the free energy. Hence, the resulting thermal expansion follows the Debye approximation.
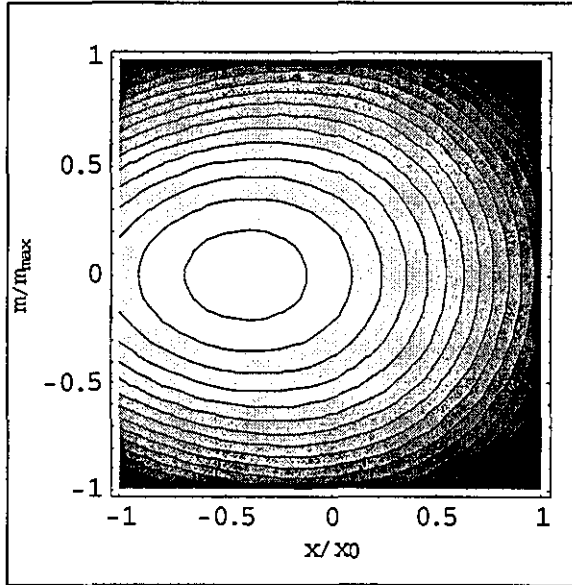
Fig. 8.12: The free energy F as function of magnetisation m and deviation x for a distance-dependent bandwidth and paramagnetic ground state.

Parameters: $n = 0.8$, $U = 0$, $W_0 / k_B \Theta_D = 5$,

$\zeta x_0^2 / k_B \Theta_D = 1$, $\beta x_0 = 0.2$.

Darker areas represent higher values of F.

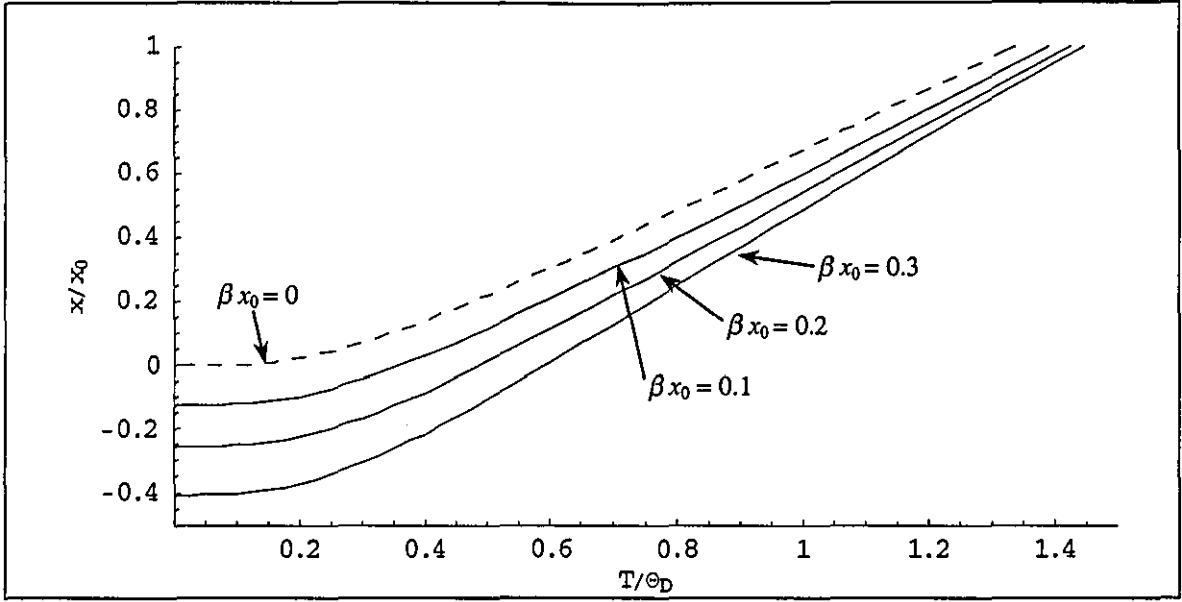The minimum of F is shifted towards smaller x-values.

Fig. 8.13: The deviation x as function of temperature T for a paramagnetic ground state.

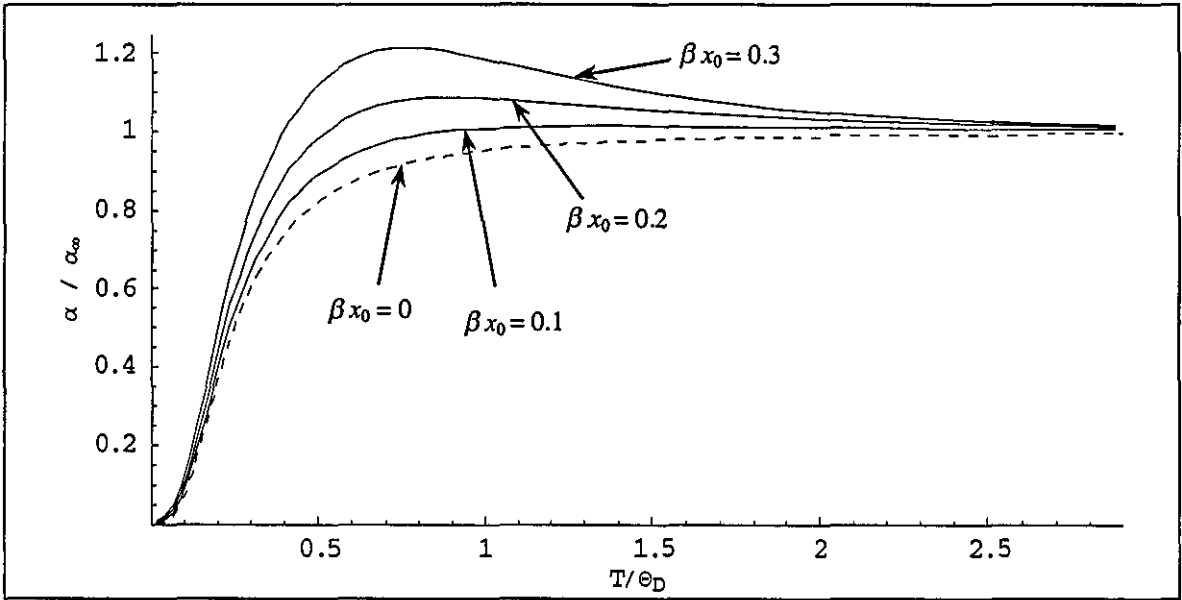Parameters: $n = 0.8$, $U = 0$, $W_0 / k_B \Theta_D = 5$, $\xi x_0^2 / k_B \Theta_D = 1$.

Fig. 8.14: The thermal expansion α as a function of temperature T for a paramagnetic ground state. Parameters: as Fig. 8.13.

The case of a band with distant-dependent bandwidth and a paramagnetic ground state is shown in Fig. 8.12 to Fig. 8.14. The inclusion of the rectangular band shifts the equilibrium deviation towards smaller values. The shift is larger for larger β, i.e. stronger distance-dependence of the bandwidth, or smaller ξ, i.e. a softer lattice. Furthermore, the shift is larger for a larger bandwidth W_0. It is also larger for a band filling closer to $n = 1$, where the gain in energy by increasing the bandwidth is largest. At higher temperatures, the

cohesive energy of the rectangular band diminishes due to thermal excitation of electrons from the lower to the upper part of the band. Consequently, the shift of the equilibrium deviation becomes smaller and the lattice parameter approaches its value without a rectangular band for $T \rightarrow \infty$. The resulting thermal expansion follows roughly the Debye approximation, but is higher than for a distance-independent bandwidth, in particular at intermediate temperatures.
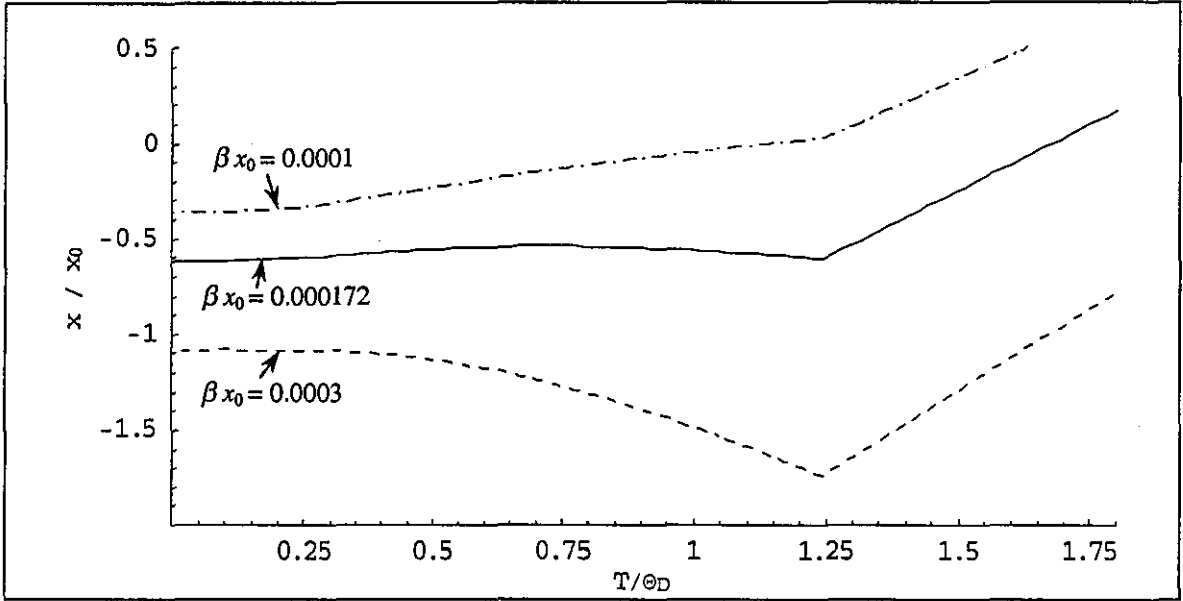

Fig. 8.15: The deviation x as function of temperature T for a ferromagnetic ground state.

Parameters: $n=0.8$, $U/k_B\Theta_D=10.5$, $W_0/k_B\Theta_D=10$, $\xi x_0^2/k_B\Theta_D=0.00022$. The kinks mark the Curie temperature.
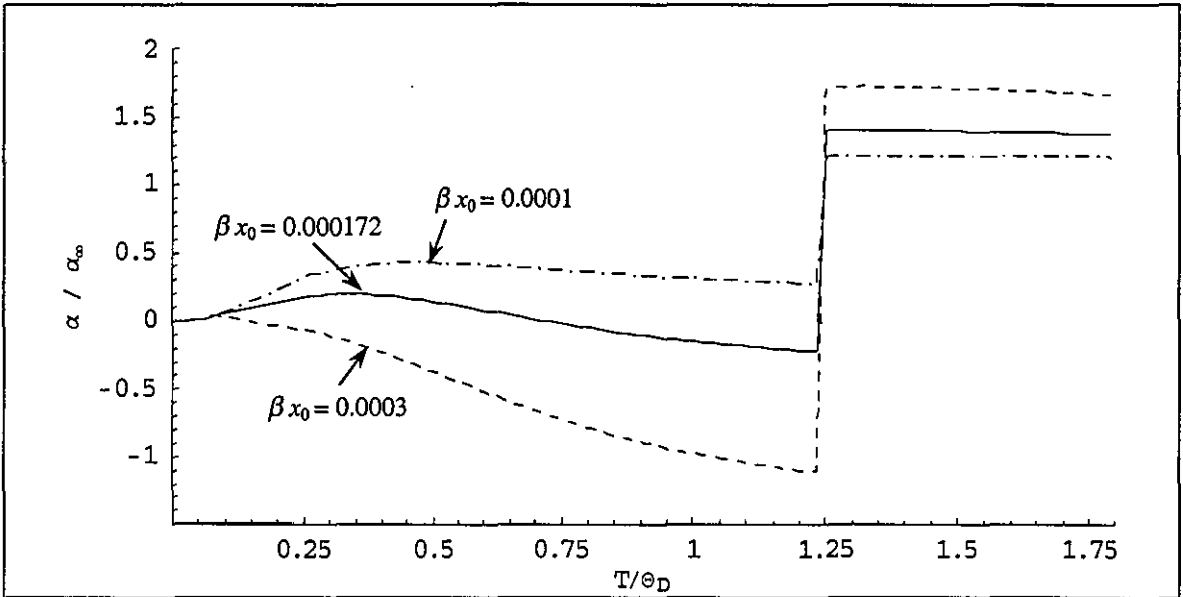

Fig. 8.16: The thermal expansion α as function of temperature T for a ferromagnetic ground state.

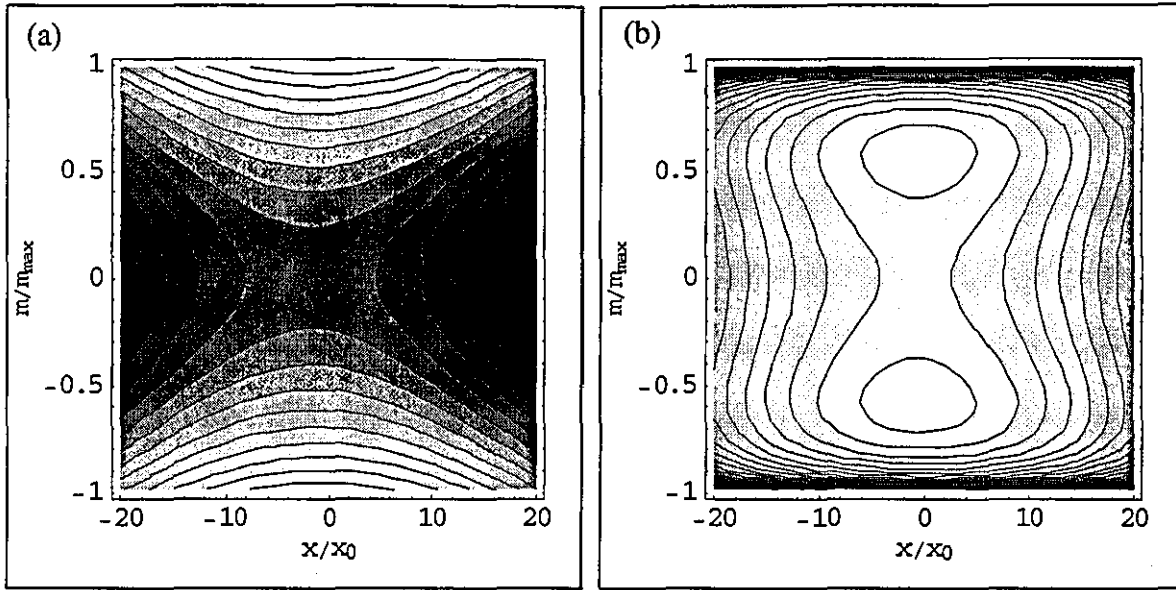Parameters: as Fig. 8.15. The jumps in the curves mark the Curie temperature.

Fig. 8.17: The free energy F as function of deviation x and magnetisation m for a ferromagnetic ground state.

Parameters: $n = 0.8$, $U/k_B\Theta_D = 10.5$, $W_0/k_B\Theta_D = 10$, $\xi x_0^2/k_B\Theta_D = 0.00022$, $\beta x_0 = 0.000172$.

(a) $T = 0$: The minima of the energy are at $(m/m_{max} = \pm 1, x/x_0 = -0.05)$.

(b) $T/\Theta_D = 1$: The minima have moved toward smaller absolute values of m.

Above $T_C = 1.244\,\Theta_D$, the shape of the free energy is similar to Fig. 8.12.
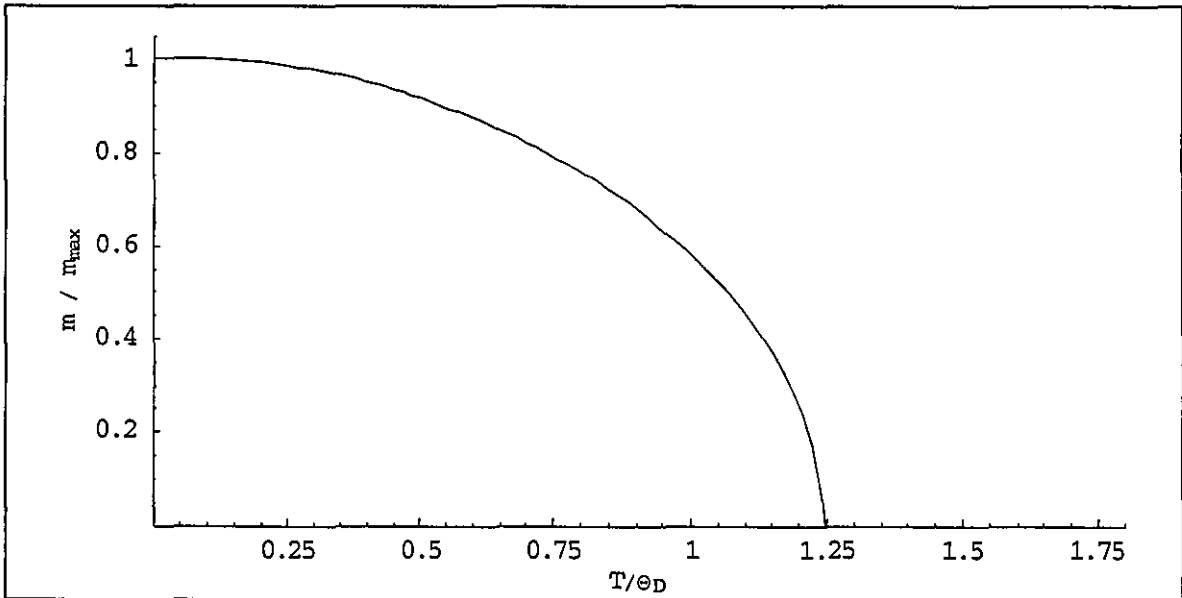

Fig. 8.18: The magnetisation m as function of T for a ferromagnetic ground state.

Parameters: as Fig. 8.17.

The curves for $\beta x_0 = 0.0003$ and $\beta x_0 = 0.0001$ are almost identical to the shown curve.
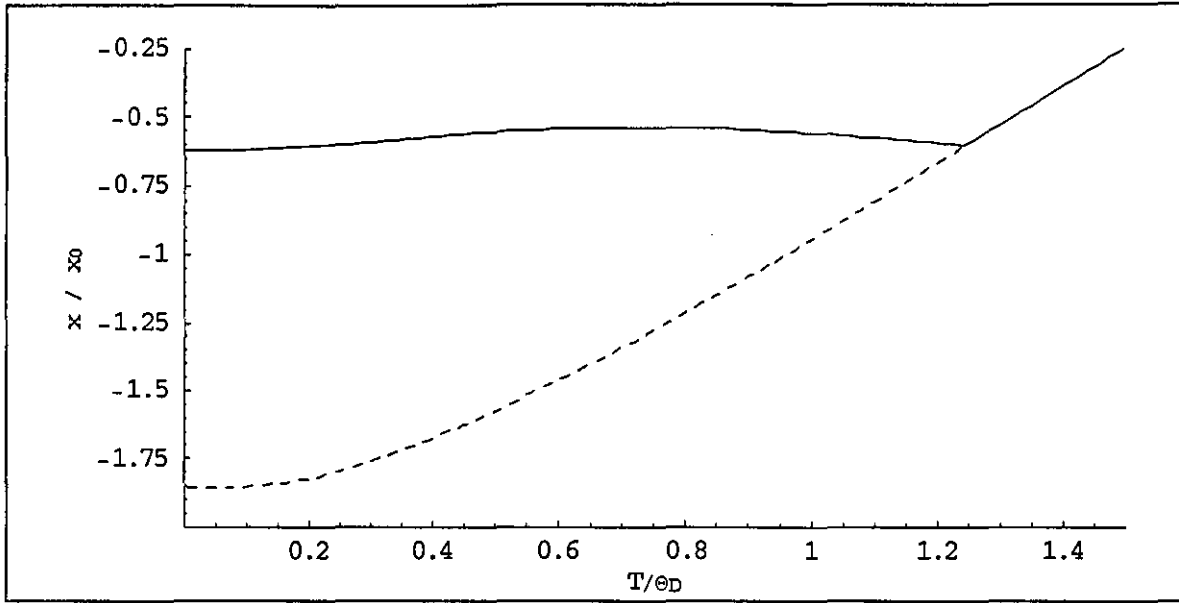
Fig. 8.19: The deviation x of a system with a ferromagnetic ground state (solid line) compared to a similar system staying paramagnetic below $T_C = 1.244\,\Theta_D$ (dashed line).
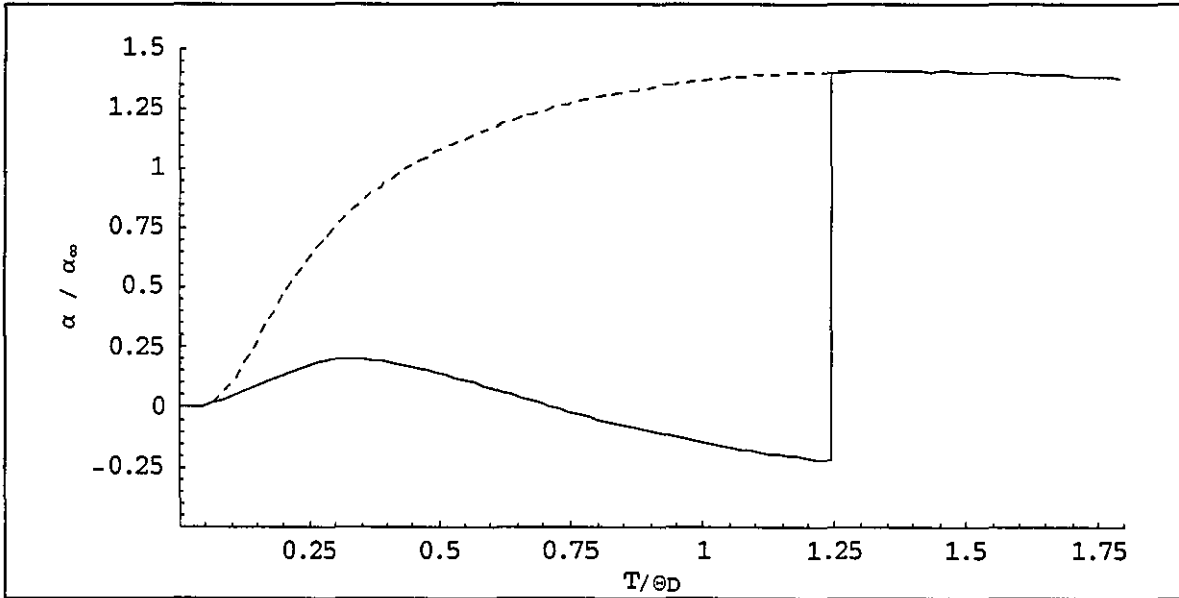
Parameters: as Fig. 8.17.

Fig. 8.20: Comparison of the thermal expansion of a system with ferromagnetic ground state (solid line) to a similar system with paramagnetic ground state (dashed line).

Parameters: as Fig. 8.17.

For a rectangular band with a ferromagnetic ground state, the behaviour is illustrated in Fig. 8.15 to Fig. 8.21. As seen in Fig. 8.18, the magnetisation as a function of temperature is very similar to the case of a distance-independent bandwidth. However, the behaviour of the deviation differs noticeably from the case of a distance-independent bandwidth. The deviation increases much slower with temperature in the ferromagnetic phase. For a large

distance-dependence, the deviation may even decrease with increasing temperature. As illustrated in Fig. 8.20, the resulting thermal expansion is decreased in the ferromagnetic phase compared to the case of a paramagnetic system and therefore, to the case of a distance-independent bandwidth. The decrease in the thermal expansion is larger for stronger distance-dependence β of the bandwidth, or smaller elastic constant ξ. Furthermore, the decrease is larger for a larger bandwidth W_0 and a band filling closer to $n = 1$. For a certain set of parameters, the thermal expansion may almost vanish or become negative.
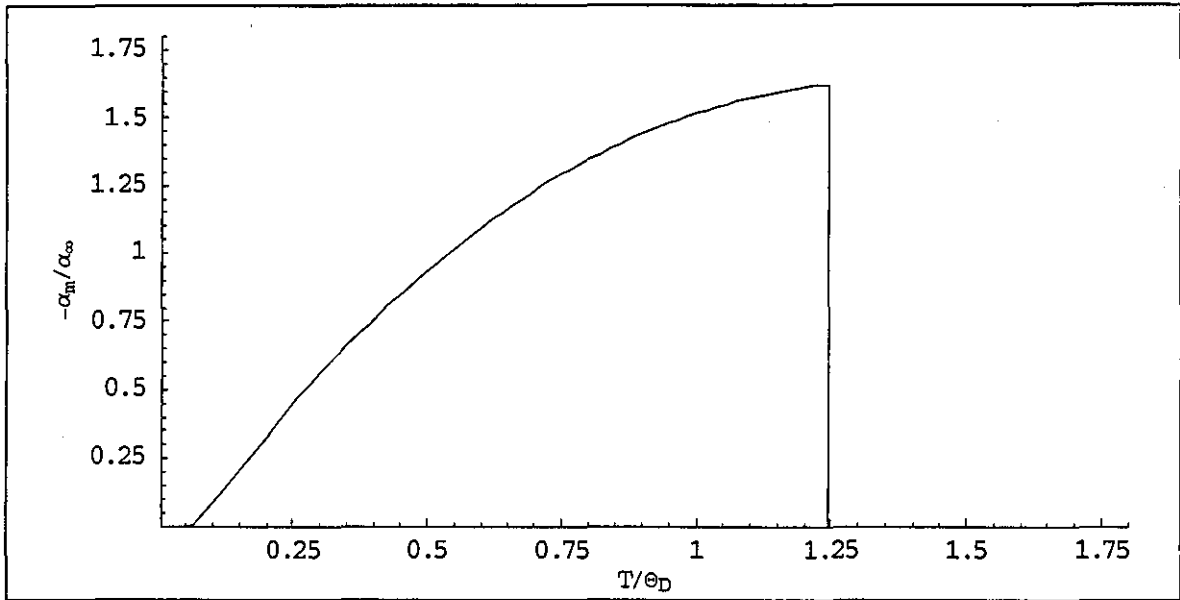

Fig. 8.21: The magnetic contribution to the thermal expansion α_m.

Parameters: as Fig. 8.17.

By comparing the thermal expansion α_{ferro} calculated for a ferromagnetic system to the thermal expansion α_{para} of a system with the same parameters, but assumed paramagnetic at all temperatures, one can calculate the magnetic contribution to the thermal expansion:

$$\alpha_m = \alpha_{ferro} - \alpha_{para} \tag{8.48}$$

This contribution is always negative for temperatures below the Curie temperature. Whereas the magnetisation and the lattice parameter change continuously at the Curie temperature, the thermal expansion jumps discontinuously from the low value in the ferromagnetic phase to the high value in the paramagnetic phase.
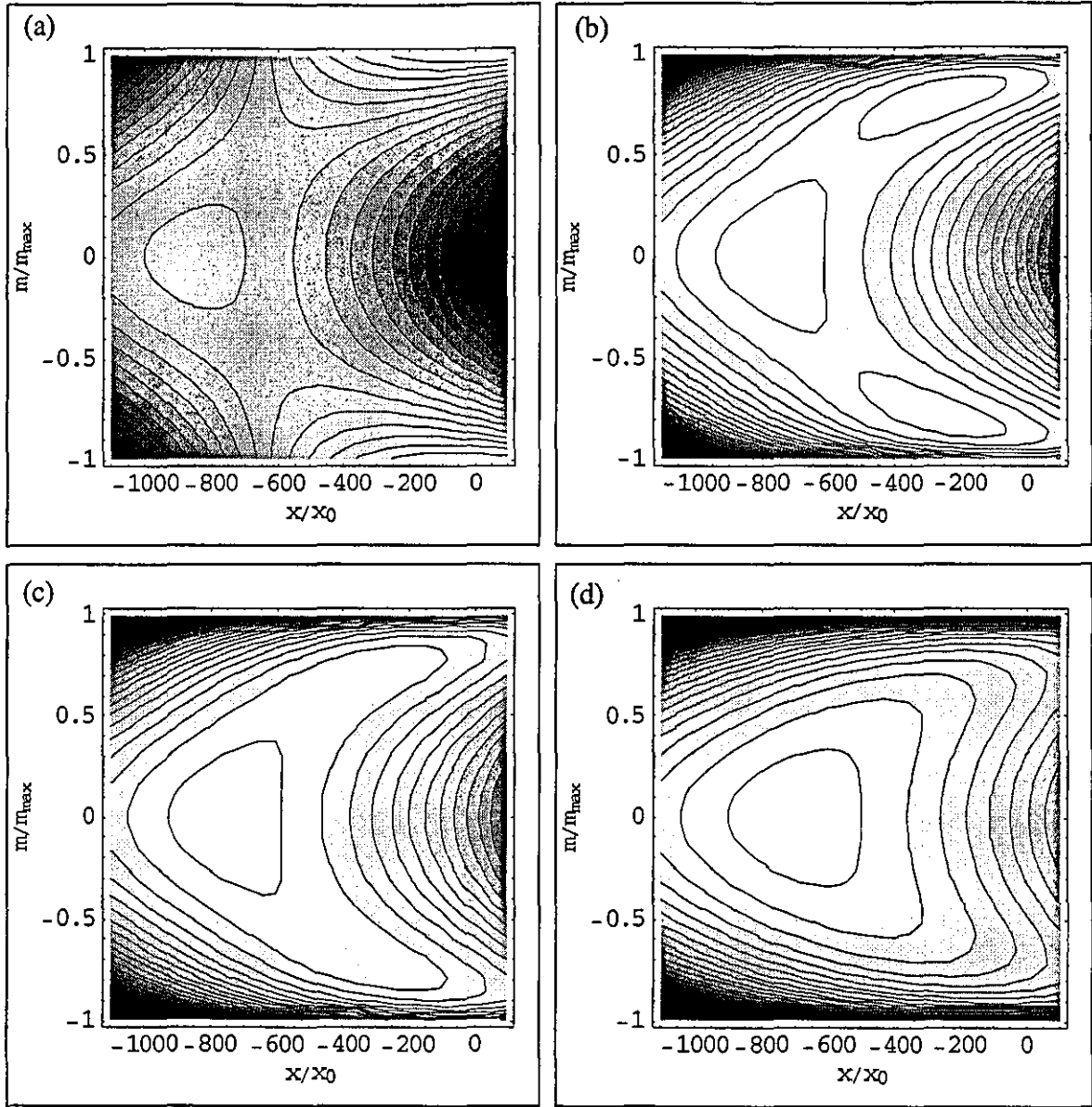
Fig. 8.22: Example of a free energy with both a ferromagnetic and a paramagnetic minimum at $T = 0$.

The free energy F is plotted as a function of magnetisation m and deviation x at different temperatures T. Darker areas represent higher values of F. The parameters are: $n = 1$, $U / k_B \Theta_D = 110$, $W_0 / k_B \Theta_D = 100$, $\xi x_0^2 / k_B \Theta_D = 0.000005$, $\beta x_0 = 0.00015$.

(a) $T = 0$: Besides the minima at $(m/m_{max} = \pm 1, x/x_0 = 0)$, there is a local minimum at $(0, -852.3)$ with higher energy. The ferromagnetic state is stable and the paramagnetic state is meta-stable.

(b) $T = T_C = 8.19\Theta_D$: The minima at $(\pm 0.78, -256.0)$ and $(0, -776.5)$ have the same energy. Above this temperature, the paramagnetic state is stable, and the ferromagnetic state is meta-stable or unstable.

(c) $T = 9.187\Theta_D$: The ferromagnetic minima vanish at $(\pm 0.51, -525.8)$. The system cannot remain in a ferromagnetic state above this temperature.

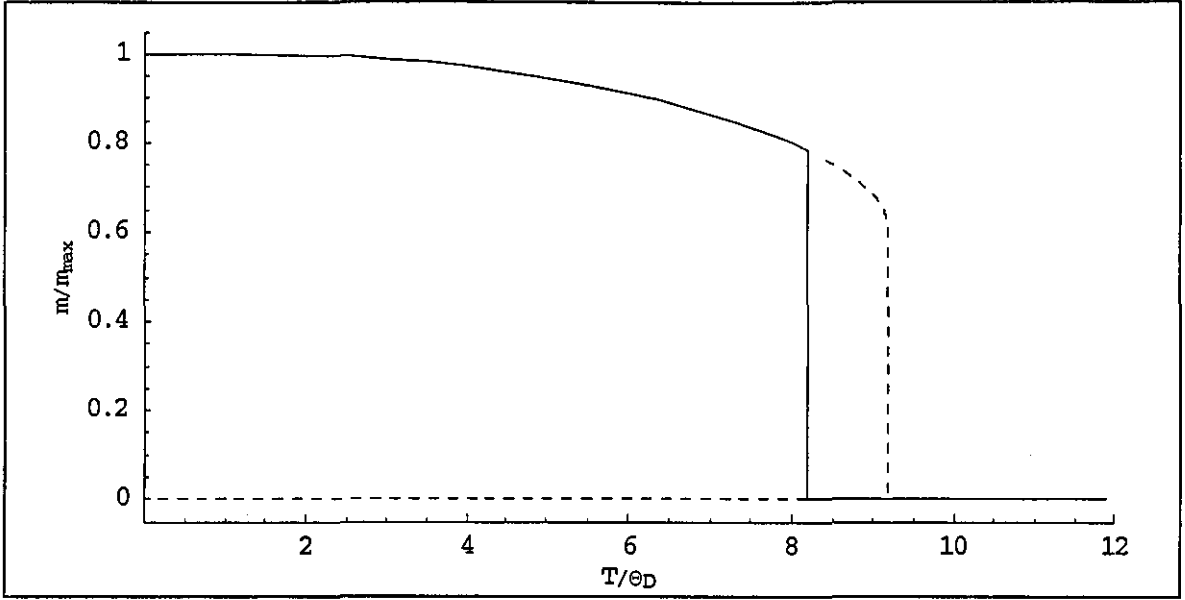(d) $T = 12\Theta_D$: The only minimum is at $(0, -840.6)$. The system is paramagnetic.

Fig. 8.23: The magnetisation *m* as a function of temperature *T*.

The parameters are the same as Fig. 8.22. The solid line represents the value of the stable state, i.e. the global minimum of the free energy, whereas the dashed line represents the values of a possible meta-stable state.
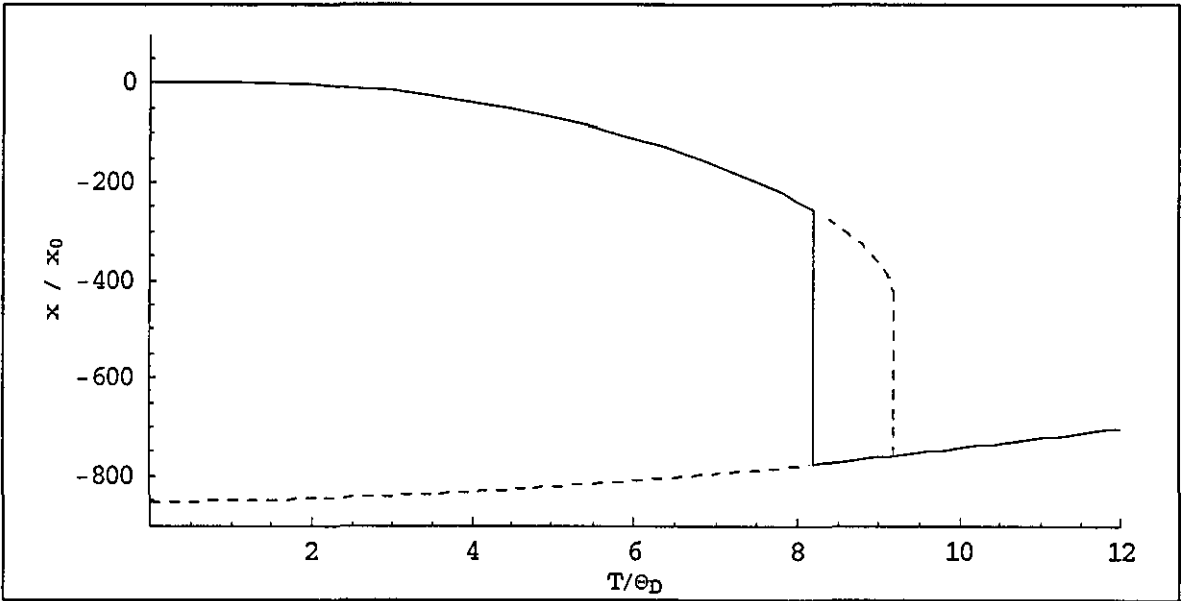

Fig. 8.24: The deviation *x* as a function of temperature *T*.

Parameters: as Fig. 8.22. The solid line represents the value of the stable state and the dashed line the values of a possible meta-stable state.

However, a system with both a stable ferromagnetic state and a meta-stable paramagnetic state at $T = 0$, may show a first-order transition from the ferromagnetic to the paramagnetic phase. Above a certain temperature T_C, the energy of the paramagnetic state may become lower than the one of the ferromagnetic state. Then the magnetisation may suddenly drop to zero and the lattice parameter may jump from its high value in the

ferromagnetic phase to its lower value in the paramagnetic phase. The thermal expansion is then singular at the transition temperature. However, there may be a temperature range around T_C, where the system remains in the meta-stable minimum during heating or cooling through T_C. Hence, the transition may exhibit hysteresis.

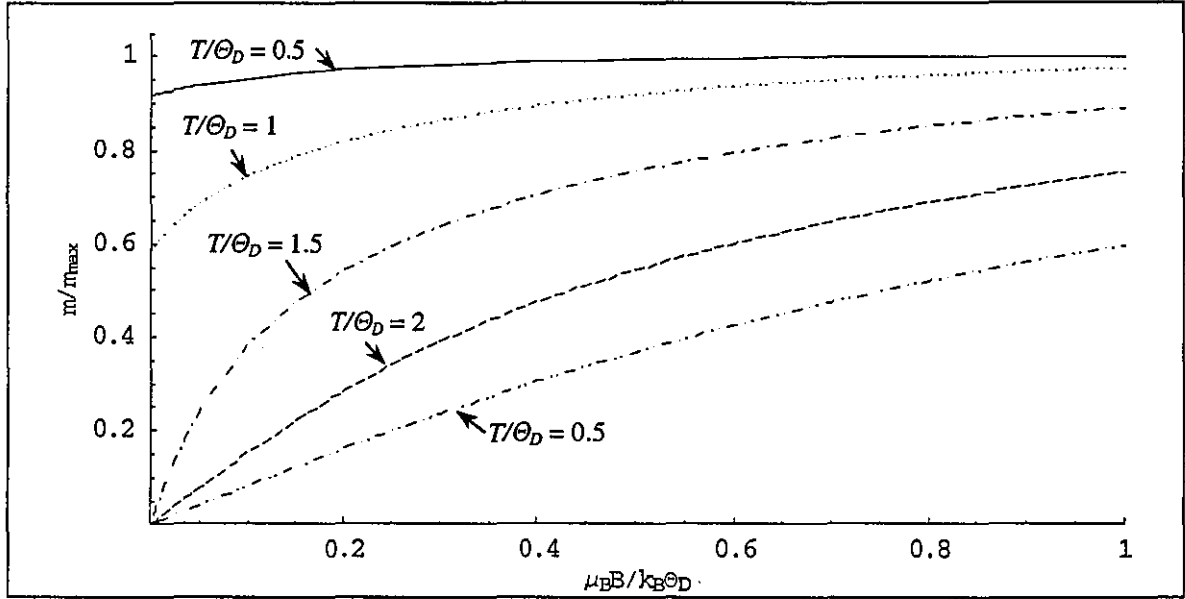**Fig. 8.25:** The magnetisation m as function of the external magnetic field B_0.
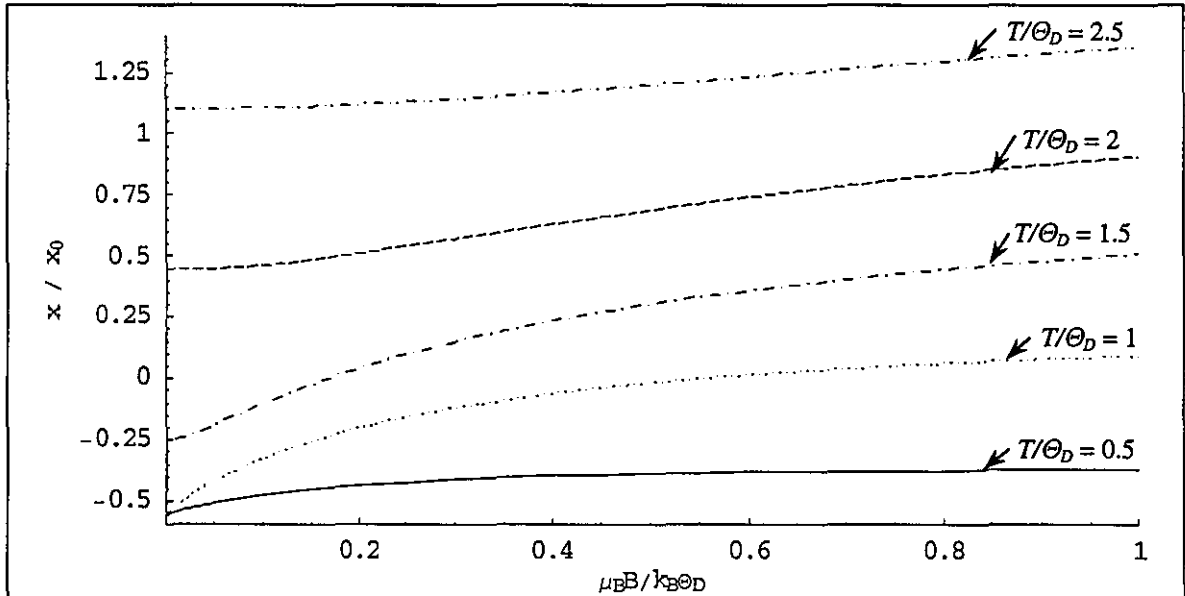
Parameters: as Fig. 8.17.

Fig. 8.26: Magnetostriction: The response of the deviation x to an external magnetic field B_0.
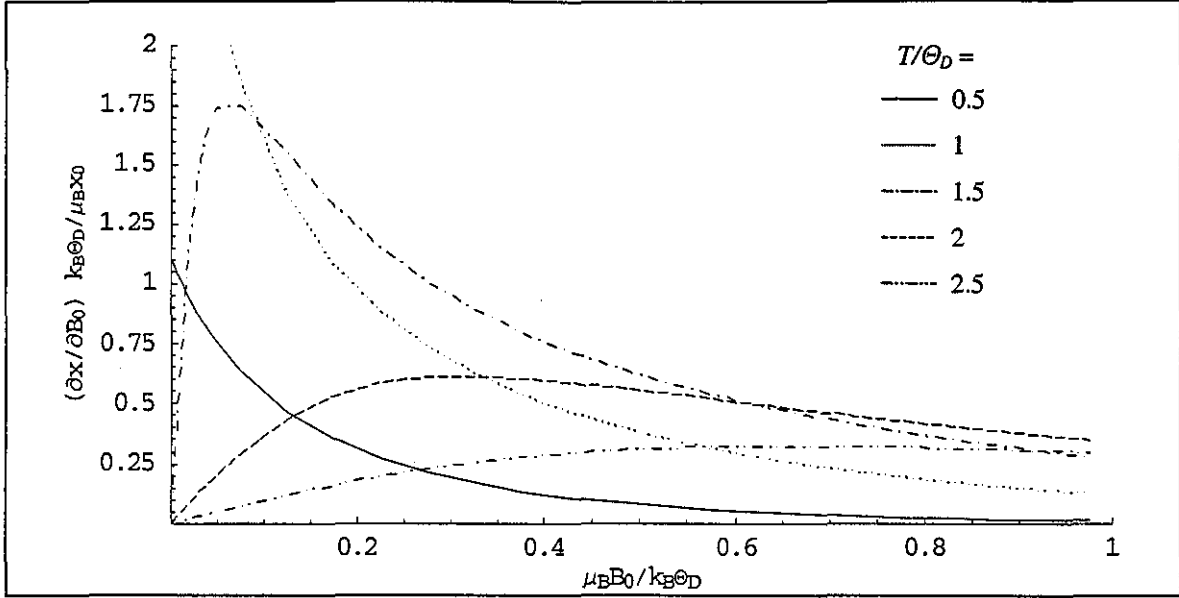
Parameters: as Fig. 8.17.

Fig. 8.27: Magnetostriction: The change of the deviation x by change of the field strength B_0. Parameters: as Fig. 8.17.

Coupled to the magnetisation, the deviation is expected to change with application of an external magnetic field. The response of the deviation to an external magnetic field B_0 is shown in Fig. 8.26. Since a state with larger moment has a larger lattice parameter, the deviation is larger for a higher external field. Furthermore, the change of deviation with changing external field $(\partial x/\partial B_0)_{T,n}$ is approximately proportional to the change of the magnetisation with B_0, i.e. to the magnetic susceptibility. Therefore, the dependence of the deviation is particularly large for a system with ferromagnetic ground state around the Curie temperature. Since the field dependence of the deviation arises from the coupling to magnetisation, it is larger for a stronger magneto-elastic coupling, i.e. smaller ξ, larger β or larger W_0. A system with more than one minimum of the free energy, as for example shown in Fig. 8.22, may show metamagnetic behaviour. There may be a discontinuous change in magnetisation and hence a discontinuous change in the lattice parameter forced by the external field.

8.9 Discussion

Although the coupling of magnetisation and lattice parameter has been treated in a particular simple way, the model studied here may give insight into the possible mechanisms of various effects arising from magneto-elastic coupling. For example, the dependence of the bandwidth on the lattice parameter results in a pressure-dependence of

magnetisation and Curie temperature. Furthermore, the model, as it has been used in section 8.5, may explain the smearing out of the ferromagnetic-to-paramagnetic phase transition in certain materials. Due to lattice vibrations, which alter the distance between neighbouring ions, and the magneto-elastic coupling, parts of the solid may have already become paramagnetic around the Curie temperature, whereas others are still ferromagnetic. The model analysed in section 8.8 can explain a very small or negative thermal expansion due to a decrease of the magnetisation. A partially filled band with increasing bandwidth for decreasing lattice parameter favours a smaller lattice parameter. The energy of the band, which is gained by decreasing the lattice parameter, is lower for a higher spin polarisation. Thus, if the magnetisation of the band is lowered, the energy gain is increased and the equilibrium value of the lattice parameter is decreased. Therefore, a decrease of the magnetisation by an increase in temperature creates a negative contribution to the thermal expansion, which counteracts positive contributions to the thermal expansion. A change of the magnetisation by application of an external magnetic field gives rise to a field-induced change in the lattice parameter. In case of various competing minima of the free energy with different values of lattice parameter and magnetisation, the transition between the various magnetic states may be discontinuous in both magnetisation and volume.

Not only the results of section 8.5 for a soft lattice are qualitatively in good agreement with experimental findings in ferromagnetic Invar materials, but also the results for other magneto-elastic effects discussed within this model. For example, the pressure-dependence of magnetisation and Curie temperature, as discussed in section 8.4 for a system with a lattice parameter slightly larger than the critical distance, follows qualitatively the behaviour observed in $Fe_{65}Ni_{35}$ [21]. The low or negative thermal expansion of Invar is reproduced in section 8.8 by a system with ferromagnetic ground state. Furthermore, the results for the magnetostriction at low field strengths render the volume-magnetostriction data of iron-nickel Invar [21]. For example, the difference in the trends for the slope of the volume-magnetostriction between the ferromagnetic and the paramagnetic phase of iron-nickel Invar is reproduced correctly in the model.

9 Particle Exchange

In solids, there may be more than one electron band with a non-vanishing density of states at the Fermi level. Then, the total number of electrons in one of these bands can not be regarded as constant any more. Electrons may be exchanged between the bands and a change of external parameters may lead to a redistribution of the electrons. Furthermore, there are processes, where electrons may be exchanged with the environment, e.g. photoemission or electric currents.

9.1 The Chemical Potential

In the derivation of the mean field Hamiltonian of the Stoner model in section 6.1, the chemical potential μ of the electrons had been substituted by two reduced chemical potentials $\bar{\mu}_\sigma$ for each spin direction $\sigma \in \{\uparrow, \downarrow\}$. The chemical potential can be recovered by the thermodynamic relation:

$$\mu = \left(\frac{\partial F}{\partial n} \right)_{T, B_0} \tag{9.1}$$

With (6.14), (6.17), (6.18) and (6.25) follows for the chemical potential of the electrons in the band for stationary values of m:

$$
\begin{aligned}
\mu &= \left(\frac{\partial F}{\partial n} \right)_{T, B_0, m} + \left(\frac{\partial F}{\partial m} \right)_{T, B_0, n} \left(\frac{\partial m}{\partial n} \right)_{T, B_0} = \left(\frac{\partial F}{\partial n} \right)_{T, B_0, m} \\
&= \frac{U}{2} n + \sum_\sigma \left(\frac{\partial \bar{F}_\sigma}{\partial n_\sigma} \right)_{T, B_0} \left(\frac{\partial n_\sigma}{\partial n} \right)_{T, B_0, m} \\
&= \frac{U}{2} n + \frac{\bar{\mu}_\uparrow + \bar{\mu}_\downarrow}{2}
\end{aligned}
\tag{9.2}
$$

For a paramagnetic system in absence of an external magnetic field, the reduced chemical potentials for both spin directions are equal:

$$\bar{\mu}_\uparrow (m = 0) = \bar{\mu}_\downarrow (m = 0) =: \bar{\mu}_{para} \tag{9.3}$$

The chemical potential is then:

$$\mu_{para}(n) = \frac{U}{2} n + \bar{\mu}_{para}(n) \tag{9.4}$$

The chemical potential is enhanced by the Coulomb repulsion. If the number of electrons in the system is raised, then the chemical potential is additionally increased by an increase in Coulomb energy.

For a system with finite magnetisation, $\bar{\mu}_{para} = (\bar{\mu}_\uparrow + \bar{\mu}_\downarrow)/2$ may not hold. Therefore, the chemical potential of a state with finite magnetisation may not be the same as for the paramagnetic state. Furthermore, the expression $(\bar{\mu}_\uparrow + \bar{\mu}_\downarrow)/2$ may depend on the magnetisation. Then the chemical potential of a ferromagnetic system might depend strongly on temperature in the range, where the magnetisation changes with temperature.

9.2 The Chemical Potential of a Band with Rectangular DOS

To understand, how the chemical potential of a ferromagnetic state differs from the paramagnetic state in the framework of Stoner theory, a band with a rectangular density of states (5.1) at zero temperature is considered first. As calculated in section 5.1, the free energy of the system is given by:

$$F = \frac{W}{4}(n^2 - 2n + m^2) + \frac{U}{4}(n^2 - m^2) \tag{9.5}$$

The magnetisation of a paramagnetic system is zero. The free energy is then given as:

$$F_{para} = \frac{W}{4}(n^2 - 2n) + \frac{U}{4} n^2 \tag{9.6}$$

From (9.6), the chemical potential can be calculated directly by differentiation with respect to n:

$$\mu_{para} = \frac{W + U}{2} n - \frac{W}{2} \tag{9.7}$$

The chemical potential depends linearly on the total number of electrons.

If the system is fully ferromagnetic and the band is less than half filled, i.e. $n < 1$, the magnetisation is equal to the total number of electrons. The free energy is then:

$$F_{ferro} = \frac{W}{2}(n^2 - n) \tag{9.8}$$

From this, the chemical potential is obtained as:

$$\mu_{ferro} = W\,n - \frac{W}{2} \tag{9.9}$$

The chemical potential depends linearly on the total number of electrons, but the slope is different from (9.7).

For $n > 1$, the magnetisation of the fully ferromagnetic state is $2 - n$. With the free energy

$$F_{ferro} = \frac{W}{2}(n^2 - n) \tag{9.10}$$

the chemical potential is:

$$\mu_{ferro} = W\,n - \frac{3W}{2} + U \tag{9.11}$$

The chemical potential is again a linear function of the total number of electrons. The slope is equal to the one for $n < 1$, but the offset is different.
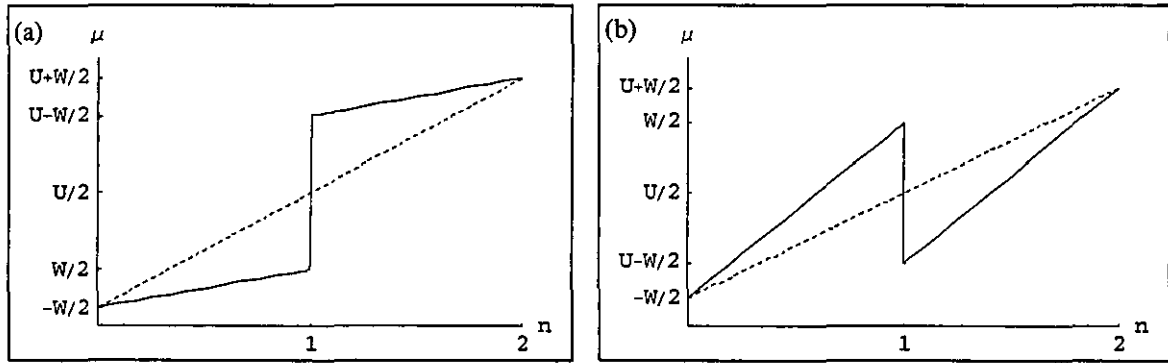

Fig. 9.1: The paramagnetic (dashed line) and the ferromagnetic (solid line) chemical potential μ as functions of the total number of electrons n for (a) $U > W$ and (b) $U < W$ (schematic).

In Fig. 9.1, the paramagnetic and the ferromagnetic chemical potential are compared as functions of the total number of electrons. For $U > W$, the ferromagnetic chemical potential is smaller than the paramagnetic for $n < 1$ and larger for $n > 1$. For $U < W$, the ferromagnetic chemical potential is larger than the paramagnetic for $n < 1$ and smaller for $n > 1$.

In section 5.1, it has been calculated that for $U > W$ the system is ferromagnetic. Then, as a function of the total number of electrons n, the chemical potential is discontinuous at $n = 1$. There it jumps from a value below to a value above the paramagnetic chemical potential.

The results of chapter 7 can be used to examine the chemical potential of the rectangular band at finite temperatures. The reduced chemical potentials $\bar{\mu}_\sigma$ are obtained by solving (7.4). The result is:

$$\bar{\mu}_\sigma = k_B T \ln\left[\operatorname{csch}\left[\frac{W(2-n-\bar{\sigma}m)}{k_B T} \right] \sinh\left[\frac{W(n+\bar{\sigma}m)}{k_B T} \right] \right] \tag{9.12}$$

Using this result and (9.2), the chemical potential is obtained as:

$$\mu = \frac{U}{2}n + \frac{k_B T}{2}\sum_\sigma \ln\left[\operatorname{csch}\left[\frac{W(2-n+\bar{\sigma}m)}{k_B T} \right] \sinh\left[\frac{W(n-\bar{\sigma}m)}{k_B T} \right] \right] \tag{9.13}$$

This expression reduces to

$$\mu = \frac{U}{2} \quad \text{for} \quad n=1. \tag{9.14}$$

For $n = 1$, the chemical potential is independent of temperature and magnetisation. For $n \neq 1$, the chemical potential depends on the temperature and on the magnetisation, which can be found by solving the minimum conditions (7.9) and (7.10).
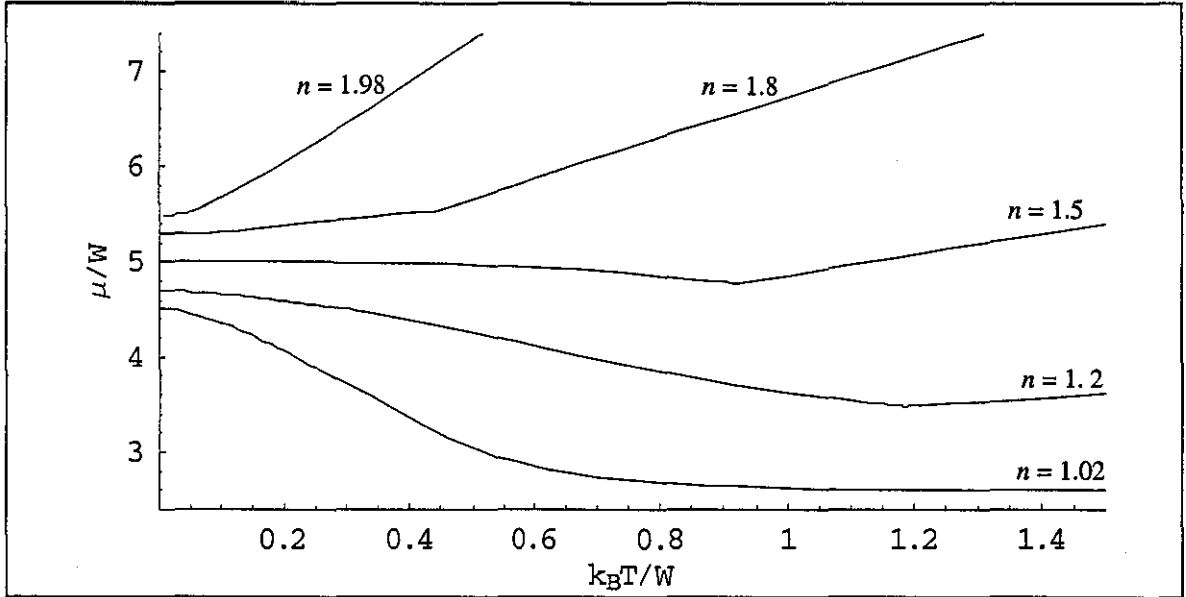

Fig. 9.2: The chemical potential μ as a function of temperature T for different band fillings $n > 1$ ($U/W = 5$).
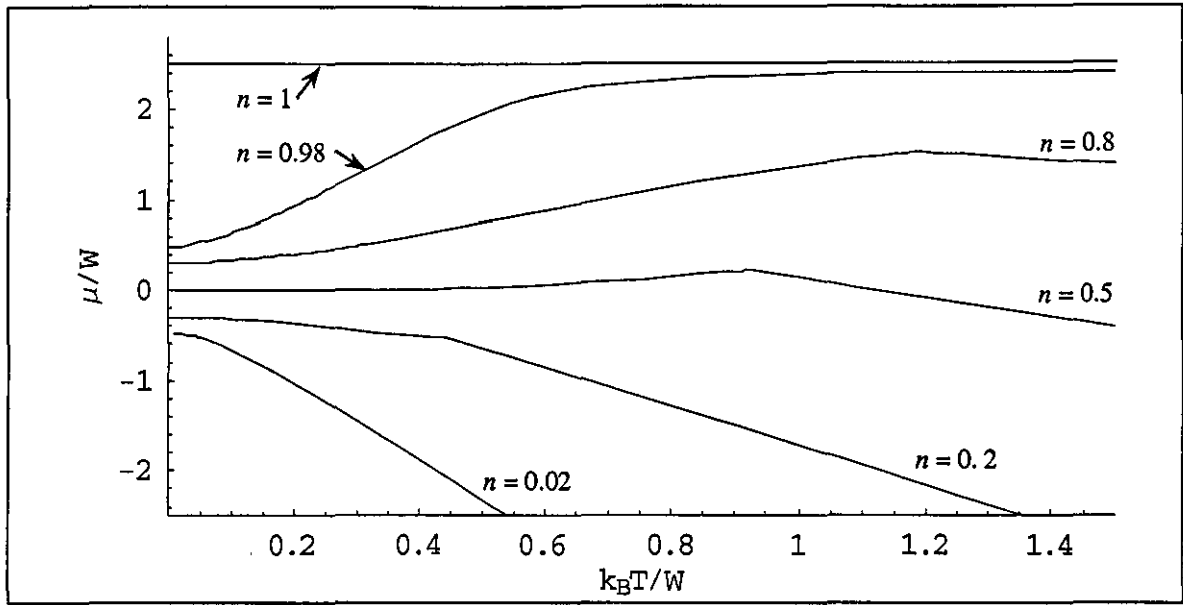
Fig. 9.3: The chemical potential μ as a function of temperature T for different band fillings $n \leq 1$ ($U/W = 5$).
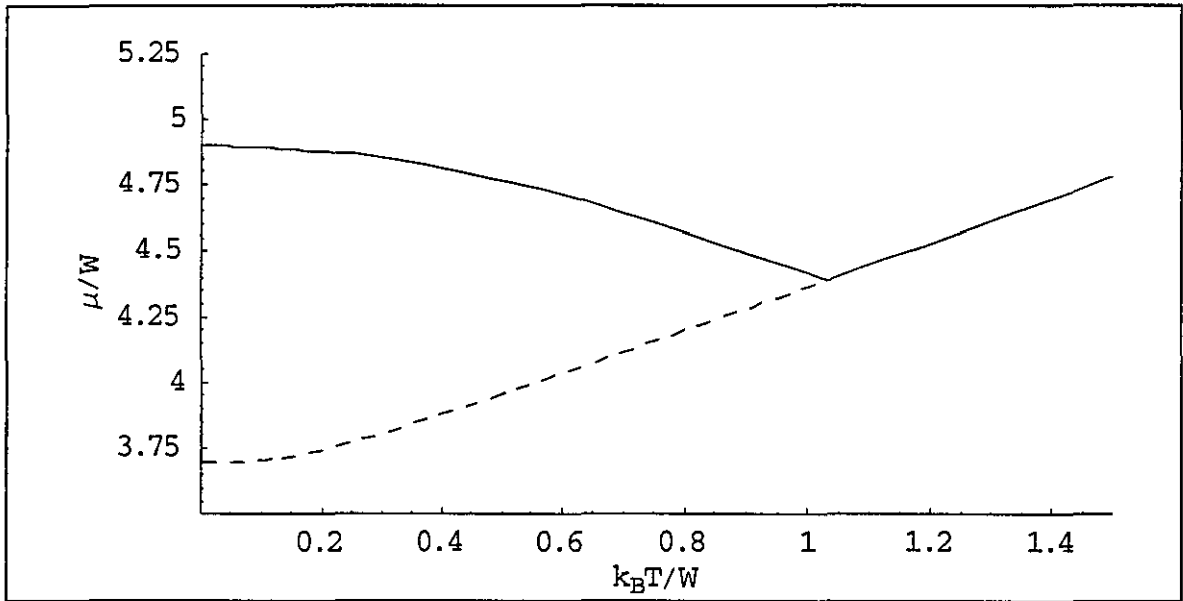

Fig. 9.4: The chemical potential μ as functions of temperature T (solid line) and of a hypothetical system staying paramagnetic below $k_B T_C = 1.03$ W (dashed line).

Parameters: $n = 1.4$, $U/W = 5$.

The chemical potential as a function of temperature for different band fillings is shown in Fig. 9.2 for $n > 1$ and in Fig. 9.3 for $n < 1$. For $n > 1$ and temperatures higher than the Curie temperature T_C, where the system is paramagnetic, the chemical potential decreases with decreasing temperature. However, for band fillings between $n = 1$ and $n \approx 1.5$, the chemical potential increases with decreasing temperature below T_C due to the increasing magnetisation. For larger band fillings, the chemical potential still decreases with

decreasing temperature, but not as rapidly as in the paramagnetic phase. The difference between the chemical potential of the ferromagnetic phase and the chemical potential as it would be expected if the system stayed paramagnetic at all temperatures is shown in Fig. 9.4 for a certain set of parameters. The chemical potential is symmetric with respect to the transformation $(n \rightarrow 2 - n, \mu \rightarrow U - \mu)$. Therefore, the behaviour of $\mu(T)$ for $n < 1$ can be obtained by exploiting this symmetry.
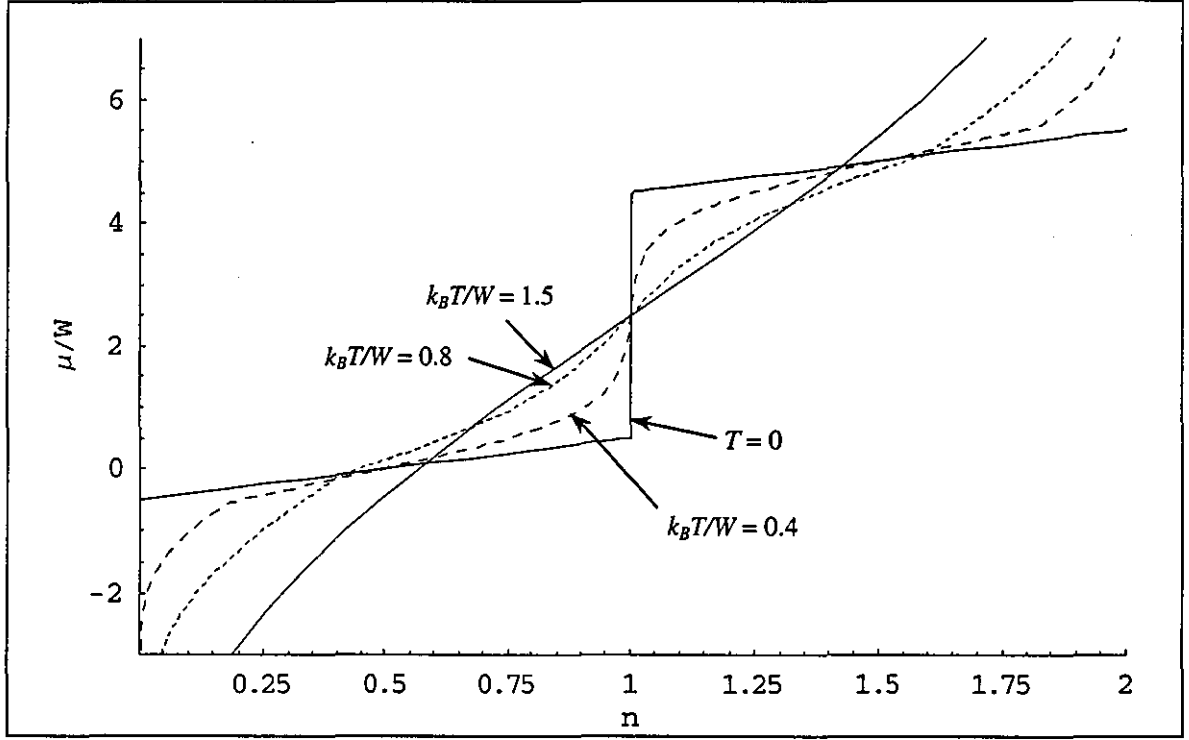

Fig. 9.5: The chemical potential μ as function of the total number of electrons n for different temperatures T. Parameters: $U/W = 5$, $k_B T_C(n=1)/W = 1.233$.

The dependence of the chemical potential on the total number of electrons for different temperatures is shown in Fig. 9.5. As discussed in the previous section, the chemical potential at zero temperature is, as a function of the total number of electrons, discontinuous at $n = 1$. For finite, but low temperatures, the change of $\mu(n)$ around $n = 1$ is rapid but continuous. For large temperatures, where the system is paramagnetic for all band fillings, the step at $n = 1$ vanishes completely. Whereas the limit of a full or empty band leads to finite values of μ for $T = 0$, infinite values result for $T > 0$.

9.3 The Grand Potential

So far, the magnetisation of the single band has been considered without the possibility of particle exchange with other parts of the electronic structure of the solid. If the electronic structure in a range around the Fermi level accessible for thermal excitations is dominated by the single band, this approach is justified. However, in most transition metals and alloys, the d-band states lie in the same energy region as states belonging to other bands, e.g. s-p-bands.

A first step towards integrating the interaction of the single band with other bands in the solid is to allow electrons to be exchanged between states of the single band and the environment. If electrons can be exchanged between the single band and a large particle reservoir, not the free energy of the band is minimal in the thermodynamic equilibrium, but the grand potential. The grand potential Ω is related to the free energy F by the Legendre transformation:

$$\Omega = F - \mu n \tag{9.15}$$

where n is the total number of electrons in the single band and $\mu = (\partial F/\partial n)_{T,B_0}$ the chemical potential. In equilibrium, the magnetisation then minimises the grand potential under the constraint of a constant chemical potential, whereas the total number of electrons may vary. Hence, the actual magnetisation satisfies:

$$0 = \left(\frac{\partial \Omega}{\partial m}\right)_\mu \tag{9.16}$$

The actual magnetisation for a constant chemical potential can be calculated using the results for the magnetisation in the case of a constant total number of electrons. With (6.19), one can express the grand potential as:

$$\Omega = \Omega(\mu, m) = F(n(\mu, m), m) - \mu\, n(\mu, m) \tag{9.17}$$

Using this expression for Ω, one obtains for its derivative:

$$\left(\frac{\partial \Omega}{\partial m}\right)_\mu = \left(\frac{F(n(\mu,m),m)}{\partial m}\right)_\mu - \mu \left(\frac{\partial n(\mu,m)}{\partial m}\right)_\mu$$

$$= \left(\frac{F(n,m)}{\partial m}\right)_n\Bigg|_{n=n(\mu,m)} + \left[\left(\frac{F(n,m)}{\partial n}\right)_m\Bigg|_{n=n(\mu,m)} - \mu\right]\left(\frac{\partial n(\mu,m)}{\partial m}\right)_\mu \tag{9.18}$$

If the magnetisation minimises the free energy under the constraint of a constant total number of electrons, i.e.

$$\left(\frac{\partial F}{\partial m}\right)_n = 0 \tag{9.19}$$

then

$$\mu = \left(\frac{\partial F}{\partial n}\right) = \left(\frac{\partial F(n,m)}{\partial n}\right)_m + \left(\frac{\partial F(n,m)}{\partial m}\right)_n \left(\frac{\partial m}{\partial n}\right) = \left(\frac{\partial F(n,m)}{\partial n}\right)_m \tag{9.20}$$

and therefore:

$$\left(\frac{\partial \Omega}{\partial m}\right)_\mu = 0 \tag{9.21}$$

Interchanging the role of F and Ω and n and μ and using the same arguments as above leads to the equivalence:

$$\left(\frac{\partial F}{\partial m}\right)_n\bigg|_{n=n(\mu)} = 0 \quad \Leftrightarrow \quad \left(\frac{\partial \Omega}{\partial m}\right)_\mu\bigg|_{\mu=\mu(n)} = 0 \tag{9.22}$$

The actual magnetisation for a given number of electrons n is the actual magnetisation for a given chemical potential equal to $\mu(n)$ and vice versa. Hence, if the actual magnetisation $m(n)$ for a given total number of electrons n is known and one can invert (9.20) to obtain $n(\mu)$, one can calculate the actual magnetisation $m(\mu) = m(n(\mu))$ for a given chemical potential μ.

A different approach is to express the grand potential as $\Omega(\mu,n,m) = F(n,m) - \mu n$ and minimise it with respect to both m and n. However, it seems convenient to perform the change of variables

$$n_\uparrow = \frac{n+m}{2} \quad \text{and} \quad n_\downarrow = \frac{n-m}{2} \tag{9.23}$$

and minimise the grand potential with respect to the total number of electrons for each spin direction $n_\uparrow$ and $n_\downarrow$. With (6.19) and (6.20), the grand potential as a function of $n_\uparrow$ and $n_\downarrow$ is:

$$\Omega(\mu,n_\uparrow,n_\downarrow) = Un_\uparrow n_\downarrow - \mu_B B\left(n_\uparrow - n_\downarrow\right) + \sum_\sigma \overline{F}_\sigma(n_\sigma,T) - \mu\left(n_\uparrow + n_\downarrow\right) \tag{9.24}$$

With (6.20) and $\left(\partial \overline{F}_\sigma / \partial n_\sigma\right)_{T,\mu,B_0,n_{-\sigma}} = \overline{\mu}_\sigma$, the conditions for the actual values of the total number of spin-σ electrons are

$$0 = \left(\frac{\partial \Omega}{\partial n_\sigma}\right)_{T,\mu,B_0,n_{-\sigma}} = U\, n_{-\sigma} - \mu_B\, B + \overline{\mu}_\sigma(n_\sigma) - \mu \tag{9.25}$$

where $\overline{\mu}_\sigma(n_\sigma)$ is calculated by solving (6.21) for $\overline{\mu}_\sigma$. From analysing the matrix of the second derivatives, one obtains the condition for the stability of the solution:

$$U^2 < \left(\frac{\partial \overline{\mu}_\uparrow}{\partial n_\uparrow}\right)\left(\frac{\partial \overline{\mu}_\downarrow}{\partial n_\downarrow}\right) \tag{9.26}$$

Noticing that $(\partial \overline{\mu}_\sigma / \partial n_\sigma) \approx D(\varepsilon_f)^{-1}$ for the paramagnetic state, this again reflects the Stoner criterion. For a large density of states at the Fermi level, the paramagnetic state is unstable. Then a ferromagnetic state must be the ground state.

9.4   The Magnetisation of a Band with Rectangular DOS

In this section, the magnetisation of a single band with rectangular density of states is considered for the situation, where electrons can be exchanged between the band and a particle reservoir. As discussed in chapter 5, a band with a rectangular density of states (5.1) at zero temperature is paramagnetic for $U < W$ regardless of the total number of electrons and, hence, for any value of the chemical potential. For $U > W$, the system is fully ferromagnetic. Using (9.9), (9.11) and (9.14), the total number of electrons, as a function of the chemical potential, is in the fully ferromagnetic phase:

$$n = \begin{cases} 0 & \text{for} \quad \mu \leq -W/2 \\ 1/2 + \mu/W & \text{for} \quad -W/2 < \mu < W/2 \\ 1 & \text{for} \quad W/2 \leq \mu \leq U - W/2 \\ 3/2 + (\mu - U)/W & \text{for} \quad U - W/2 < \mu < U + W/2 \\ 2 & \text{for} \quad \mu \geq U + W/2 \end{cases} \tag{9.27}$$

From this and (5.7), it follows for the magnetisation for $U > W$:

$$
m = \begin{cases}
0 & \text{for} & \mu \leq -W/2 \\
1/2 + \mu/W & \text{for} & -W/2 < \mu < W/2 \\
1 & \text{for} & W/2 \leq \mu \leq U - W/2 \\
1/2 - (\mu - U)/W & \text{for} & U - W/2 < \mu < U + W/2 \\
0 & \text{for} & \mu \geq U + W/2
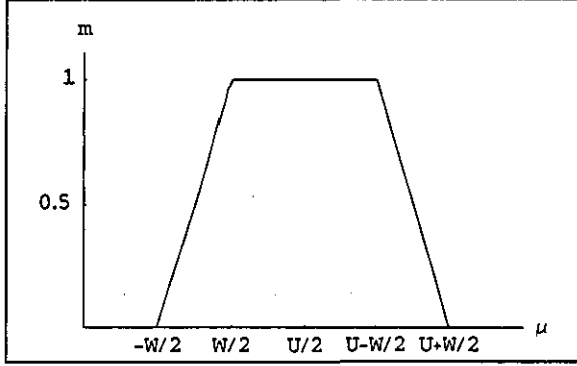\end{cases}
\tag{9.28}
$$

Fig. 9.6: The magnetisation m as a function of the chemical potential μ.

The result is shown in Fig. 9.6. For a chemical potential below the lower edge of the band, the band is empty and hence the magnetisation is zero. For $-W/2 < \mu < W/2$, the magnetisation increases with increasing chemical potential by filling the up-spin states. Since the spin-down states are all pushed above the chemical potential by the Coulomb repulsion, they remain empty. For a chemical potential between the upper edge of the spin-up band at $W/2$ and the lower edge of the spin-down band, which is shifted by the Coulomb repulsion above the spin-up band to $U/2$, the magnetisation remains constant. Only if the chemical potential rises above the lower edge of the spin-down band, the magnetisation decreases by filling the spin-down states with electrons. For a chemical potential above the upper edge of the spin-down band, both sub-bands are completely filled and the magnetisation is zero.

For calculating the magnetisation of a band with rectangular DOS at finite temperatures, the results of chapter 7 in conjunction with those of section 9.2 can be used. The equation (9.13) for the chemical potential $\mu(n, m(n))$ as a function of the total number of electrons is numerically inverted to find the total number of electrons $n(\mu)$ as a function of the chemical potential and, with it, the magnetisation $m(n(\mu))$.
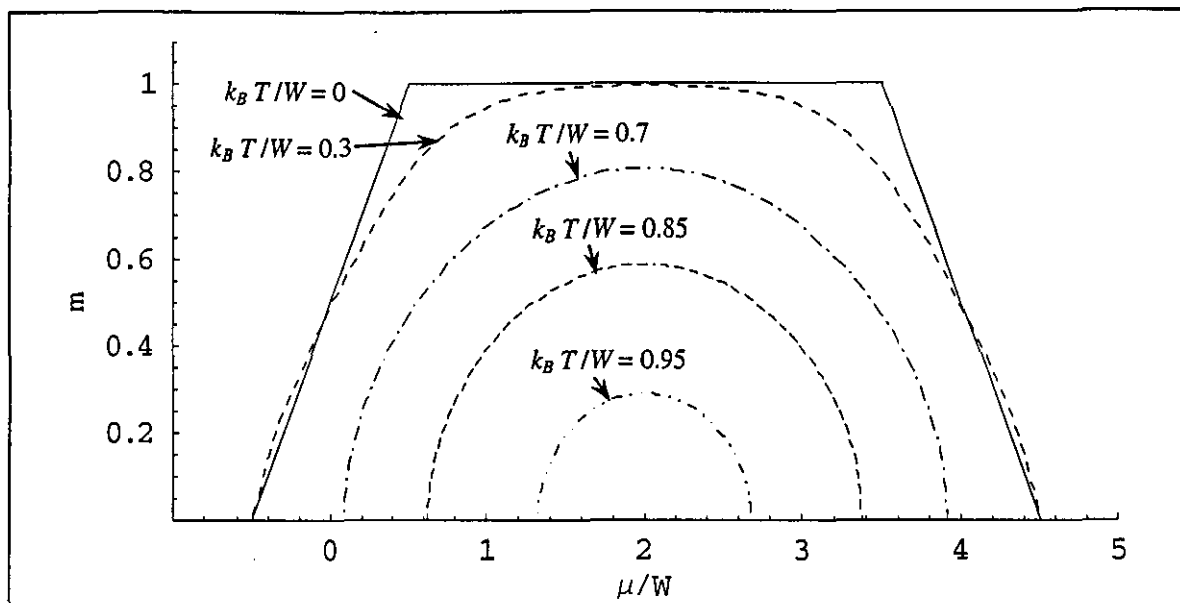
Fig. 9.7: The magnetisation m as a function of the chemical potential μ at different temperatures T.
Parameters: $U / W = 4$, $k_B T_C / W = 0.979$ for $\mu = U/2$.

In Fig. 9.7, the magnetisation as a function of the chemical potential is shown for different temperatures. For a chemical potential close to the bottom of the band, the magnetisation may be larger at finite temperatures than at zero temperature since, in this case, the band contains more electrons at higher temperature.

9.5 Lattice Distortions

In section 8.6, a periodic lattice distortion has been considered and the resulting magnetisation has been calculated under the assumption that the number of electrons is locally conserved. However, the very small time scale of the dynamics of the electrons and their itinerant character imply that the electrons may spatially redistribute to adjust to any lattice distortion. This can be included into the model by assuming a constant chemical potential throughout the crystal instead of a constant electron density.

Consider a lattice at zero temperature, which is distorted by a sinusoidal modulation of the inter-ionic distance:

$$a(\mathbf{r}) = a_0 + A \sin(\mathbf{k} \cdot \mathbf{r}) \qquad (A > 0, \mathbf{k} \neq \mathbf{0}) \qquad (9.29)$$

Here, a_0 is the inter-ionic distance in absence of the distortion, i.e. the lattice parameter, A the amplitude and $\mathbf{k}$ the wave vector of the distortion. The whole crystal may be seen as being composed of many small regions with a local lattice parameter $a_l = a(\mathbf{r})$. The width

$W(\mathbf{r})$ of the local electron band in a region around $\mathbf{r}$ is assumed to depend on the local lattice parameter:

$$W_l(\mathbf{r}) = W_0 \exp[-\beta\, a(\mathbf{r})] \tag{9.30}$$

Because of the symmetry between spin-up and spin-down band and between electrons and holes, it is sufficient to consider a positive magnetisation and $\mu < U/2$. This implies that one may focus the consideration to the spin-up states, since the local band is either paramagnetic or the spin-down band is empty for $m > 0$ and $\mu < U/2$.

Using (9.31), the magnetisation of each region is given at zero temperature by:

$$m_l(\mathbf{r}) = \begin{cases} 0 & for & W_l(\mathbf{r}) < U & or & -W_l(\mathbf{r})/2 \geq \mu \\ 1/2 + \mu/W_l(\mathbf{r}) & for & W_l(\mathbf{r}) > U & and & -W_l(\mathbf{r})/2 < \mu < W_l(\mathbf{r})/2 \\ 1 & for & W_l(\mathbf{r}) > U & and & W_l(\mathbf{r})/2 \leq \mu \leq U/2 \end{cases} \tag{9.31}$$
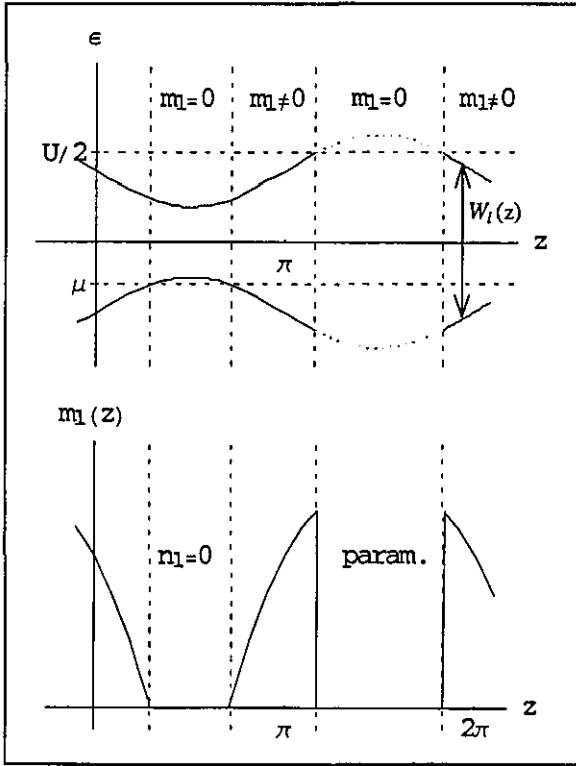
Fig. 9.8: The lower and the upper edge of the local spin-up band and the local magnetisation m_l (schematic).

In regions, where the local bandwidth $W_l(z)$ is larger than the on-site repulsion U, the local band is paramagnetic. In regions, where the lower edge of the band lies above the chemical potential μ, the band is empty.

The resulting average magnetisation can then be calculated by integrating over the whole volume V of the crystal:

$$m = \frac{1}{V} \int_V m_l(\mathbf{r})\, d\mathbf{r} \tag{9.32}$$

Without any distortions, the average magnetisation is given by:

$$m = \begin{cases} 0 & for \quad W_0 < U \quad or \quad -W_0/2 \geq \mu \\ 1/2 + \mu/W_0 & for \quad W_0 > U \quad and \quad -W_0/2 < \mu < W_0/2 \\ 1 & for \quad W_0 > U \quad and \quad W_0/2 \leq \mu \leq U/2 \end{cases} \tag{9.33}$$

The following definitions will be used to calculate the average magnetisation for a finite distortion:

$$a_m := -\beta^{-1} \ln(U/W_0) \tag{9.34}$$

$$a_{\mu 0} := \begin{cases} -\beta^{-1} \ln(-2\mu/W_0) & for \ \mu < 0 \\ \infty & for \ \mu \geq 0 \end{cases} \tag{9.35}$$

$$a_{\mu 1} := \begin{cases} -\beta^{-1} \ln(2\mu/W_0) & for \ \mu > 0 \\ \infty & for \ \mu \leq 0 \end{cases} \tag{9.36}$$

$$z := \mathbf{k} \cdot \mathbf{r} \tag{9.37}$$

$$a_l(z) := a_0 + A\sin(z) \tag{9.38}$$

$$W_l(z) := W_0 \exp[-\beta a(z)] \tag{9.39}$$

$$m_l(z) = \begin{cases} 0 & for \ a_0 + A\sin(z) < a_m \ \vee \ a_0 + A\sin(z) \geq a_{\mu 0} \\ 1/2 + \mu/W_l(z) & for \ a_0 + A\sin(z) > a_m \ \wedge \ a_0 + A\sin(z) < \min\{a_{\mu 0}, a_{\mu 1}\} \\ 1 & for \ a_0 + A\sin(z) > a_m \ \wedge \ a_0 + A\sin(z) \geq a_{\mu 1} \end{cases} \tag{9.40}$$

With these definitions, the average magnetisation can be written as:

$$m = \frac{1}{V} \int_V m_l(\mathbf{r}) \, d\mathbf{r} = \frac{1}{2\pi} \int_0^{2\pi} m_l(z) \, dz \tag{9.41}$$

In the following cases, one finds for the average magnetisation:

$$m = \begin{cases} 0 & for \quad A < \min\{a_m - a_0, a_0 - a_{\mu 0}\} \\ 1/2 + \dfrac{\mu}{W_0 e^{-\beta a_0}} I_0(\beta A) & for \quad A < \min\{a_0 - a_m, a_{\mu 0} - a_0, a_{\mu 1} - a_0\} \\ 1 & for \quad A < \min\{a_0 - a_m, a_0 - a_{\mu 1}\} \end{cases} \tag{9.42}$$

Here, $I_n(z)$ is the modified Bessel function of the first kind, which satisfies the differential equation $z^2 f''(z) + z f'(z) - (z^2 + n^2) f(z) = 0$. These cases are characterised by a small amplitude A of the distortion compared to other length scales associated with the local lattice parameter. Then the local magnetisation is given by the same branch of (9.40) for all regions of the crystal. Furthermore, one obtains:

$$m = \begin{cases} \dfrac{1}{\pi} \arccos\left(\dfrac{a_m - a_0}{A} \right) & for \quad |a_0 - a_m| < A < a_0 - a_{\mu 1} \\[3mm] \dfrac{1}{2\pi} \arccos\left(\dfrac{a_m - a_0}{A} \right) & for \quad |a_0 - a_m| < A \quad and \quad \mu = 0 \end{cases} \tag{9.43}$$

In these cases, some regions of the crystal are paramagnetic and others ferromagnetic, but the local magnetisation has the same value in all ferromagnetic regions. This situation has been implicitly discussed in section 8.6.

For large amplitudes, there are regions in the crystal with a local magnetisation given by different branches of (9.40), which complicates the calculation of the average magnetisation. However, the situation simplifies for very large amplitudes. In the limit $\beta A \rightarrow \infty$, on obtains:

$$\lim_{\beta A \to \infty} m = \begin{cases} 0 & for \quad \mu < 0 \\ 1/2 & for \quad \mu \geq 0 \end{cases} \tag{9.44}$$

For $\mu < 0$, all regions of the crystal are either paramagnetic or do not contain any electrons at all. For $\mu \geq 0$, all regions of the crystal are either paramagnetic or have a completely filled local spin-up band and an empty local spin-down band. In other situations, an expression in terms of standard functions has not been found for the average magnetisation.

An impression of the possible complexity of the behaviour of the average magnetisation gives Fig. 9.9, where m is plotted against the amplitude A of the distortion for a certain set of parameters with $-W_0 e^{-\beta a_0}/2 < \mu < 0$ and $a_m < a_{\mu 0} < a_0$. For small amplitudes, the magnetisation decreases as the amplitude increases. However, when the amplitude well exceeds $a_{\mu 0} - a_0$, the magnetisation increases again with increasing amplitude until $A = a_0 - a_m$. From this point, the magnetisation decreases drastically with increasing amplitude, because parts of the crystal become paramagnetic. For $A \rightarrow \infty$, the magnetisation goes to zero.
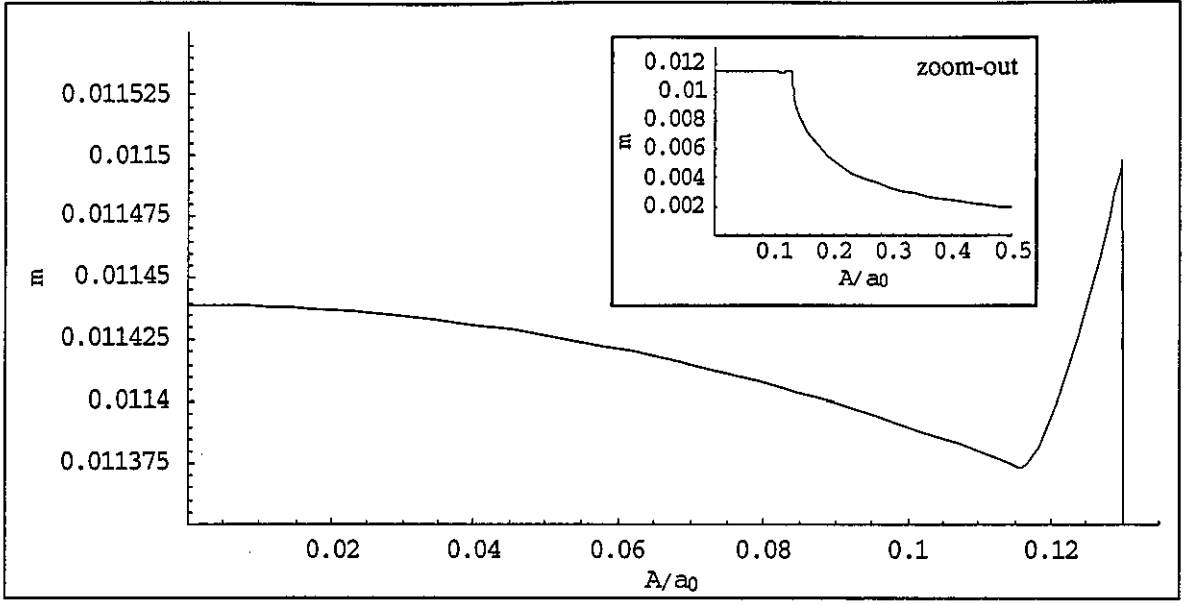
Fig. 9.9: The average magnetisation m as a function of the amplitude A of the distortion.
Parameters: $\mu / W_0 = -0.4$, $a_m / a_0 = 0.87$, $\beta a_0 = 0.2$.

However, if the electrons are confined to the rectangular band, they may redistribute to establish a constant chemical potential throughout the band, but their total number N will be constant. With the average number of electrons

$$n = N/V \tag{9.45}$$

and the maximum magnetisation

$$m_{\mathrm{max}} = \min\{n, 2 - n\} \tag{9.46}$$

one obtains for the average magnetisation:

$$m = m_{\mathrm{max}} \begin{cases} 1 & for & A < (a_0 - a_m) \\ 0 & for & A < (a_m - a_0) \end{cases} \tag{9.47}$$

For $-A < (a_0 - a_m) < A$, one may use (9.7) and (9.27) to calculate the local number of electrons as a function of the chemical potential:

$$n_l(\mathbf{r}, \mu) = \begin{cases} 0 & for & W(\mathbf{r}) < U & \& & \mu \leq -W(\mathbf{r})/2 \\ 1/2 + \mu/W(\mathbf{r}) & for & W(\mathbf{r}) < U & \& & -W(\mathbf{r})/2 < \mu < W(\mathbf{r})/2 \\ 1 & for & W(\mathbf{r}) < U & \& & W(\mathbf{r})/2 \leq \mu \leq U - W(\mathbf{r})/2 \\ \dfrac{W + 2\mu}{W + U} & for & W(\mathbf{r}) > U \end{cases} \tag{9.48}$$

Then the average number of electrons is calculated as:

$$n(\mu) = \frac{1}{V} \int_V n_l(\mathbf{r}, \mu) \, d\mathbf{r} = \frac{1}{2\pi} \int_0^{2\pi} n_l(z, \mu) \, dz \qquad (9.49)$$

This relation then may be inverted to obtain the chemical potential as a function of the average number of electrons. Then the chemical potential for the specific number of electrons may be used to calculate the magnetisation using (9.41). The resulting magnetisation may again show a non-trivial dependence on the amplitude of the distortion.

9.6 Discussion

The assumption of a constant chemical potential alters the results for the magnetic properties of the system compared to the assumption of a constant total number of electrons. As shown in section 9.4 for the case of a rectangular density of states, the magnetisation for an almost empty band may increase with increasing temperature at low temperatures. This rather unusual effect, which is due to electrons flowing into the band, does not occur, if the number of electrons is fixed. Furthermore, the effect of lattice distortions on the magnetisation value may show a quite complex behaviour as a function of the distortion amplitude.

10 Summary and Outlook

This work was aimed at studying aspects of the interaction between lattice deformation and magnetisation of itinerant electron systems. Therefore, an approach based on the Stoner model within mean field approximation has been used. The introduction of a lattice-parameter dependence of the bandwidth enabled the discussion of a wide range of effects arising from magnetisation-lattice interactions. The obtained results are qualitatively in good agreement with experimental findings in ferromagnetic Invar materials.

As pointed out in the discussion of the localised model, many properties found in transition metals and alloys require a description that considers the itinerant character of the magnetic carriers. Consequently, the d-electrons in transition metals have to be described within a band model. Here, the Stoner model has been used to describe band magnetism. Its finite-temperature properties, including the various magnetic states and the ferromagnetic-to-paramagnetic phase transition, have been discussed within MFA.

The Stoner theory provides an explanation of the non-integral values of the saturation magnetisation in units of μ_B. In particular, experimental findings of magnetic properties at zero temperatures, such as the Slater-Pauling curve, are well explained by this model. The model also explains a possible deviation of the susceptibility from the Curie-Weiss law. In summary, the Stoner model gives a qualitatively satisfactory explanation of many properties of transition metals and alloys.

The Stoner model in mean field approximation has been used to study the finite-temperature properties of a single band with a rectangular DOS. A rectangular shape can be seen as a first approximation for more complicated band shapes. Furthermore, it permits a large part of the calculations to be carried out analytically. This facilitated the discussion of the magnetic properties of the system and their dependence on the system parameters. According to the ratio of bandwidth and on-site repulsion, the model can describe the magnetic behaviour of a paramagnet, or a strong ferromagnet.

The model of the single band with a rectangular DOS has been extended to incorporate the interaction of lattice and magnetic degrees of freedom by introducing a dependence of the bandwidth on the lattice parameter. This extended model gives insight into the possible mechanisms of various effects arising from magneto-elastic coupling. For example, the pressure dependence of the magnetisation and the Curie temperature are explained by a change in the kinetic energy of the magnetic electrons if the inter-ionic distance is

changed. Furthermore, the smearing-out of the ferromagnetic-to-paramagnetic phase transition, as it is observed in some materials, is explained by local variations of the inter-ionic distance due to lattice vibrations.

Furthermore, the model explains a small or negative thermal expansion and magnetostriction due to magneto-elastic coupling. For a partially filled band with increasing bandwidth for decreasing lattice parameter, the energy gained by decreasing the lattice parameter is lower for a higher spin polarisation. If the magnetisation of the band is lowered, the energy gain is increased and the equilibrium value of the lattice parameter is decreased. Therefore, a decrease of the magnetisation caused by an increase in temperature creates a negative contribution to the thermal expansion. The application of an external magnetic field increases the magnetisation and consequently, increases the lattice parameter.

The results of the model for the pressure dependence of the magnetisation and the Curie temperature, the reduced thermal expansion, the magnetostriction and the smearing-out of the ferromagnetic-to-paramagnetic phase transition are all in good qualitative agreement with the experimental findings for ferromagnetic iron-nickel Invar. This supports that the basic assumptions of the model are correct. Quantitatively, the results may not agree very well with experimental findings due to the coarse approximations made. A more extensive analysis of the details of the magnetisation-lattice interaction may improve the quantitative agreement.

A feature of the model, which is not observed in Invar materials, is the sharp step in the thermal expansion at the Curie temperature. A model including fluctuations, as it has been used to describe lattice vibrations, into the approach of a free energy depending on magnetisation and volume, as used for the discussion of the thermal expansion, may remedy this discrepancy.

The model has also been used to study the influence of periodic lattice distortions on the magnetisation. Whereas in certain situations, the magnetisation is not affected by the lattice distortion, in other cases, the magnetisation shows a complex dependence on the amplitude of the distortion. The results may be used to discuss the effect of static lattice distortions on the magnetisation. Furthermore, they may be used to discuss the interaction of a single phonon with the magnetisation.

The consideration of the chemical potential and the grand potential in the last part of the work provides a firm basis for a further development of the model. The model may be

extended to two or more interacting electron bands. Furthermore, the model may be extended to study transport processes in polarised bands.

References

1   D. C. Mattis, *The theory of magnetism*, Harper & Row, New York, London (1965)

2   W. Heisenberg, Zeit. Phys. **49**, 619 (1928)

3   F. Bloch, Zeit. Phys. **57**, 514 (1929)

4   N. F. Mott, Proc. Phys. Soc. London **47**, 571 (1935)

5   J. C. Slater, Phys. Rev. **49**, 537, 931 (1936)

6   E. C. Stoner, Phil. Mag. **15**, 1018 (1933)

7   E. C. Stoner, Proc. Roy. Soc. A **154**, 656 (1936)

8   E. C. Stoner, Proc. Roy. Soc. A **165**, 372 (1938)

9   E. C. Stoner, Proc. Roy. Soc. A **169**, 339 (1938)

10   C. Herring, *Exchange Interactions among Itinerant Electrons*, in *Magnetism, Vol. IV*, edited by G. T. Rado and H. Suhl, Academic Press Inc, New York, United States of America (1966)

11   A. Blandin, *Band Magnetism*, in *Theory of Condensed Matter*, International Centre for Theoretical Physics, Trieste, International Atomic Energy Agency (1968)

12   F. Gautier, *Itinerant Magnetism*, in *Magnetism of Metals and Alloys*, edited by M. Cyrot, North Holland Publishing Company, Amsterdam, New York, Oxford (1982)

13   *Metallic Magnetism*, edited by H. Capellmann, Springer-Verlag Berlin Heidelberg, Germany (1987)

14   H. Watanabe, J. Phys. Soc. Japan **3**, 12 and 317 (1948)

15   K. L. Hunt, Proc. Roy. Soc. A **216**, 103 (1953)

16   E. P. Wohlfahrt, Phil. Mag. **42**, 374 (1953)

17   E. C. Stoner, Rept. Progr. Phys **11**, 43 (1947)

18   E. P. Wohlfahrt, Rev. Mod. Phys. **25**, 211 (1953)

19   R. Hauser, E. Bauer, E. Gratz, Th. Häufler, G. Hilscher, and G. Wiesinger, Phys. Rev. B **50**, 13493 (1994)

20   C. E. Guillaume, C. R. Acad. Sci. **125**, 235 (1897)

21   E. F. Wassermann, *Invar: Moment-Volume Instabilities in Transition Metals and Alloys*, in *Ferromagnetic Materials 5*, edited by K. H. J. Buschow and E. P. Wohlfarth, North Holland, Netherlands (1990)

22   J. Mathon and E. P. Wohlfarth, Phys. Status Solidi **30**, K131 (1968)

23   E. P. Wohlfarth, Phys. Lett. A **28**, 569 (1969)

24   M. Shiga and Y. Nakamura, J. Phys. Soc. Jpn. **26,** 24 (1969)

25   J. F. Janak and A. R. Williams, Phys. Rev. B 14, 4199 (1976)

26   *Ferromagnetic Materials 1*, edited by E. P. Wohlfarth, North Holland, Netherlands (1980)

27   R. M. Bozorth, *Ferromagnetism*, IEEE Press, Piscataway, N.J. (1993)

28   C. Kittel, *Einführung in die Festkörperphysik*, 12. Auflage, R. Oldenbourg Verlag, München, Germany (1999)

29   N. W. Ashcroft, N. D. Mermin, *Solid State Physics*, Library of Congress Cataloging in Publication Data, Saunders College, Philadelphia, United States of America (1976)

30   W. Nolting, *Grundkurs Theoretische Physik, 4 Spezielle Relativitaetstheorie - Thermodynamik*, Friedr. Vieweg & Sohn Verlagsgesellschaft mbH, Braunschweig/Wiesbaden, Germany (1997)

31   W. Nolting, *Grundkurs Theoretische Physik, 5 Quantenmechanik: Grundlagen*, Friedr. Vieweg & Sohn Verlagsgesellschaft mbH, Braunschweig/Wiesbaden, Germany (1997)

32   W. Nolting, *Grundkurs Theoretische Physik, 5 Quantenmechanik: Methoden und Anwendungen*, Friedr. Vieweg & Sohn Verlagsgesellschaft mbH, Braunschweig/Wiesbaden, Germany (1997)

33   W. Nolting, *Grundkurs Theoretische Physik, 6 Statistische Physik*, Friedr. Vieweg & Sohn Verlagsgesellschaft mbH, Braunschweig/Wiesbaden, Germany (1997)

34   G. Fabricius, A. M. Llois and H. Dreyssé, Phys. Rev. B **48**, 6665 (1993)

35   P. M. Marcus and V. L. Moruzzi, Phys. Rev. B **38**, 6949 (1988)

36   R. Strack and D. Vollhardt, Phys. Rev. Lett. **72**, 3425 (1994)

37   J. E. Hirsch, Phys. Rev. B **40**, 2354 (1989) and 9061 (1989)

38   Mathematica 4.0, Wolfram Research (1998-1999)

39   P. Entel, E. Hoffmann, H. C. Herper, E. F. Wassermann, V. Crisan, H. Ebert and H. Akai, J. Phys. Soc. Jpn. **69,** Suppl. A. 1pp. 112-118 (2000)

40   V. L. Moruzzi, Phys. Rev. B **41**, 6939 (1990)

41   P. Entel and M. Schröter, Physica B **161**, 160 (1989)

42   R. J. Weiss, Proc. Phys. Soc. London **82**, 281 (1963)

43   P. J. Brown, K. U. Neumann and K. R. A. Ziebeck, J. Phys.: Condens. Matter **13**, 1 (2000)

44   S. J. Hilbert, unpublished